

**SOUND PROPAGATION IN POROUS MEDIA WITH
APPLICATION TO DIESEL PARTICULATE FILTERS**

By
Sayel M. Fayyad

Supervisor
Dr. Mohammad A. Hamdan, Prof
and

Co- Supervisor
Dr. Mohammad N. Hamdan, Prof

This Dissertation was Submitted in Partial Fulfillment of the Requirement
for the Doctor of Philosophy Degree in Mechanical Engineering

Faculty of Graduate Studies
University of Jordan

September, 2006

Committee Decision

This Dissertation (Sound Propagation in Porous Media with Application to Diesel Particulate Filters) was successfully defended and approved on 20/9/2006.

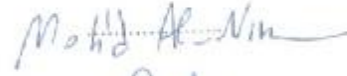
Examination Committee

Signature

Prof. Mohammad A. Hamdan
Professor of mechanical engineering
University of Jordan



Prof. Moh'd A. Al-Nimr
Professor of mechanical engineering
Jordan University of Science and Technology



Dr. Ahmad Al-Qaisia
Associate professor of mechanical engineering
University of Jordan



Dr. Jehad Yamin
Assistant professor of mechanical engineering
University of Jordan



Dedication

-To my father

-To my mother

-To my wife and my children

Acknowledgment

I would like to express my great appreciation to my supervisor Prof. Mohammad A. Hamdan and my co-supervisor Prof. Mohammad N. Hamdan for their great efforts and patience in supervising my thesis, and for their ultimate support, sacrifices and encouragement in all stages of preparing this work.

Also, I am deeply grateful to the mechanical engineering department instructors and employees for their help all over the way.

List of Contents

Subject	page
Committee Decision	ii
Dedication.....	iii
Acknowledgment	iv
List of Contents.....	v
List of Tables.....	ix
List of Figures and Plates.....	x
List of Abbreviation	xv
List of appendices.....	xix
Abstract.....	xix
Chapter one: Introduction and objectives.....	1
1.1 Introduction.....	1
Chapter two: Literature Review.....	6
Chapter Three: Introduction to Porous media and flow in porous media.....	12
3.1 Introduction.....	12
3.2 Porous media.....	12
3.3 Characteristics of porous media	14
3.3.1 Porosity.....	14
3.3.2 Permeability.....	14
3.3.3 Pore structure	16
3.3.4 Capillarity in porous media.....	16
3.4 Flow through porous media.....	16
3.5 Numerical solution for laminar flow in porous media.....	21

Subject	page
Chapter four: Diesel Particulate Filter (DPF).....	23
4.1 Introduction.....	23
4.2 diesel particulate filter (DPF).....	25
4.2.1 diesel particulate filter (DPF).....	25
4.2.2 DPF regeneration.....	25
Chapter five: Acoustic theoretical Back Ground	29
5.1 Introduction.....	29
5.2 Waves.....	29
5.2.1 Velocities in wave motion.....	30
5.2.2 The wave equation	30
5.2.3 Sound waves in gasses.....	31
5.2.4 sound fields.....	33
5.3 propagation constant, and sound attenuation.....	34
5.4 pressure drop model.....	35
5.5 Reverberation and Noise Reduction.....	36
5.6 Sound absorption and speed of sound.....	39
5.6.1 sound absorption.....	39
5.6.2 speedof sound.....	40
5.7 Anechoic termination.....	41
5.8 Acoustics impedance.....	42
5.9 Predicted damping for a DPF at operating conditions.....	45
5.10 Characterization of DPF performance.....	45
5.11 noise and noise control.....	46

Subject	page
Chapter six: Time domain DPF Acoustical Model (four-port model).....	48
6.1 Introduction.....	48
6.2 Derivation of Governing Equations.....	50
6.2.1 Physical model.....	50
6.2.2 Governing equations derivation.....	52
Chapter seven: six-port DPF Acoustic Model	64
7.1 Introduction.....	64
7.2 Governing equations of six-port model.....	64
Chapter eight: Acoustics impedance and transmission losses of DPF unit.....	69
8.1 Introduction.....	69
8.2 Finding the T2 Matrix.....	69
8.3 The lumped impedance model for the DPF.....	72
Chapter nine: Results and Discussion	79
9.1 Introduction.....	79
9.2 Results.....	79
9.3 Discussion.....	100
Chapter ten: Conclusions And Recommendations	111
10.1 Conclusion.....	111
10.2 Recommendations.....	112
References	113
Appendix A	117
Appendix B.....	120

Subject	page
Appendix C.....	122
Appendix D	133
Appendix E	141
Abstract in Arabic	142

List of Tables

Table Number	Title	Page
1	Numerical values for DPF filter material (SiC)	22
2	propagation constants at hot conditions, four-port model.....	63
3	propagation constants at hot conditions, T=1000 C, four-port model.....	63
4	propagation constants at cold conditions, six-port model	68
5	propagation constants at hot conditions, T=1000 C, SIX-port model.....	68
B.1	Numerical values for typical DPF filter.....	120
B.2	Numerical values for different types of DPF filter.....	120
B.3	some physical quantities	121

List of Figures and Plates

Figure Number	Figure Title	Page
1	Velocity of particles during flow through a porous medium.....	19
2	DPF unit.....	23
3	DPF component	24
4	DPF operation.....	26
5	progressive transverse waves moving along a string	29
6	sound waves transferring through DPF unit(four- port model.....	32
7	Anechoic termination.....	41
8	DPF sections an 2D gas flow.....	50
9	Exhaust emission gases motion in DPF unit.....	51
10	Real parts of Γ vs. shear wave number (Attenuation)-HOT conditions, time harmonic variation.....	79
11	real parts of Γ vs. shear wave number (attenuation) – hot.....	80
12	imaginary parts of Γ vs. shear wave number (phase shift)-hot, time.....	80
13	imaginary parts of Γ vs. shear wave number (phase shift) – hot.....	81
14	Real parts of Γ vs. shear wave number (Attenuation)-cold, 2-D space and time harmonic variation.....	81
15	Real parts of Γ vs. shear wave number (Attenuation)-hot, Space.....	82
16	Imaginary parts of Γ vs. shear wave number (phase shift)- hot.....	82
17	Imaginary parts of Γ vs. shear wave number (phase shift)- hot.....	83
18	TL vs. w, for typical filter, time H.V., hotcond, M=0.02, with and withno no soot layer.....	83
19	TL vs. w, for typical filter, hot cond., M=0.02, no soot layer.....	84
20	TL vs. w, for RC:200/12., hot cond., M=0.02, no soot layer.....	84
21	TL vs. w, for EX80:100/17., hot cond., M=0.02, no soot layer.....	85

Figure Number	Figure Title	Page
22	TL vs. w, for EX80:200/14., HOT cond., M=0.02, no soot layer.....	85
23	TL vs. w, for RC80:200/12., HOT cond., M=0.02, no soot layer.....	86
24	NRF vs. frequency for TYPICAL DPF., HOT cond., M=0.02, with no soot layer.....	86
25	TL vs. w, for typical filter, hot cond., M=0.02, time, with and with no soot ...	87
26	TL vs. w, for typical filter, hot cond., space and time, with and with no soot ..	87
27	TL vs. w, for RC: 200/12., hot cond., M=0.02, with/no soot layer.....	88
28	TL vs. w, for RC:200/20., hot cond., M=0.02, with/no soot layer.....	88
29	TL vs. w, for EX80:100/17., hot cond., M=0.02,with/ no soot layer.....	89
30	TL vs. w, for EX80:200/14., hot cond., M=0.02, with/no soot layer.....	89
31	TL vs. w, for four types of DPF., hot cond., M=0.02, with soot layer.....	90
32	NRF vs. w, for typical filter, hot cond., M=0.02,with/ no soot layer.....	90
33	NRF vs. frequency typical filter, hot cond., M=0.02,with/ no soot layer	91
34	transmission losses vs. frequency, time H.V., hot T=1000 C, and T=500 C,With soot layer,M=0.02.....	91
35	TL vs. channel width at hot cond. Time H.V., with soot layer.....	92
36	TL vs. permeability at hot cond. Time H.V., with no soot layer.....	92
37	TL vs. permeability at hot cond. space H.V., with no soot layer.....	93
38	TL vs. wall thickness at hot cond. Time H.V., with no soot layer.....	93
39	Pressure drop vs. axial velocity for typical filter.....	94
40	TL vs. pressure drop at hot cond. Time H.V., with no soot layer.....	94
41	TL vs. channels/m ² at hot cond. plane H.V., with no soot layer. W=700Hz.....	95
42	TL vs. channels/m ² at hot cond. time H.V., with no soot layer. w=700Hz.....	95
43	TL vs. porosity at hot cond. time H.V., with no soot layer. w=700Hz....	96
44	TL vs. w, for typical filter, hot cond., M=0.02, no soot layer. Comparing between time and space	96

Figure Number	Figure Title	Page
45	Pressure drop vs. axial velocity for different types of DPF units.....	97
46	Attenuation vs. shear wave number for Allam and presented study, at hot conditions.....	97
47	Phase shift vs. shear wave number for Allam and presented study, at hot conditions.....	98
48	TL vs. w, for RC: 200/12., hot cond., M=0.02, no soot layer. TIME H.V., comparing with Allam(2006).....	98
49	TL vs. w, for EX80:200/14., hot cond., M=0.02, no soot layer. time H.V., comparing with Allam(2006).....	99
50	TL vs. w, for RC:200/14., hot cond., M=0.02, no soot layer. TIME H.V., comparingwithAllam(2006).....	99
51	Some DPF types and designs.....	117
52	DPF units.....	118
53	DPF styles and specifications.....	119
54	2-D model for porous media pipe and gas flow through.....	122
55	VX, VY, and pressure rate of change for the gas flow through porous media.....	122
56	Axial velocity profile for gas emission through the porous media.....	123
57	Temperature profile for gas emission through the porous media.....	123
58	Nodal solution for axial velocity.....	124
59	Transverse velocity (VY) distributions.....	124
60	Pressure distribution through the porous media.....	125
61	Total pressure change across the porous media.....	125
62	Wall shears distributions.....	126
63	Temperature distribution through the porous media.....	126

Figure Number	Figure Title	Page
64	VX, VY, and Pressure rate of change for the gas flow through porous media at hot conditions (T=773°K).....	127
65	Axial velocity profile for gases emission through the porous media at hot conditions (T=773°K).....	127
66	Temperature profile for gases emission through the porous media at hot conditions (T=773°K).....	128
67	Nodal solution for axial velocity at hot conditions (T=773°K).....	128
68	Nodal solution for transverse velocity at hot conditions (T=773°K).....	129
69	Pressure distribution through the porous media at hot conditions (T=773°K).....	129
70	Nodal solution for temperature distribution at hot conditions (T=773°K).....	130
71	Total pressure change across the porous media at hot conditions (T=773°K).....	130
72	Vector solution for velocity at hot conditions (T=773°K).....	131
73	Element solution in x-direction at hot conditions (T=773 K).....	131
74	Element solution in y-direction at hot conditions (T=773 K).....	132
75	Wall shear stress distributions at hot conditions (T=773°K).....	132
76	DPF cleaning unit.....	141

List of Abbreviations and Symbols

A	Area or cross sectional area[m ²]
A ₀	constant
a _j	channel width [m]
a _{mn}	x-constant in Fourier series.
a _{ln}	y-constant in Fourier series.
'a _n	modal amplitude[m]
ATD	after treatment devices
B ₀	constant
B'	specific surface[1/m]
B''	bulk modulus [Pa]
b _{mn}	Fourier series constant
b _{ln}	Fourier series constant
C	speed of sound [m/s]
CFD	computational fluid dynamics
CC	catalytic converter
C _p	specific heat at constant pressure[J/kg.k]
c _j	a curve around the channel perimeter[m]
D	diameter[m]
D _p	effective particle diameter[m]
D ₀	constant
D _{0j}	constant
D _{0jj}	constant
DPF	diesel particulate filter
DOE	department of energy
d	diameter of cavity[m]
dB	decibel
E ₀	sound energy density[W/m ²]
E _{inst}	instantaneous sound energy density[W/m ³]
e	eigenvector
F	function in space
FEM	finite element method
g	acceleration of gravity[m/s ²]
H	function in space
He	Helmholtz number
H _{soot}	wall thickness with soot layer[m]
Hz	hertz
h _t	wall thickness[m]
I	sound intensity[W/m ²]
IL	insertion loss[dB]
IL'	sound intensity level [W/m ²]
i	index
j	index=1,2
K	pressure drop coefficient[m/s]
K _{th}	thermal conductivity[W/mk]
k _{1, 2}	wave numbers[1/m]
L	length[m]
Ls	sound pressure level[dB]
l	odd integer

l'	end correction length[m]
M_j	Mach number
M_{in}	Mach number at inlet
M_{out}	Mach number at outlet
m_{in}	open area ratio at inlet
m_{out}	open area ratio at outlet
m	odd integer
N	number of channels
N'	number of particles
NRF	noise reduction factor[dB]
n	odd integer
P	pressure [Pa]
P_0	ambient pressure or reference pressure[Pa]
PM	particulate matter.
Pr	Prandtl number
$P_j(\cdot)$	acoustic pressure[Pa]
P_{rms}	root mean square pressure[Pa]
PWL	sound power level[W]
Q	volumetric flow rate [m ³ /s]
$q_j(\cdot)$	acoustic volume velocity[m/s]
R	gas constant[J/kg k]
R_1	viscous flow resistance[Ns/m ³]
R_2	second order flow resistance[Ns ² /m ⁴]
R_w	wall acoustic resistance [Ns/m ³]
Re	Reynold's number
R_H or R_h	hydraulic radius[m]
R_{ac}	acoustic resistance[Ns/m ⁵]
r	specific acoustic resistance[Ns/m ⁵]
S	S-matrix
S_p	surface area of the particle[m ²]
SPL	sound pressure level[Pa]
SEM	scanning electron microscope
T	temperature[k]
T_0	ambient temperature[k]
T_g	gas temperature[k]
TL	transmission losses[dB]
T_{rev}	reverberation time[s]
U, U_0	mean flow velocity in x-direction[m/s]
$ULSD$	ultra-low sulfur diesel.
u'	discharge average velocity[m/s]
u_x	axial (variable) velocity
u_w	acoustic velocity through the wall[m/s]
V, V_0	mean flow velocity in y-direction[m/s]
V_o	volume of enclosure[m ³]
VX	axial velocity[m/s]
VY	transverse velocity[m/s]
V_p	pore volume [m ³]
V_t	total volume[m ³]
V_s	solid volume[m ³]
v	pore velocity[m/s]

W	sound power[W]
W_0	reference power[W]
W_i	incident sound power[W]
W_t	transmitted sound power[W]
w	frequency[1/s]
Y	resistance coefficient
Y1	plug mass impedance of section one[kg/m ² s]
Y3	plug mass impedance of section three[kg/m ² s]
y	specific acoustic reactance[kg/m ² s]
Z	acoustic impedance[kg/m ² s]

Greek Symbols

α	sound absorption coefficient.[sabins]
$\acute{\alpha}$	average sound absorption coefficient [sabins]
Γ	Wave propagation constant
ϕ	Porosity (void fraction) [%]
Γ'	attenuation[dB/m]or neper
$i\Gamma''$	phase shift[dB/m]or neper
ΔP	pressure drop[Pa]
ρ	density[kg/m ³]
ϕ_A	2D porosity[%]
μ	viscosity[Ns/m ²]
σ	permeability[Darcy] or [m ²]
$^{\circ}C$	degree centigrade
ρ_0	ambient density[kg/m ³]
μ_w	dynamic viscosity[Ns/m ²]
σ_w	wall permeability[Darcy] or [m ²]
σ_{soot}	permeability with soot[Darcy] or [m ²]
σ_0	viscous permeability[Darcy] or [m ²]
σ_1	thermal permeability[Darcy] or [m ²]
Λ	viscous length[m]
Λ'	thermal length[m]
η	a constant
σ'	open area ratio
γ	ratio of Cp to Cv.
ϵ	Young's modulus of elasticity[Pa]
ψ	Poisson's ratio.

List of Appendices

Appendix Number	Title	Page
A	Some DPFs types, designs, and styles.....	117
B	Numerical values for different types of DPF units.....	120
C	Numerical results for flow in porous media.....	122
D	Some of software commands.....	133
E	Cleaning and regeneration unit of DPF.....	141

SOUND PROPAGATION IN POROUS MEDIA WITH APPLICATION TO DIESEL PARTICULATE FILTERS

By
Sayel M. Fayyad

Supervisor
Prof. Mohammad A. Hamdan
and

Co-Supervisor
Prof. Mohammad N. Hamdan

ABSTRACT

This work presents a 2-D space acoustic model for sound propagation in a diesel particulate filter (DPF) unit using two approaches. In the first approach the 2-D space model is formulated, using linearized forms of momentum, energy, and continuity equations, along with ideal gas law and Darcy's equation and assuming harmonic variations in time for the field variables: acoustic velocity, temperature, pressure and density. The model retains the normal as well as transverse component of gas velocity and accounts for the mean axial flow, thermal and viscous effects. Approximate analytical solutions to the obtained model are obtained using assumed Fourier sinus series solutions for the field variables and an averaged form of the continuity equation. This approach leads to a four-port acoustic model for the DPF unit. In the second approach the 2-D space model is obtained using the same linearized forms of the governing equations in the first approach but assuming harmonic in time and 2-D space for the field variables, this approach led to a six-port acoustic model for the DPF unit which is not available in previous studies. The obtained four-port and six-port models were analyzed for the effect of various system parameters such as frequency,

temperature, pressure drop, porosity, permeability, presence of soot layer, and number of channels on the transmission losses and noise reduction factor. The obtained results using the above two models, presented in graphical forms where compared against each other and with those available in the published literature.

The results of the present four-port approach, which take into account the effect of transverse velocity, where found to be in fairly good qualitative and quantitative agreement with those of other four-port models and with those obtained experimentally by other investigators. The results obtained from the 2-D acoustic model i.e. six-port model where achieve some improvements in transmission losses and noise reduction compared with all last four-port models presented in the literature.

The flow in porous media has a significant role in producing noise and vibration in exhaust systems of the automobiles, so this flow is analyzed and studied numerically in this thesis using some appropriate software. Temperature, pressure, and velocity profiles and distributions are presented in graphical forms. These numerical results give a complete description for the flow in porous media (DPF unit) and help in studying this type of flow in such media.

This study focuses on solving analytically the acoustic models which is developed as mentioned above taking into account the porosity of DPF unit and the effect of transverse velocity.

Chapter 1

Introduction and Objectives

1.1 Introduction

The propagation of sound in a narrow tube containing a viscous, heat conducting fluid is a topic that has attracted considerable interest over the years, mainly because of its generalization to the acoustics of porous media. With rising oil prices and global warming, which is a dominant environmental issue, the search for better ways to utilize present energy sources or find new alternatives to it became inevitable. This problem is quite important in Jordan due to the increased number of traffic automobiles currently on the streets, in addition to the fuel properties which are far below the international standards, i.e., the diesel fuel currently used in Jordan. According to international standards, the amount of sulfur content is not to exceed 50-150 PPM or (0.005-0.015) %, while here in Jordan it is about 1.15%.

Diesel engines have many environmental problems which can be summarized in two important forms, the most critical and extremely problem that affects the harmful of humans is the very high noise produced by these engines, since diesel engines are usually very noisy machines because of their big size and high power and heat produced. The second environmental problem of diesel engines is that its high production of NO_x and other exhaust gasses and particulate matters (PM). The exhaust gasses cause high pollution problems for the environment represented by acidic rain, effects on ozone layer, and global warming, since NO_x has the ability to react with other compounds and forms new complicated compounds affect humans harmful.

One of the efficient tools used to reduce the pollutants is the diesel particulate filter (DPF). The DPF is connected on the exhaust pipe, hence noise and vibration

characteristics of exhaust system are changed and consequently affect the performance of the engine by developing back pressure, changing temperature, density, and velocity of the exhaust gases...etc. DPF can make noise reduction and has the ability to make transmission loss for sound waves propagates through the system. Muffler can do noise reduction, but it is not as efficient as diesel particulate filters which can make both noise reduction and particulate matters reduction with high efficiency. So it is very important to build an acoustic model for this new technology which will be one of the most important tools in future to make both noise and pollutants reduction.

Jordan is one of the countries suffering from pollution resulted from exhaust gasses emission of heavy diesel vehicles, and also from noise which is considered as a pollution. Ministry of environment lately attempted to study the ability of use some technologies that may help in some gasses emission reduction, and one of these suggested technologies is the DPF technology. But the usage of this new technology in Jordan may face many problems can be summarized in both things:

1-The poor specifications of the diesel used here in Jordan, which is represented by the sulfur contents which is, as be discussed, about 1.15%. Since as the sulfur contents increase the performance of the DPF in gasses emissions reduction decreases rapidly.

2- The high prices of this technology

It can be concluded that Jordan can not decide to use this technology unless diesel specifications be improved by decreasing sulfur contents or uses some appropriate additives; in addition this project must be funded from government or other environmental organizations.

The present study is concerned with developing a 2-D acoustic model for a gas flow in a porous media with application to DPF following two approaches: according to the first approach, the field parameters (temperature, pressure, density, and velocities) are

considered to be varying harmonically in time only, and according to the second approach these parameters are considered to be varying harmonically in time and in 2-D space. In first approach a traditional four-port model (depend on time only) was obtained, while in the second approach a new six-port model has been found, in which six roots for the eigenvalue problem were obtained which represented the wave propagation constants against four roots in last traditional four-port models. The six-port model achieves good improvements over last four-port model in both transmission losses and noise reduction.

The flow in a DPF is usually considered as thermo–viscous gas flow. This flow through the diesel particulate filter is considered in the presented study as a 2-D flow. All previous studies treat the problem as a 1-D, but in the real case it should be 2-D model. Generally the propagation of acoustic waves in such a bounded fluid flow, involves reactive and dissipative processes. These processes can be characterized in the frequency domain, by a complex-valued wave number. The imaginary part of this number is in general proportional to the shear and bulk viscosity coefficients and the heat conduction coefficient. In a bounded domain (pipe or cavity), reactive and dissipative processes at rigid walls- arise from interactions between the acoustic field and the entropy (diffusion of heat) and the vorticity fields (diffusion of shear waves) are created on the boundary walls and that extracts energy from the acoustic wave. It is known that the entropy and vorticity fields decay exponentially in the direction normal to the walls and, with the exception of low frequencies and narrow ducts, only play a role in a thin acoustic boundary layer region. When this is the case the effect of resulting reactive and dissipative effects can still be handled by introducing a complex wave number. For the case of interest here with sound propagation in a narrow channel (width around 1-2mm) the boundary layers will extend over the cross-section and a full

analysis of the coupled field problem is necessary. It is known that for the diesel particulate filters there is a need to analyze wave propagation in narrow tubes which should be considered partially as porous media. The present study gives an approximate analytical solution in which the effects of mean flow are taken into accounts. The mean flow profile is assumed to be uniform and both the temperature and pressure gradients are assumed to be constant.

The main objectives of this study can be summarized as follows

- Building a 2-D acoustic model for the exhaust gases emission with the existence of the diesel particulate filter.
 - Evaluating the wave propagation constant which includes both attenuation, and phase shift.
 - Evaluating the acoustics impedance of the DPF unit.
 - Calculating the values of transmission losses (TL) for the typical filter, and for other types of DPF.
 - Selecting the appropriate DPF type corresponding to its properties and on its capability on sound transmission losses.
 - Calculating the noise reduction factor (NRF) which is an additional evaluation tool in comparison between different types of DPFs units.
 - Asses the effect of frequency, wall permeability, porosity, pressure drop, channels width, wall thickness, and number of channels of porous DPF units on TL.
 - Find the velocity, temperature, pressure distributions and profiles for the gasses flow through the porous media numerically-using some appropriate software packages.
- All results from last two approaches mentioned above (four-port and six-port models) were compared with both theoretical and experimental results available in the literature and a fairly good qualitative and quantitative agreement can be noticed.

This dissertation consists of ten chapters, chapter one gives an introduction for this study, while chapter two gives a literature review for last studies which have been concerned the problem, chapter three gives a description for porous media, its specifications, types, and some important methods and theories described the behavior of these materials. Also in chapter four a description for diesel particulate filter (DPF) including its construction, types, properties, and flow in both porous media and DPF are presented. Chapter five establishes for some acoustic concepts and background in order to make necessary calculations for the models resulted later. In chapter six a full description, assumptions, and derivation of the model are made at the case of time harmonic variation. In chapter seven there is a full derivation for the invented model (six-port model) at the case of harmonic in time and 2-D space. In chapter eight the DPF impedance, the transfer matrix (S-matrix), transmission losses (TL) , and noise reduction factor (NRF) for DPF are evaluated for the two cases, time harmonic variation and harmonic in time and 2-D space case. All results are listed and discussed in chapter nine; also a conclusions and recommendations are listed in chapter ten.

Chapter 2

Literature Review

A variational treatment of the problem of sound propagation or transmission in narrow tubes is described and it has been the subject of much research over many years.

Cummings (1993) studied the sound propagation in a narrow tubes of arbitrary cross-section, he also build an analytical model which can be used for any cross-sectional geometry, as long as the cross-section of the tube is uniform along its length. Very simple low frequency and high frequency approximate solutions are obtained by the use of idealized trial functions. These models give results of acceptable accuracy in comparison with the exact or numerical solutions. One appealing feature of this type of method is that there is considerable scope for improvement the results, by the choice of more versatile trial functions that can more nearly approach the true solutions to the governing equations.

Peat (1994) made an approximation to the effect of mean flow on sound propagation in capillary tubes. The paper began with the derivation of the governing equations by the use of boundary layer approximations. It was shown that these equations reduced to those for the low reduced frequency solution equations in the limit of zero steady flow. In practical, the radial velocity component is retained in the equations under these approximations, even though one might suppose that it would be negligible in a capillary tube. In this study, a first approximation was sought for the effect of the steady flow upon sound propagation in capillary tubes. For simplicity, the background temperature was assumed to remain constant and tubes of circular cross-section were considered. The results given in this paper indicated the effect of steady flow-upon the axial propagation of sound waves in capillary tubes, in terms of both decay rate and phase velocity. In the zero flow limits these factors were the same for both forward and

backward propagation waves but, with steady flow, the forward convected waves behaved differently from that of the backward waves, which propagates into the flow. It was also found that a third wave was generated in the steady flow case, unless either the acoustic disturbances were assumed to be isentropic or else the Prandtl number is unity. Dokumaci (1995) studied the sound transmission in narrow pipes with superimposed uniform mean flow and made an acoustic modeling of automobile catalytic converters. The paper was mainly concerned with the acoustic modeling of the honeycomb structure in automobile catalytic converters, in the large shear wavenumber limit, which was valid for the standard pipes in internal combustion engine exhaust systems; this study provided a useful alternative to the one-dimensional theories. In this study a two-port elements have been presented for the acoustic modeling of the honeycomb structure in monolithic catalytic converters. Also this study predicted a marked frequency dependence model for the honeycomb structure at the lower frequencies. Astley and Cumings (1995) presented FEM solutions, based on simplified equations for waves in a visco-thermal fluid, for the problem of sound propagation in capillary tubes. They made analysis for the laminar flow with a parabolic velocity distribution and a quadratic cross-section. The simplification of the governing equations is based on that the axial gradients are much smaller than the gradients over the cross-section. They derive the linearized fluid-dynamical differential governing wave motion in a narrow tube containing a viscous, heat-conducting fluid and discussed the boundary conditions that must be applied at the tube walls. Ih et al. (1996) have developed analytical solutions for sound propagation in capillary ducts with mean flow. In this study the transverse of particle velocity, temperature, and viscosity were considered. A fully developed laminar steady flow was assumed and the concept of a complex propagation constant was introduced in the formulation. The final equation formed reduces to Kummer-type

differential equation and its solution was obtained in terms of confluent hypergeometric functions. The dispersion equation for the complex propagation constants was taken on a recursive form. A simplified form of the analysis permitted comparison with previous results dealing with visco-thermal effects and included the features of Poiseuille-type laminar steady flow for low and medium shear wave numbers. Jeong and Ih (1996) showed by numerical solutions of the governing equations, that including the radial particle velocity has a small but noticeable effect. They made a numerical study on the propagation of sound through capillary tubes with mean flow. They used the general formulations of conservation equations with non-isentropic conditions based on the low reduced frequency solutions, the linearized governing equations were solved by the recursive use of numerical methods. Also they investigated the characteristics of the forward and backward propagation acoustic waves, and the characteristics of the hydrodynamics waves were also investigated when steady flow was present. In this study the effect of the radial and axial temperature gradient was excluded.

Dokumaci (1998) extended his earlier work to the case of rectangular narrow tubes with a plug flow. The solution procedure is now based on a weak (Galerkian) formulation, where the fields over the channel cross-section are expanded as double Fourier sinus series. The paper presented a comparative study of these for pipes having circular and rectangular cross-sections. The results indicated that the assumptions of a uniform mean flow profile closely predicted the results based on a parabolic profile. The in-plane velocity terms were retained in this study, and they had been used in the continuity equation. Dokumaci (2001) derived an approximate dispersion equation for sound waves in a narrow pipe with ambient gradients. The paper presented an approximate solution in which the presence of mean flow, which is assumed to have a uniform velocity profile, was taken into account. The solution also included the effect of constant

pressure gradient. A dispersion equation was derived by assuming that the spatial variations of the ambient variables can be lumped. Allam and Abom (2002) build up theoretical models to predict the acoustic 2-port (4-pole) of a diesel particulate filter (DPF) unit. In the first model the steady flow resistance was used to calculate an equivalent lumped resistance. In this model the wave propagation in the DPF monolith was neglected and was a low frequency approximation. To include wave propagation effects the monolith was described using a coupled wave guide model, where the coupling was via the porous walls of the monolith. Darcy's law was used to describe the pressure drop in the porous walls. Based on this an improved theoretical model was obtained. Both models were compared to measured data from a test rig with clean air operating at 20 C. The agreement for the 1-D wave propagation model was quite good but for low frequencies (< 300 Hz) the lumped resistance model also seems satisfactory. Fairbrother and Tonsa (2003) described work on simulating the acoustic behavior of catalysts and DPF devices using both linear and nonlinear techniques. In this paper two existing computer simulation codes (one linear, one non linear) had been extended and combined into a single package. The linear method was carried out in the frequency domain and made use of plane wave assumptions. This was done with the transfer matrix method, also called the four pole method. Specific models of after treatment components were used to generate transmission loss predictions versus frequency. The non linear method solved the mass, movement and energy equations in the time domain and made use of white noise excitation and Fast Fourier Transforms (FFT) to obtain results in the frequency domain. Allam and Abom (2003) made an acoustic modeling of an after-treatment device (ATD). In this paper Allam and Abom presented an acoustical model of a complete ATD for a passenger car. The model was built up to four basic elements: 1) conical

inlet/outlet; 2) straight pipe; 3) catalytic converter (CC) unit and 4) DPF unit. For the DPF unit two models had been developed. One simple 1-D model with no influence of wall boundary layers and one based on a 1-D CC model suggested by Dokumaci (1998) including wall boundary layers. Both models neglected the effects of chemical reactions. Both models were compared with experimental data and the agreement was satisfactory. Wijnant, et.al. (2003) made an investigation for the boundary layer induced noise. They describe a method to design trim panels containing a large number of coupled tubes to effectively reduce noise. The theory of visco-thermal wave propagation in tubes was discussed. They calculated the absorption coefficient for a panel containing a number of non-coupled tubes. Initial results optimized the tubes' length and radii for a desired fictive absorption coefficient; also the applicability of the method was proved. Allam (2005) studied the acoustic modeling and testing of DPF and considered it as an eigenvalue 1D problem. This paper presented a first attempt to describe the acoustic behavior of DPFs and to present models which allow the acoustic two-port to be calculated. The simplest model neglected wave propagation and treated the filter as an equivalent acoustic resistance modeled via a lumped impedance element. This simple model gave a constant frequency independent transmission loss and agreed within 1 dB with measured data on a typical filter (length 250 mm) up to 200–300 Hz (at 20 C). In the second model, the ceramic filter monolith is described as a system of coupled porous channels carrying plane waves. The coupling between the channels through the porous walls is described via Darcy's law. This model gave a frequency-dependent transmission loss and agreed well with measured data in the entire plane wave range.

Allam and Abom, (2006) modified the 1-D model using the classical (exact) Kirchhoff solution for a plane wave in a narrow tube. The model was in close agreement with the

predictions of the new model. Furthermore this model, which assumed isothermal sound propagation, worked satisfactorily up to 800-1000 Hz for a typical filter at operating (hot) conditions. This study formed the backbone of the presented study, where a 1D linear acoustic model for a DPF unit had been developed.

Based on last revision of the main last studies concerned the problem, it is obvious that the problem was treated in most of these studies as a 1-D model, but really it should be a 2-D one by taking into account the effect of the transverse velocity and the partial porosity of DPF unit.

Chapter 3

Introduction to Porous Media and Flow in Porous Media

3.1 Introduction

Porous media having now a vital role in manufacturing, because of their distinctive properties rather than solids, one of these important technologies depending on these properties is the diesel particulate filter (DPF) which considered as a porous media. In this chapter there is a brief description for porous media, their properties like porosity, permeability, their usage, and some relations governing the behavior and flow through porous media. There are many examples of porous materials in everyday life and the environment: textile and leathers are highly porous; they owe their thermal insulating. On the other side there are many artificial porous media which having many manufacturing usage such as diesel particulate filters.

3.2 Porous Media

Porous media is an aggregates of solid elements (grains matrix etc.) between which the voids form the pore space itself. These voids within the porous body give rise to the wide differences in physical behavior between dense solids (such as minerals) and porous substances such as DPF units, Holzbecher (1998).

To describe a material as a porous media, it should have one of the following:

1. It must contain spaces, so-called pores or voids, free of solids, imbedded in the solid or semisolid matrix. The pores usually contain some fluid, such as air, water, oil, etc., or a mixture of different fluids as in the case of DPF unit.
2. It must be permeable to a variety of fluids, i. e. Fluids should able to penetrate through one face of a septum made of the material and emerge on the other side. In this case one refers to a "permeable porous material".

The most important areas of technology that, to a great extent, depend on the properties of porous media are:

1- Hydrology, which relates to water movement in earth and sand structures, such as dams, flow to wells from water-bearing formations, intrusion of sea water in coastal areas, filter beds for purification of drinking water and sewage, etc.

2- Petroleum engineering which is mainly concerned with petroleum and natural gas production, exploration, well drilling, and logging, etc. Despite the great similarity of the physical systems and processes in these two fields of technology, each of them has a distinct technical literature and terminology, Dewiest (1969).

3- In chemical engineering, heterogeneous catalysis is an important technology where pore diffusion of gases as well as impregnation of porous catalysts with catalyst precursor and distribution of molten catalyst is a process that depends on pore structure. Flow through packed beds is equally important in operations involving chemical reactions or separation of chemical components.

4- Chromatography and, in particular, gel permeation chromatography are relatively new but increasingly important processes, the latter of which depends on both diffusion and flow through porous media. Other separation processes use porous polymer, biological, and inorganic membranes. Filtering of gases and liquids and drying of bulk goods are equally important technologies based on flow or diffusion through porous media. The impregnation of plastics with plasticizers also depends on pore structure.

5- In medicine and biochemical engineering, biological membranes and filters, the flow of blood and other body fluids, and electro-osmosis are a few examples where the role played by porous media is critical.

6- In electrochemical engineering, porous electrodes and permeable and semi permeable diaphragms for electrolytic cells play important technological roles in the struggle to obtain improved current efficiencies. Sintering of granular materials is a very large tonnage technology where pore structure is of importance.

7-In manufacturing diesel particulate filters (DPF), which is a good example of porous media. This device has the ability to make gas emission reduction about 70-90%; it is made of ceramics which considered as porous media.

3.3 Characteristics of porous media

There are two important quantities describing the properties of a porous medium: the porosity ϕ and the permeability σ .

3.3.1 Porosity

Porosity which defined as is the ratio of the pore volume V_p to the total volume V_t of the body considered. The solid volume V_s is given by $V_s = V_t - V_p$. Hence it suffices to measure two of these three parameters to calculate porosity. Porosity also plays an important role in metallic, plastic, and enamel coatings, where its presence is definitely. There are two kinds of porosity of the medium defined as three-dimensional porosity, ϕ , and two-dimensional porosity, ϕ_A , the both quantities can be given as

$$f = \frac{\text{void volume}}{\text{bulk volume}} \quad (3.1)$$

$$f_A = \frac{\text{cross - sectional void area}}{\text{total cross - sectional area}} \quad (3.2)$$

Hence the void volume of the porous medium can be written as

$$\text{void volume} = \frac{f}{1-f} (\text{volume of particles}) \quad (3.3)$$

3.3.2 Permeability

Permeability" is the term used for the conductivity of the porous medium with respect to permeation by a Newtonian fluid. "Permeability," used in this general

sense, is of limited usefulness only because its value in the same porous sample may vary with the properties of the permeating fluid and the mechanism of permeation. It is both more useful and more scientific to separate out the parameter which measures the contribution of the porous medium to the conductivity and is independent of both fluid properties and flow mechanisms. This quantity is the "specific permeability" σ , or it is just called "permeability", its value is uniquely determined by the pore structure, Holzbecher (1998) and Dewiest (1969).

Practical unit of permeability is the "Darcy." A porous material has permeability equal to 1 Darcy if a pressure difference of 1 Atm, will produce a flow rate of 1 cm/sec of a fluid with 1 unit of viscosity through a cube having sides 1 cm in length. Thus 1 Darcy is equal to $0.987 \mu\text{m}^2$. For very "tight" materials the unit millidarcy = 0.001 Darcy is used. Often the porosity can be chosen as constant for the whole medium. Since the permeability σ describes the ability of the fluid to flow through the porous medium, so σ is often called the absolute permeability and is a quantity depending on the geometry of the medium only. There has been much effort to establish relations between the permeability and the porosity. However, a general formula seems impossible to find a relate permeability to porosity but the permeability is found to be proportional to Φ^m when m is in the range of 3 to 6 depending on the geometry of the medium. The fluid flowing in the pore space is characterized by the dynamical viscosity μ . The viscosity indicates the resistance in the fluid due to shear and angular deformations. At microscopic level there are friction forces in the fluid caused by the interchange of momentum in collisions between the molecules. The strength of the friction forces sets the viscosity of the fluid. Another expression for the viscosity which is often used, is the kinematic viscosity ν defined as $\nu = \mu / \rho$, where ρ is the density of the fluid. Moreover, the viscosity of incompressible Newtonian fluids (which will be the

case of interest here) is assumed to be isotropic, thus, such fluids are characterized by only one viscosity coefficient μ , Dewiest (1969).

3.3.3 Pore Structure

Pores are invisible to the naked eye in the majority of porous media. The porous nature of a material is usually established by performing any one of a number of experiments on a sample and observing its behavior, because porous materials behave differently from nonporous ones in a number of respects.

3.3.4 Capillarity in Porous Media

In a "capillary system" the surfaces separating the various bulk phases play a significant role in determining the physical-chemical state of the system. According to this definition, the vast majority of porous media are capillary systems. In the case of capillary systems, mechanical equilibrium, i.e., the absence of net mechanical force acting on the system is determined not only by the hydrostatic pressure and gravitational attraction but also by forces associated with surface tension, Holzbecher (1998).

3.4 Flow through porous media

In the present thesis the coupled steady state axial mean laminar flows of incompressible viscous Newtonian fluids in porous media are discussed. The flow in the pure fluid region is usually described by the Navier-Stokes system of equations. The most popular models for the flow in the porous media are those suggested by Darcy and by Brinkman, the flow of several components and several phases through a porous medium is generally described by introducing macroscopic mass-balance equations under the form of generalized dispersion equations. Porous medium consists of a matrix with a large amount of microscopic pores and throats which are typically narrow tubes where fluid can pass through. Soil and sand are both

examples of porous media and fluid flow in a porous medium can be considered as pouring a cup of water over soil and letting the water flow into the soil due to the gravitational forces. The description of flow in porous media is extremely difficult because of the complexity of the medium. Even though flow in a single tube is given by simple equations, the network of the tubes is impossible to know in detail. Fluid flow through a porous medium is often given by the phenomenological Darcy equation. Consider a porous medium of absolute permeability σ in a homogeneous gravitation field where one fluid of viscosity μ is injected through the medium by applying a pressure gradient ΔP across the matrix. Then the flow rate Q of the fluid through the medium is given by Darcy's equation, such that

$$Q = -\left(\frac{\sigma A}{m}\right)\left(\frac{\Delta P}{L}\right) \quad (3.4)$$

This is a linear law, similar to Newton's law of viscosity, Ohm's law of electricity etc. In equation (3.4), Q is the volumetric flow rate (or "discharge"), A the normal cross-sectional area of the sample, L the length of the sample in the macroscopic flow direction, P "piezometric pressure," Stanley, H., et.al. (1979).

There are four conditions that are required for this equation to be valid:

1. Creeping flow – The modified Reynold's number based on superficial velocity must be on the order of 1.
2. The porous media itself is not reactive with the flowing fluid.
3. No accumulation.
4. Single-phase flow

Using equation (3.4), it is possible to determine the permeability (σ) of the porous media. Darcy's equation is applied for those porous media which have regions with a smaller pores which also treated as a permeable medium as in the case presented (partially porous media not highly porous). The most general equation describes the

matching of boundary conditions at an interface between the larger pores and the permeable medium is the Brinkman's equation, such that:

$$\Delta P = -\frac{m}{S}V + m_e \nabla^2 V \quad (3.5)$$

where

V : is the fluid velocity

μ : is the fluid viscosity

μ_e : is the effective fluid viscosity

σ : is the permeability.

ΔP : is the pressure drop.

The equation satisfied two boundary conditions at the pore/ permeable medium interface which are continuity of the fluid velocity and the shear stress.

Although liquids display a permeability that depends on the media only, gases display a permeability that also depends on the identity of the gas and the pressure differential across the media. This variation with the identity and pressure of the gas is known as slippage. This effect was originally detected with gas flow through capillary tubes, and becomes more pronounced when the diameter of the capillary tubes approach the mean free path of the gas molecule. The mean free path is a function of the molecular weight and kinetic energy of a gas.

Flow in porous media requires a description of both the media and the flow. In the broadest sense an open pipe is a limiting case of a porous medium. Usually the number of holes or pores is sufficiently large that a volume average is needed to calculate pertinent properties. Pores which occupy some definite fraction of the bulk volume form a complex network of voids.

Flow in a porous medium is usually a creeping flow where the modified Reynolds number defined for a porous medium is less than one. In order to define the Reynolds

number for flow in porous media, the concept of hydraulic radius, R_H can be used. The hydraulic radius is defined as the void volume of a porous medium divided by the surface area of the medium such that

$$R_H = \frac{\text{void volume of porous medium}}{\text{surface area of porous medium}} \quad (3.6)$$

If V_p : is the particle volume, and the surface area of the particle, S_p , for spherical particles, the specific surface, B (which has dimension m^{-1}) can be defined as

$$B = \frac{6}{D} = \frac{S_p}{V_p} \quad (3.7)$$

where D is the diameter of a particle.

The hydraulic radius can be rewritten in terms of the porosity, ϕ , the number of particles, N , the volume of the particles, V_p , and the surface area of a particle, S_p , in the following way:

$$R_H = \frac{fV_p \left(\frac{N}{1-f} \right)}{S_p N} = \frac{fV_p}{S_p(1-f)} \quad (3.8)$$

For nonspherical particles, an effective particle diameter, D_p , can be defined as:

$$D_p = \frac{6}{B} \quad (3.9)$$

The discharge velocity, \bar{u} , and the pore velocity, v , (as shown in figure (1)) are related by the mass balance as in the following equation

$$\bar{u}A_{tot} = vA_{void} \quad (3.10)$$

This gives the result:

$$\bar{u} = f_A v \quad (3.11)$$

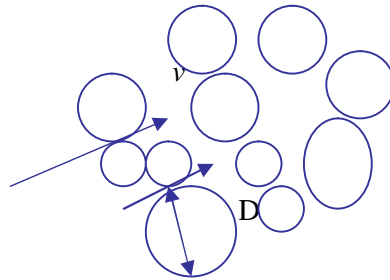


Fig (1) Velocity of particles during flow through a porous medium.

Hence Reynolds number for flow in a pipe is:

$$\begin{aligned} \text{Re} &= \frac{r \bar{u}^2}{m \left(\frac{\bar{u}}{D} \right)} \\ &= \frac{\bar{u} D r}{m} \end{aligned} \quad (3.12)$$

Where

μ : is viscosity;

\bar{u} : is the discharge velocity;

ρ : is density of the fluid;

D: is the diameter of a pipe;

v: is the pore velocity (m/s).

For porous media, the length scale corresponds to the hydraulic radius, R_H , while the velocity scale is the discharge velocity \bar{u} , divided by the porosity ϕ .

Therefore, for porous medium, the Reynolds number can be rewritten as

$$\begin{aligned} \text{Re} &= \frac{4R_H \bar{u} r}{f m} \\ &= \frac{2}{3(1-f)} \frac{D_p \bar{u} r}{m} \end{aligned} \quad (3.13)$$

Usually for convince of definition the numerical constants are dropped and in some definitions the $(1-\phi)$ term is also dropped. The Reynolds number then becomes:

$$\text{Re}_p = \frac{D_p \bar{u} r}{m} \quad (3.14)$$

For the case of porous media used in this study which represents the DPF and the flow which is represented here by the exhaust gas emission having the following properties ($\bar{u}=8\text{m/s}$, $\rho_g=0.35 \text{ kg/m}^3$, $\phi=0.45$, $\mu=4.15\text{E}^{-5}$, and $D=5\text{E}^{-6} \text{ m}$, see table (1) below) and by applying equations (3.13) or (3.14) yields that:

Re=0.408, but at low temperatures the exhaust gases properties is changed.

This results means that Darcy's law is applied for the case of flow in this type of porous media and that the flow is laminar.

3.5 Numerical Solution for Laminar Flow in Porous Media

The flow in porous media is analyzed numerically using some appropriate software programming. This appropriate software program is used in order to find velocity distributions in both directions, x and y through the porous media, and also to find temperatures profile and distribution through porous media. The results describe in addition the pressure distribution, wall shear, and contours and profiles for temperature, pressure, velocities V_x , and V_y for the flow in porous media which represents the a DPF unit made of silicon carbide (SiC) which having the following properties (see table (1)) below. All numerical results are listed in appendix C, from figure (78) to figure (102). Also a discussion for these results will be demonstrated later in chapter 9.

Table (1) DPF's material specifications*

Quantity	value
pore size(μm)	23
porosity (%)	45
Air through wall permeability ($10 \times 12/\text{m}^2$ Darcy) at 20°C	0.70
Thermal conductivity- 25°C [W/mK]	40
Thermal conductivity- 630°C [W/mK]	15
Specific heat- 25°C [J/kg/K]	750
Specific heat- 800°C [J/kg/K]	1250
Weight gained after 10000hours use in air at 1000°C	low
Weight gained after 10000hours use in air at 1000°C	low
Weight gained after 10000hours use in air at 1000°C	low
Expansion/radial $\times 10^{-6}/^\circ\text{C}$ - 25°C	4.20
Expansion/radial $\times 10^{-6}/^\circ\text{C}$ - 650°C	3.9
Thermal shock parameter , TSP 3	85-750
Long life maximum temperature in air- ($^\circ\text{C}$)	1200
Modulus of elasticity –E[GPa]	50
Poisson's ratio- ν	0.10
Compress strength, longitudinal Q_a [MPa]	30
Bending strength –MOR/a MPa	>25
Bending strength –MOR/b MPa	1.70
Bending strength –MOR/c MPa	2.60
Specific weight-[gram/ cm^3 /monolith]	1.8
Monolith pitch 2.8 bulk weight [gram/ cm^3]	0.95
Electric resistance- [ohm .cm]	1

* Source: laa@liqtech.dk, www.liqtech.dk.

Chapter 4

Diesel Particulate Filter (DPF)

4.1 Introduction

All countries now are seeking from pollution especially that produced from heavy diesel vehicles, Jordan is one of these countries which has many problems in this field can be represented by the poor specifications of diesel fuel- sulfur content (about 1.15%)-, and the very rapid increase in number of automobiles which cause more pollution, in addition to the shortage in energy sources which is a main reason in increasing prices of fuel in Jordan recently.

Diesel particulate filters are considered as a good example of a porous media and also considered as one of the leading technologies for meeting future particulate matter (PM) emission; see figure (2) and (3) below. These devices generally consist of a wall-flow type filter positioned in the exhaust stream of a diesel vehicle. As the exhaust gases pass through the system, particulate emissions are collected and stored. Because the volume of diesel particulates collected by the system will eventually fill up and even plug the filter, a method for controlling trapped particulate matter and regenerating the filter is needed.



Figure (2) DPF unit (source: Joe Kubsh, www.meca.org) .

It is very important to explain and understand the construction of DPF units, their properties, types, and their operation especially if it is known that all countries (including Jordan) attempt to use such devices in the close future, and in order to complete understanding about the way to derive the acoustics governing equations for the DPF unit after it is connected on the exhaust system.



Figure (3) some DPF components (source: Joe Kubsh, www.meca.org) .

There are many new technologies that recently developed to make exhaust gasses emission reduction especially that produced from diesel engines includes

- Diesel particulate filters (DPF)
- Diesel oxidation catalysts (DOC)
- Crankcase emission controls
- Enhanced combustion modifications: e.g. cams, coating, superchargers, and engine rebuild kits.

From last technologies DPF is considered as one of the most efficient devices and the easier to be installed and to maintenance.

4.2 Diesel Particulate Filter (DPF)

4.2.1 Diesel Particulate Filter (DPF)

Diesel particulate filter is a superior system in the reduction of particulate matters because it can reduce about 70% PM. It contains a large numbers of thin tubes or cavities with a diameter of about (1-2 mm), and (0.15-0.5 m) length see figure (3) below. There are many types of DPF's (see appendix (A)), such as: electric heater type, burner type (ceramic filter), and fuel additive type; the latter type is a honey-comb ceramic. The honey-comb type constitutes an additive supply and an electronic system. In this type Fe is used as an additive whereby iron oxide is formed which reacts with carbon and then it is converted to iron. When certain temperature is reached, the O₂ formed around iron oxide reacts with the particulate matter (PM) so that these particles could be regenerated in the existence of O₂ of catalyst. For many diesel engines, the exhaust gas temperature is insufficient to regenerate the filter.

4.2.2 DPF Regeneration

For filter regeneration to work effectively, exhaust temperatures need to exceed about 500° C for non-catalyzed systems, and 250° to 300° C for catalyzed systems. Some diesel particulate filters use a “passive” approach, and do not require an external or active control system to dispose of the accumulated soot. Passive filters are installed in place of the muffler. At idle or low power operations, particulate matter is collected on the filter. As the engine exhaust temperatures increase, the collected material is then burned or oxidized by the exhaust gas, thus cleaning or regenerating the filter. See appendix E which shows some cleaner and regeneration units of DPFs, Oh, S. et. al. (2002),and (Washington state university extension in energy program).

To ensure filter regeneration, various strategies (or combinations) are used.

Regeneration methods include:

- Coating the filter substrate with a base or precious metal, thereby reducing the temperature needed for oxidation of the diesel particulate matter;
- Installing a catalyst upstream of the filter, and again lowering the exhaust temperature needed to burn off the particulate.
- Using fuel-borne catalysts to reduce the burn-off temperature of the collected particulates;
- Installing fuel burners, electrical heaters or some other active method to heat the exhaust gas to a high enough temperature to ensure PM oxidation.

While limited to primarily off-road applications, another strategy which avoids filter regeneration altogether is to use a disposable particulate trap. The disposable system is sized to collect diesel particulate matter over a set period of operation. When full, the system is removed from the vehicle and replaced with a new unit.

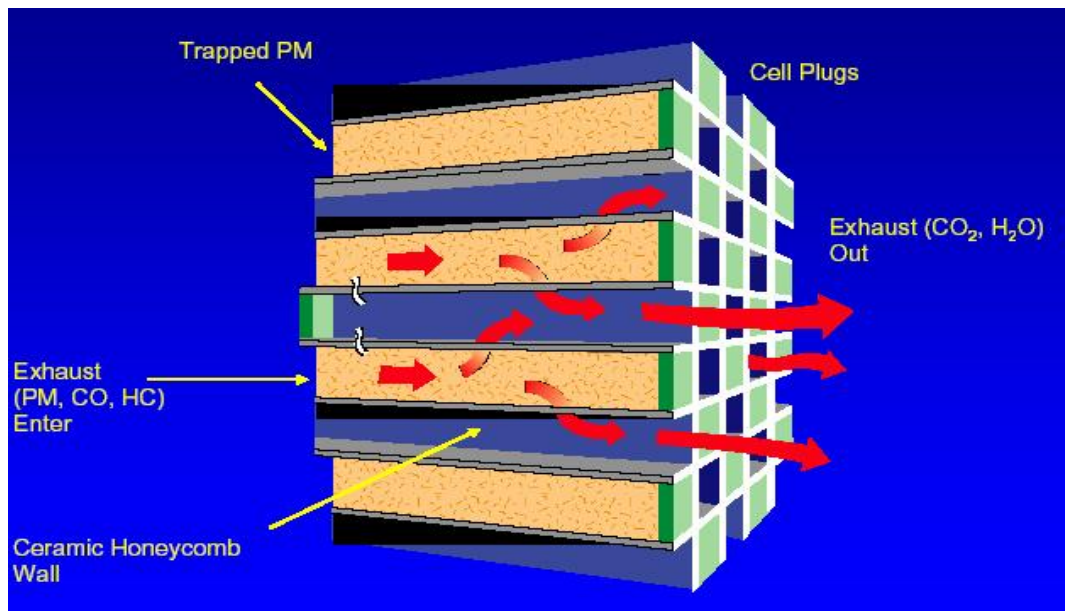


Figure (4) DPF operation (source: Joe Kubsh, www.meca.org).

Diesel particulate filters are also very sensitive to exhaust gas temperatures and fuel sulfur content which affects on the performance of the DPF system, other factors affected the DPF performance are its dimensions, soot layer thickness, and heat losses. For most continuously regenerating catalyzed particulate filters to work properly, an engine must operate at around 300° C for 30 percent of the duty cycle or 30 minutes. Some other types of diesel particulate filters require an average exhaust temperature of at least 270° C for 40 percent of the engine duty cycle, (Washington state university extension in energy program).

Exhaust gas temperatures are highly application dependent. Excessive heat loss in the exhaust system can cause lower exhaust gas temperatures, as can over-size engines that are operated low on their torque/power curve. Although many diesel applications generate sufficient exhaust gas temperatures for successful DPF operations, device manufacturers and regulators recommend that certain vehicle applications are equipped with data loggers to continuously monitor exhaust back pressure and temperature. Once it is determined that sufficient exhaust gas temperatures exist for filter regeneration, the monitoring can be stopped. Fuel sulfur content also affects the performance of passive DPFs, Oh, S. et. al. (2002),and (Washington state university extension in energy program).

The Department of Energy (DOE) in USA recently concluded a study examining the effects of sulfur on diesel particulate filters. Two passive regeneration systems were tested: a catalyzed DPF (the filter is directly coated with a catalyst) and a continuously regenerating DPF (a catalyst is located upstream of the filter). DOE found that DPFs cease to reduce PM emissions with fuels containing 150 ppm sulfur and become a source of PM emissions with 350 ppm sulfur fuels. Overall, baseline PM emissions increased as the fuel sulfur level increases. At 3 ppm sulfur both devices reduced PM

emissions by 95 percent, and at 30 ppm sulfur the PM reduction efficiencies of both devices dropped to the around 72 percent. Diesel particulate filters can be installed on new and used automobiles, but must be used in conjunction with ultra-low sulfur diesel (ULSD) – fuel with a sulfur content of less than 15 parts per million, Oh, S. et. al. (2002),and (Washington state university extension in energy program).

The combination of diesel particulate filters and ULSD can reduce emissions of hazardous particulates, smog causing hydrocarbons, and poisonous carbon monoxide by 60 to 90 percent. In fact, it is possible to produce an engine that is cleaner in particulates than a natural gas engine. Furthermore, studies have shown that diesel particulate filters need not cause additional maintenance on bus or truck engines, or create a fuel economy penalty.

Chapter 5

Acoustic Theoretical Background: Sound and Waves

5.1 Introduction

In this chapter some acoustical quantities will be defined as an introduction to make calculations for different aspects of sound waves propagation in porous DPF units. In section one, sound and waves and their properties, constructions, velocities, and types are discussed, in addition to the wave equation. After that some wave propagation quantities are discussed including wave propagation constant (which includes attenuation and phase shift) and which is determined later for both four-port and six-port models. Another acoustical quantities described here include shear wave number, reverberation time, noise reduction factors, anechoic termination, transmission losses, acoustic impedance of DPF unit, and pressure drop model...etc.

5.2 Waves

One of the simplest ways to demonstrate wave equation is to take the loose ends of a long rope (string) which is usually fixed at the other end and to move the loose end quickly up and down. Crests and troughs of the waves move down the rope, and if the rope were infinitely long such waves would be called progressive waves which is defined as the waves traveling in an unbounded medium free from possible reflexion, see figure (5) below.

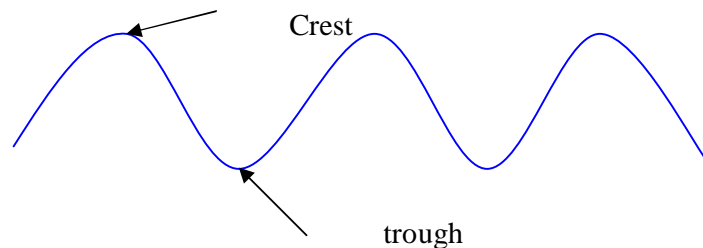


Figure (5) progressive transverse waves moving along a string.

Waves on strings are transverse waves where the displacements or oscillations in the medium are transverse to the direction of wave propagation. When the oscillations are parallel to the direction of wave propagation the waves are longitudinal. Sound waves are longitudinal waves; a gas can sustain only longitudinal waves because transverse waves require a shear force to maintain them. Also both transverse and longitudinal waves can travel in a solid. If the wave motion is seen to be as in a series of crests and troughs it can be described as a vibrational oscillator in a plane of the medium which at the instant of observation, have the same phase in their vibrations. If a plane perpendicular to the direction of wave propagation and all oscillators lying within that plane have a common phase is taken, then it can be observed that with time how that plane of common phase progresses through the medium.

5.2.1 Velocities in wave motion

There are three velocities in wave motion

- 1) The particle velocity, which is the simple harmonic velocity of the oscillator about its equilibrium position.
- 2) The wave or phase velocity, the velocity with which planes of equal phase, crests or troughs, progress through the medium.
- 3) The group velocity. A number of waves of different frequencies, wavelengths and velocities may be superposed to form a group.

5.2.2 The wave equation

It is an equation that relates the displacement y of a single oscillator to distance x and time t . The mass of the uniform string per unit length or its linear density is ρ , and a constant tension T_e exists throughout the string although it is slightly extensible. Wave equation for the string is a second order differential equation which can be simply written as

$$\frac{\partial^2 y}{\partial x^2} = \frac{r}{Te} \frac{\partial^2 y}{\partial t^2} \quad (5.1)$$

The quantity $(Te/ \rho)^{0.5}$ is called the wave or phase velocity (c), this velocity also represents the velocity with which planes of common phase are propagated. In the case of string the velocity arises as the ratio of the tension to the inertial density of the string. It is obvious that wave equation relates the acceleration of a simple harmonic oscillator in the medium to the second derivative of its displacement with respect to its position, x , in the medium. While the wave equation for a beam is of 4th order equation, Pain (1989).

5.2.3 Sound waves in gases

sound is a wave-type phenomenon by which vibrational energy is propagated through elastic media or it can be defined as a disturbance that propagates through an elastic medium at a speed characteristic of that medium. Sound can propagate gases, liquids ,and solids, but it cannot propagate in vacuum. Normally, two types of waves can be generated in an elastic medium: transverse waves and longitudinal. Shearing forces are required to cause motion of particles transverse to the direction of particles of wave propagation. Hence, transverse waves are sometimes referred to as shear waves. On the other hand, normal forces, or pressure, are required to cause motion of particles in the direction of wave propagation, and for this reason longitudinal waves are sometimes called pressure waves. A viscous fluids such as water, can sustain both shearing and compression forces, so that both types of waves exist for sound in water. However, gases can sustain very little shearing forces, so that sound propagation in air is predominantly the result of pressure waves.

Sound waves are considered as longitudinal waves and also they described as pressure waves as mentioned above. If there is a fixed mass of gas, at a pressure P_0 occupies a volume V_0 with a density ρ_0 . These values define the equilibrium state of the gas which

is distributed, or deformed, by the compressions and rarefactions of the sound waves.

Under the influence of the sound waves it assumed that

$$P = P_0 + P \quad (5.2a)$$

$$V = V_0 + V \quad (5.2b)$$

$$\rho = \rho_0 + \rho_d \quad (5.2c)$$

$$u = u_x + U_0 \quad (5.2d)$$

where

P_0 : is the ambient pressure

V_0 : is the original volume

ρ : is the gas density

ρ_d : is a density small change

u_x : is the particle (acoustic) velocity

U_0 : is the mean flow velocity.

This means that if there is a sound waves enters a medium filling by some gas the volume, density of this gas, pressure, and velocity of sound waves will be changed too, and a transferring for these waves is taking on as shown in the following figure which represented the DPF case

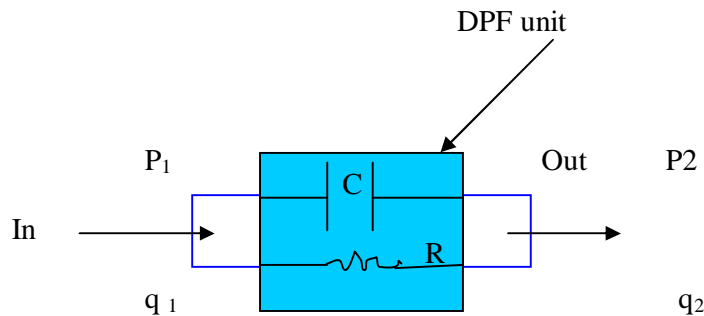


Figure (6) sound waves transferring through DPF unit (four- port model), and shows a DPF unit as a resistive and capacitive element.

From last figure the transferring operation can be represented in the form of matrices such that

$$\begin{bmatrix} p_1 \\ q_1 \end{bmatrix} = \begin{bmatrix} A & B \\ C & D \end{bmatrix} \begin{bmatrix} p_2 \\ q_2 \end{bmatrix} \quad (5.3)$$

where

$\begin{bmatrix} A & B \\ C & D \end{bmatrix}$: is called the transfer matrix (some times called ABCD matrix) which played

an important role in calculating the transmission losses in sound waves. Sound waves propagation has many characteristics as it would be explained below.

5.2.4 Sound Fields

sound has been defined as vibrations in an elastic medium. If a fluctuating disturbance is created at some point in an elastic medium, the vibrational energy (sound) generated at this point will spread as waves to fill the surrounding medium. The fluctuating mechanism causing the disturbance is called sound source, and the resulting disturbance in the medium is called the sound field. To get a complete description for the sound field it is necessary to know the sound-pressure level at any point in the field. The basic instrument used to evaluate sound field is the sound –level meter, which obtains a quantitative measure of the effective root-mean-square sound pressure at any point in the field. This quantity can be related to the sound intensity, I , at the point under certain conditions, such that:

$$I = P\bar{u} = \frac{P_{rms}^2}{r_0 C_0} \quad (5.4)$$

where

P_{rms} : is the root-mean-square value of the acoustic pressure= $P_{max}/ 2^{0.5}$

ρ_0 : is the constant equilibrium density;

u : is the particle velocity in x-direction, Lord (1980).

As the acoustic wave propagates outwards from the source the intensity of the signal is reduced with increasing range due to:

-spreading

-attenuation.

5.3 Propagation Constant " G ", and Sound Attenuation

Waves have many characteristics which help in studying them and building the acoustics model and determining the acoustic impedance for the DPF unit. It is very important to find the propagation constant for sound waves propagate in DPF unit, because these propagation constants represent the eigenvalues and for each of them there is an eigenvector which can be used later to find the transfer matrix, "S-matrix".

-propagation constant " G "

The axial acoustic wave motion has been assumed to have a complex propagation constant " Γ ", which can be expanded as:

$$G = G' + iG'' \quad (5.5)$$

Where G' represents the wave attenuation and iG'' represents the phase shift.

Attenuation " G' "

Attenuation also refers to the decrease in sound pressure levels between two points. However attenuation is more commonly used for describing the acoustical properties of heating, ventilation, DPF, and air condition ducts lined with sound absorbing materials. Attenuation is the real part of wave propagation constant and it can be reported in decibels per unit length of ducts.

-Phase shift " iG'' "

The Imaginary part of the propagation constant represents the phase shift of the sound wave. This part is in general proportional to the shear and bulk viscosity coefficients and the heat conduction coefficient.

-shear wave number

The shear wave number is a measure for the ratio between inertial and viscous effects.

A low shear wave number indicates that the viscous effects are dominant, whereas for high shear wave numbers the inertial effects dominate, Seto (1971).

5.4 Pressure Drop Model

The pressure drop in DPF unit, Δp , Can be written as a function of velocity and filter resistances as (Allam (2005))

$$DP = R_1 U + R_2 U^2 \quad (5.6)$$

where

U: is the axial mean flow speed

R_1 : is the viscous flow resistance which can be written as

$$R_1 = \eta m \Gamma_g \frac{L}{d_h^2} \quad (5.7)$$

While R_2 : is the second order flow resistance which can be given as

$$R_2 = 0.5 Y r_g T_g \quad (5.8)$$

where

η : is some constant [-]

μ : is the dynamic viscosity [kg/(m s)]

T_g : is the gas temperature [K]

L: is the length of catalyst [m]

d_h : is the hydraulic diameter of the substrate [m]

Y: is the resistance coefficient of the substrate [-]

ρ_g : is the gas density [kg/m³]

For this model a pressure drop coefficient K can be calculated such that

$$K = \frac{\Delta P}{0.5 r U^2} \quad (5.9)$$

where K is dependent on the open area ratio and Reynolds number which can be written as

$$\text{Re} = \frac{U d r}{mS} \quad (5.10)$$

where

σ : is the open area ratio.

d: is the diameter of the cavity.

5.5 Reverberation and Noise Reduction

Reverberation is the persistence of sound in an enclosure as the result of continuous reflection of sound at the walls after the sound source has been turned off. The reverberation time is the time required for the sound intensity level to decay 60 dB of the room. The reverberation time (T_{60}) is the single most important parameter used to judging the acoustical propagation of a room. If T_{60} is large (i. e., it takes many reflections to absorb the acoustical energy), there will be a large buildup of sound in the room. Two factors influence the reverberation time of an enclosure: the total room absorption α_s and the room volume V. If α_s is increased, more sound is absorbed with each reflection, resulting in a shorter time for sound decay and less sound buildup. Similarly if the volume of the room is decreased, the sound doesn't have to travel as far between absorptive reflections, resulting in a shorter reverberation time and less sound buildup. T_{60} can be given as:

$$T_{60} = \frac{KV}{A} \quad (5.11)$$

where:

K: is a constant of proportionality;

V: is the enclosure volume;

A: is the total absorption of the room.

As resonant free vibration with damping, reverberation depends on the size and shape of the enclosure as well as the frequency of the sound. Reverberation time T_{rev} at a

specific frequency is the time in seconds for the sound pressure to decrease to 10^{-6} of its original value (or 60 dB drop) after the source is turned off. i.e.

$$T_{Rev} = 0.161 V/a \quad (5.12)$$

where

V: is the volume of the enclosure in (m^3)

α : is the total sound absorption factor of the enclosure in (metric sabins) or sabins.

Equation (5.12) is valid for the decay of diffuse sound field in a rather live room, say , $\alpha \leq 0.2$. For large absorption rooms for example $\alpha = 1$, all the sound would be absorbed on the first reflection, implying reverberation time of zero. In such rooms assume that a diffuse sound field has been built-up in a room and that its initial intensity is I_0 at the time the source is shut off. The intensity of the sound energy absorbed by the first reflection on all surfaces of the room would be $I_0 \alpha$. Hence, after the first reflection the intensity of the sound energy remaining in the room would be $I_1 = I_0 (1 - \alpha)$. Similarly, after two reflections the intensity is $I_2 = I_0 (1 - \alpha)^2$ and after n reflections, $I_n = I_0 (1 - \alpha)^n$, so from definition of T_{rev} :

$$\frac{I_{60}}{I_0} = \frac{I_n}{I_0} = (1 - \alpha)^n = 10^{-6} \quad (5.13)$$

the sound wave will travel in the room between successive reflections a distance d, which is called the mean free path, which can be defined as

$$d = \frac{4V}{S} \quad (5.14)$$

where

V: is the total volume;

S: is the surface area of the room.

The time required for n reflections will be given as

$$T_{60} = \frac{nd}{C} = \frac{4Vn}{SC} = -\frac{0.161V}{S \ln(1-a)} \quad (5.15)$$

this equation gives a reverberation time of zero for room average source absorption coefficient of unity, Lord (1980).

If reverberation time is too short, the sound may not be sufficiently loudness in all portions of the enclosure (DPF) unit. If it is too long, echoes will be present. Short reverberation time decreases sound intensity in the enclosure, Seto (1971).

To establish the noise reduction coefficient, to test the sound control efficiency of materials and structures. The growth of sound intensity in a reverberation chamber is given by:

$$I(t) = \frac{w}{a} (1 - e^{-ac/4V}t) \quad (5.16)$$

while decay of intensity is given as:

$$I(t) = 1/4E_0 C e^{-(ac/4V)t} \quad (5.17)$$

where

w : is the sound power output in (watt).

α : is the total sound absorption in metric sabins.

C : is the speed of sound (m/s).

V : is the volume of the DPF unit. (m^3).

E_0 : is the Sound energy density Joul/m³.

a : is the channel width.

t : is the time.

-Noise Reduction and Insulation

Machine Noise generally indicates poor balance, excessive clearance, turbulent flow or other improper working of some components of the machine. Most machine noises can be reduced and attenuated by proper redesign or using sound proofing enclosures lined with absorptive materials. Acoustical filters such as mufflers, catalytic converters,

sound traps, and DPF units should be employed wherever necessary. Impact noise can be reduced by using some equipment, It is necessary to calculate space average sound pressure level L_s such that:

$$L_s = 10 \log \frac{P_1^2 + P_2^2 + \dots + P_n^2}{nP_0^2} \quad (5.18)$$

where

$p_0 = 2 \times 10^{-5}$ (Pa) is the reference sound pressure

$p_1, p_2 \dots p_n$ is the Sound pressures in (Pa), Seto (1971).

n : is the number of sound pressure sources.

5.6 Sound Absorption and Speed of Sound

5.6.1 Sound Absorption

Sound absorption is a process in which energy of sound is converted partly into heat by frictional and viscous resistance of the pores of acoustical materials like porous materials (DPF unit) and partly into mechanical vibration of the materials. There are many types of equipment to absorb sound such as Helmholtz resonators and resonator-panel absorbers which are considered as efficient tools for sound absorption at their resonant frequencies. Mufflers and DPF impede the transmission of sound but permit the free flow of air.

The sound absorption coefficient α of a material is defined as the decimal fraction of perfect absorption that it has, e.g. $\alpha=0.6$ means 60% absorption. It is the efficiency of a material in absorbing sound energy at a specified frequency, and varies with the angle of incidence and the thickness of the material, also $\alpha_{\text{space}} = 1$.

Absorption coefficient (α) is obtained by statistically averaging the ratio of absorbed to incident energy over all possible angles of incidence. The average sound absorption coefficient α' is determined by averaging the absorption coefficient over all the absorbing areas. Also α' can be given as

$$a' = \frac{\sum_i^n a_i S_i}{S} \quad (5.19)$$

where

S_i : is the area of the source;

S : is the total surface of the room.

n : is the total number of the absorption surfaces in the room.

In general when sound is impinges on a wall, some of the acoustical energy will be reflected (r), some will be absorbed, and some will be transmitted (t) by the wall. Sound absorption coefficient α_{abs} can be defined as

$$a_{abs} = \frac{I_i - I_r}{I_i} \quad (5.20)$$

Transmission coefficient α_{Tran} can be defined as:

$$a_{Tran} = \frac{I_t}{I_i} \quad (5.21)$$

5.6.2 Speed of sound

The speed of sound is the speed of propagation of sound waves through the given medium. The speed of sound in air can be given as

$$C = \sqrt{\gamma P / \rho} \quad (5.22)$$

where

γ : is the ratio of the specific heat of air at constant pressure to that at constant volume.

P : is the pressure in (pa).

ρ : is the density in kg/m^3 .

At room temperature and standard atmospheric pressure, the speed of sound in air is 343.3m/s and increases approximately 0.6 m/sec for each degree centigrade rise. The speed of sound in air is independent of change in barometric pressure, frequency and wavelength but it is directly proportional to absolute temperature (T) i.e.

$$\frac{C_1}{C_2} = \sqrt{T_1/T_2} \quad (5.23)$$

where

C_1 : is the speed of sound at temperature T_1

C_2 : is the speed of sound at temperature T_2

The speed of sound in Solids having large cross- Sectional area is given by:

$$C = \sqrt{\frac{e(1-y)}{r(1+y)(1-2y)}} \quad (5.24)$$

where

ϵ is she young's modulus of elasticity.

Y : is the Poisson's ratio.

ρ : is the density in kg/m^3 .

The speed of sound, C , in fluids can be written as

$$C = \sqrt{B'/r} \quad (5.25)$$

where

B' is the bulk modulus (pa)

5.7 Anechoic Termination

Anechoic Termination is characterized by highly absorptive wedges or long pyramids mounted to the walls of the room (DPF) to absorb all incident sound energy. It simulates a free field or unbounded space. See fig (7) which represents the anechoic termination.

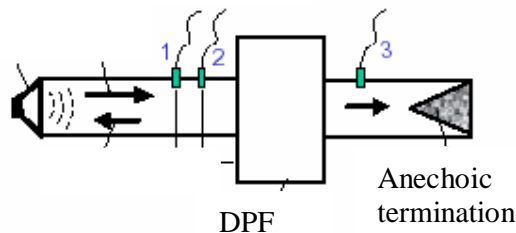


Figure (7) Anechoic Termination, (source: Tao (2001)).

The decay of sound intensity in an anechoic termination is given by

$$I(t) = I_0 e^{(AC/AV)(1-\alpha')t} \quad (5.26)$$

where

I_0 : is the sound intensity in watts/m² when the source shut off

A: is the total area of wall in m²

V: is the volume of DPF unit

α' : is the average sound absorption coefficient, Seto (1971).

An anechoic sound field is one that is "without echoes" or reflections. However, anechoic (free-field) conditions can be approached if the back ground levels resulting from reflected sound are sufficiently low. In an anechoic chamber the walls of the room are designed to be almost 100% absorptive from a specified range of frequencies, and free-field conditions exist nearly to the boundaries of the room. Thus, it is possible to determine the directional properties and the sound power of a noise source in an anechoic room by taking a number of sound-level measurements in the far field surrounding the source. Two types of anechoic tests chambers are commonly used; the fully anechoic room has a highly absorbent material on all of its interior surfaces, including the floor, while the semi-anechoic chamber has a hard floor. The high degree of absorption of anechoic termination is achieved through the use of porous wedge at the walls of the room (as in DPF unit).

5.8 Acoustics Impedance

-Specific Acoustic Impedance

Specific acoustic impedance Z of a medium is defined as the ratio (real or complex) of sound pressure to particle velocity

$$Z = P/U \quad (5.27)$$

where:

$P=A+B\angle \theta$, is the acoustic pressure amplitude at the termination, obtained by vector combinations of incident and reflected sound-waves amplitudes.

$U= A-B\angle \theta/\rho c$ is the net particle-velocity amplitude at the termination, obtained by vector summation of particle velocities associated with incident and reflected sound waves.

$\angle \theta$ is the phase angle between incident and reflected sound waves.

A, B : are some constants.

For harmonic plane acoustic waves traveling in the positive x direction the acoustic impedance can be given as

$$Z = \frac{-rCwA}{-wA} = rC \quad (5.28)$$

and in negative x - direction

$$Z = \frac{-rCwA}{wA} = -rC \quad (5.29)$$

ρC is known as the characteristic impedance or resistance of the medium in (rayls).

For air (as an example) at 20°c , $\rho= 1.21 \text{ kg/m}^3$, $C=343.3\text{m/s}$, give the air impedance as $Z = 415 \text{ rayls}$.

For standing waves, the specific acoustic impedance will vary from point to point in the x - direction. In general, it is a complex value such that:

$$Z = r + i y \quad (5.30)$$

where

r is the specific acoustic resistance.

y is the specific acoustic reactance.

The real part of this impedance will reflect flow induced losses and the imaginary part contains effects of non-propagating acoustic modes (the "end correction").

-Sound Measurements

Because of the very wide range of sound power, intensity and pressure encountered in our acoustical environment, it is customary to use the logarithmic scale known the decibel Scale (dB) to describe these quantities, i.e. to relate the quantity logarithmically to some standard reference. Decibel (dB) is a dimensionless unit for expressing the ratio of two powers, which can be acoustical, mechanical, or electrical. The number of decibels is 10 times the logarithm to the base 10 of the power ratio.

Four things should be kept in mind when expressing sound levels in decibels:

- level indicates the logarithmic ratio of power-related quantities (W, I, and P).
- the decibels is defined as 10 times the logarithm (base ten) of this ratio.
- the level expressed in decibels always implies a reference quantity.
- level is a dimensionless quantity, Lord (1980).

One bel is equal to 10dB. The sound power level PWL is defined as

$$PWL = 10 \log W/W_0 \quad (5.31)$$

where

W : is the power in watts

W_0 : is the reference power = 10^{-12} watt

According to this sound power level can be written as

$$PWL = (10 \log W + 120) \quad (5.32)$$

The acoustical power radiated by a large rocket for example, is approximately 10^7 watts or 120 dB, while for soft whisper, it's 10^{-10} watts or 20 dB, Seto (1971).

Sound intensity level IL is defined as

$$IL = 10 \log (I/I_0) \quad (5.33)$$

where

I_0 : is the sound intensity reference = 10^{-12} watts/m²

Another quantity that is sound pressure level SPL which is defined as:

$$SPL = 20 \log (P/P_0) \quad (5.34)$$

where

P_0 is the Sound pressure reference= 0.00002 Pa, so

$$SPL=(20 \log P + 94) \text{ dB} \quad (5.35)$$

5.9 Predicted damping for a DPF at operating conditions (hot conditions).

For clean filters and without soot loading DPF's wall resistance, R_w , can be written as (Allam (2005))

$$R_w = \frac{m_w h_t}{S_w} \quad (5.36)$$

While with soot loading (not clean) DPF unit the wall resistance can be written as:

$$R_w = m_w \left(\frac{h_t}{S_w} + \frac{h_{soot}}{S_{soot}} \right) \quad (5.37)$$

where

$\sigma_{soot} = 1.5 \times 10^{-14}$ (permeability with soot)

$h_{soot} = 1/10 h_t$

h_t is the wall thickness.

5.10 Characterization of DPF Performance

-Transmission losses (TL)

It is the difference between the sound power incident on the DPF unit and that transmitted down stream into an anechoic termination. It can be given as

$$TL = 10 \log (W_i/W_t) \quad (5.38)$$

Where

W_i : is the incident power in watts

W_t : is the transmitted power in watts.

For DPF unit transmission losses can be given as

$$TL = 20 \log (0.5 |T_{DPF}|) \quad (5.39)$$

where

T_{DPF} is the transformation matrix of the DPF unit.

-Noise Reduction factor NRF

Noise reduction factor is the difference in sound pressure levels LP at two arbitrary selected points in the exhaust pipe and tail pipe. It doesn't need or require an anechoic termination because it uses the standing wave pressures, Seto (1971).

Depending on noise reduction factor definition it can be given as

$$NRF = LP_2 - LP_1 = 20 \log \frac{P_2}{P_1} \quad (5.40)$$

NRF is an efficient tool to distinguish between different types of DPF which can be rewritten as

$$NRF = TL + 10 \log \left(\frac{\alpha}{A} \right) \quad (5.41)$$

where

A: is the area of the partition. (m²)

TL: is the transmission loss;

α : is the sound absorption factor.

These two quantities (TL and NRF) will be used to compare between different types of DPF unit.

- insertion loss

insertion loss is defined as the difference between the sound power levels, Lw, radiated without any filter (W1) and that with a filter (W2). Mathematically IL in dB can be expressed as:

$$IL = Lw_1 - Lw_2 = 10 \log W_1/W_2 \quad (5.42)$$

5.11 Noise and Noise Control

Noise is defined as unpleasant or unwanted sound. Technically noise is the combined result of single-frequency sound or pure tones, and has essentially a continuous frequency spectrum of irregular amplitudes and waveform. Air borne noise is due to the

fluctuations of air pressure about the mean atmospheric pressure, structural-borne noise results from mechanical vibrations of elastic bodies, and liquid-borne noise is caused by pulsation of liquid pressure about the mean static pressure. Ultrasound is noise of frequency greater than 20 kHz while infrasound is noise of frequency less than 20Hz. Noise causes both strain and fatigue, loss of appetite and indigestion, irritation and headache, Seto (1971). The noy has been suggested as a possible acoustic unit to rank and compare the noisiness or annoyance of noises as the ear hears them.

Chapter 6

Time Domain DPF Acoustical Model (Four-Port Model)

6.1 Introduction

The problem of sound propagation in gas-filled rigid porous media is studied; it can be characterized by a complex-valued gas density and complex-valued gas incompressibility. These two so-called scaling functions are frequency-dependent and governed by the geometry of the pore structure. The former function describes the inertial and viscous interactions between the gas and the pore space, and the latter one describes the heat exchange effects between the two domains.

Assuming wide separation between the characteristic pore size and the wavelength, i.e., between the microscopic and the macroscopic length scales, the porous medium can be characterized by several measurable quantities, like the porosity ϕ , the viscous and thermal permeabilities σ_0 and σ_1 , and the viscous and thermal length scales Λ and Λ' . These are called the macroscopic pore properties, determining the scaling functions. In porous materials (fibrous and granular), the absorption process of the acoustic waves takes place through viscosity and thermal losses of the acoustic energy inside the micro tubes forming the material. This kind of material is widely used in room acoustics, in order to control reverberation time, to avoid undesired reflections, to fill double wall cavities, floors and ceilings, and exhaust gases emission reduction devices (DPF) units etc.

Usually it is assumed that the material has a rigid frame and the fluid filling the medium inside the pores can be considered as homogeneous, with complex frequency dependent characteristic impedance, Z , and a propagation constant, k . The thermo viscous effects in the fluid filling interstices among the fibers or the particles are responsible for the

energy loss of the propagating acoustic wave. Generally, thermal losses are much lower than viscous losses in this kind of material.

A more sophisticated approach is to perform an analysis of wave propagation in an idealized microstructure corresponding to the form of real materials. For a model of identical, parallel, cylindrical pores, in a rigid frame, there are two distinct methods of analysis: one of which is based upon the idea of a complex or frequency-dependant density for the air within the pores. The other method introduces the idea of a frequency-dependant viscosity operator.

Many theories of acoustical wave propagation in porous media are evolved from an initial conceptual model of a medium containing identical parallel cylindrical capillary pores running normal to the surface. In this thesis there will be more focus on the capillary pore approach for a medium. The frame of which is assumed to be rigid, and an interest with a statement of the results of an analysis of wave motion in a single capillary pore and a consideration for viscous and thermal effects will be taken into accounts. Zwikker and Kosten theory : (Allam (2006)) have showed that, at least in the limiting cases of low and high frequency, such independent treatments give the correct results for motion in a viscous, conducting fluid contained within a cylindrical channel, when expressed in terms of a complex density and a complex incompressibility. As they point out, given this results, there is considerable merit (from the point of view of simplicity of derivation), in stating only the independent treatments.

In the following sections there will be a description for the physical model, the derivation of governing equations from basic equations (momentum, energy ,and continuity) , the continuity equation is also written in average form and some results from solving both momentum and energy equations, and from state equations with the help of Darcy's equation are substituted in the average form of continuity equation to

get the final tractable linear partial differential equations (by making some complicated mathematical operations), which will be solved by helping of Fourier sinus series to find the propagation constants, and other needed quantities.

6.2 Derivation of the Governing Equations

6.2.1 Physical Model

Figure (8) below shows obviously how DPF works, and it can be noticed that the started flow is in x-direction, but after it enters the filter it was forced to go transversely in y-direction, hence the flow is 2-D.

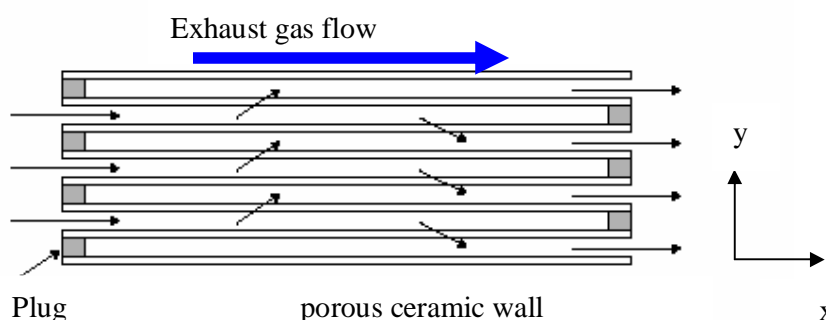


Figure (8) Exhaust emission motion in DPF unit (Muter (1998)).

The DPF may be manufactured from different materials (Cordierite or Silicon Carbide for example) and in its most common form consists of a substrate of narrow channels in which each channel is blocked at one end. Adjacent channels have this blockage at alternate ends with this construction exhaust gas may enter at one end, but must pass through the permeable wall of a channel before exiting and is thus termed a wall flow device, Mutter (1998). From this it is clear that the flow in y-direction has a considerable effect i.e. the transverse velocity has a vital role and it has an affect in the form of making the problem like as a 2-D problem.

The structure of diesel particulate filler (DPF) cells will be considered approximately square in the cross-section with a usual width of (1-2) mm. To develop an acoustic model for the sound propagation in DPF unit after it is connected

on the exhaust pipe, the knowledge of the propagation constant for two neighboring cells in the filter is required see fig (9). To derive the governing equations that describe behavior of sound propagation in the filter and which will help in controlling noise and vibration of the exhaust pipe after DPF unit is connected, the following assumptions are to be taken into account:

- The axial mean flow velocity is taken into account.
- DPF unit will be considered partially filled with porous media-Darcy's equation applied.
- The transverse “normal” component of velocity (v) will not be neglected i.e. the model will be treated as a 2-D model.
- Flow in porous DPF unit will be considered as viscous-thermal flow, incompressible, laminar ($Re=0.408$, see chapter 3), a steady (axial mean flow) and Newtonian ideal gas flow.
- Chemical reactions are neglected.

As shown in figure (9) DPF unit will be split into five areas each described by an acoustic two- port and each one has an acoustic impedance to be calculated, and depending on

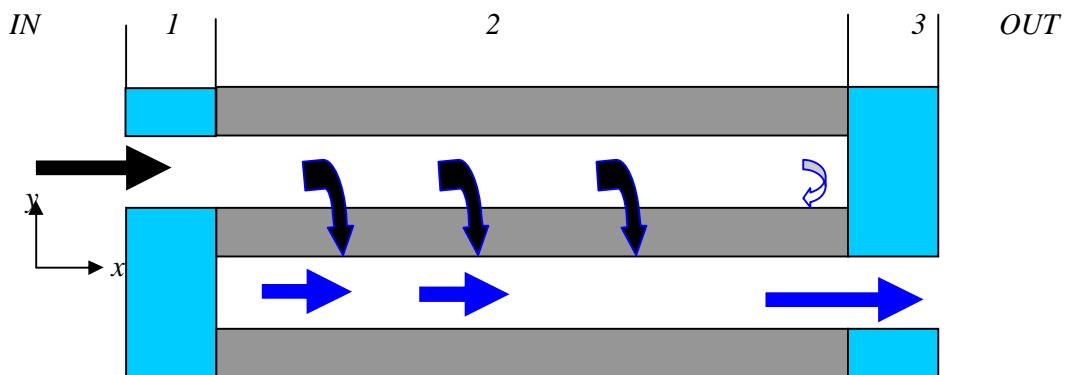


Figure (9) DPF sections and the 2D flow of gases.

this splitting of DPF unit the transfer matrix for filter unit is then can be written as

$$T_{DPF} = T_{IN} T_1 T_2 T_3 T_{out} \quad (6.1)$$

6.2.2 Governing Equations Derivation

The propagation of sound is always associated with a medium; sound does not propagate in a vacuum. Sound is generated when the medium is dynamically disturbed. Such disturbance of the medium affects its pressure, density, velocity, and temperature. Thus the vibrations are defined as sound and usually they are longitudinal waves or vibrations, i.e., the particles move in the direction of propagation of the sound waves. The relative displacement of the particles within the sound wave generates a small change of pressure, density, temperature, and also the particles velocity as mentioned above in chapter 5, equation (5.2a, b, c, d). The total particle velocity of gases flow through the DPF unit can be given as

$$u = u_{xj} + U_{0j} \quad (6.2)$$

Where

u_{xj} : is the acoustic particle velocity;

U_{0j} : is the axial mean flow velocity.

To derive the governing equations the following linearized conservation of Navier – Stokes (momentum) equations, continuity equation, and energy equation, are simplified in the manner appropriate for narrow pipes see Allam (2006), and Dokumaci (2001).

Navier -Stokes equation in general is given as:

$$r_{0j} \left[\frac{\partial \mathbf{u}}{\partial t} + \mathbf{u} \cdot \nabla \mathbf{u} \right] = -[\nabla P]_i + m[\nabla^2 u_{xj}]_i \quad (6.3)$$

This equation can be expanded in both x and y directions such that:

In x-direction (assume no axial mean flow speed in y-direction, i.e $V_{0j}=0$):

$$r_{0j} \left[\frac{\partial u}{\partial t} + u \frac{\partial u}{\partial x} + v_{yj} \frac{\partial u}{\partial y} + w_{zj} \frac{\partial u}{\partial z} \right] = -[\nabla P]_i + m[\nabla^2 u_{xj}]_i \quad (6.4)$$

In y-direction

$$r_{0j} \left[\frac{\partial v}{\partial t} + u_{xj} \frac{\partial v}{\partial x} + v_{yj} \frac{\partial v}{\partial y} + w_{zj} \frac{\partial v}{\partial z} \right] = -\frac{\partial P_j}{\partial y} + m_j \left(\frac{\partial^2 v_{yj}}{\partial x^2} + \frac{\partial^2 v_{yj}}{\partial y^2} + \frac{\partial^2 v_{yj}}{\partial z^2} \right) \quad (6.5)$$

Now by substituting equation (6.2) in equation (6.4) yields

$$r_{0j} \left[\frac{\partial(u_{xj} + U_{0j})}{\partial t} + ((u_{xj} + U_{0j})\hat{i} + v_{yj}\hat{j} + w_{zj}\hat{k}) \cdot \left(\frac{\partial u}{\partial x} \hat{i} + \frac{\partial u}{\partial y} \hat{j} + \frac{\partial u}{\partial z} \hat{k} \right) \right] = -[\nabla P]_i + m[\nabla^2 u_{xj}]_i \quad (6.6a)$$

Equation (6.6a) can be written as:

$$r_{0j} \left[\frac{\partial u_{xj}}{\partial t} + \frac{\partial U_{0j}}{\partial t} + u_{xj} \frac{\partial u_{xj}}{\partial x} + U_{0j} \frac{\partial u_{xj}}{\partial x} + v_{yj} \frac{\partial u_{xj}}{\partial y} + w_{zj} \frac{\partial u_{xj}}{\partial z} + u_{xj} \frac{\partial U_{0j}}{\partial x} + U_{0j} \frac{\partial U_{0j}}{\partial x} + v_{yj} \frac{\partial U_{0j}}{\partial y} \right] = -[\nabla P]_i + m[\nabla^2 u_{xj}]_i \quad (6.6b)$$

By making the following assumptions:

-Steady axial mean flow, i. e. $\frac{\partial U_{0j}}{\partial t} = 0$,

- $\frac{\partial u_{xj}}{\partial y}$ is neglected –no change in x component velocity in y-direction.

- $u \frac{\partial u}{\partial x}$, and $U_{0j} \frac{\partial U_{0j}}{\partial x}$: are very small quantities to be neglected depending on both

Dokumaci(2001) and Allam(2006) by the usual process of linearization. Both of them applied an order magnitude analysis, in the manner of Zwicker and Kosten theory: in order to dispense with the dual terms. $u \frac{\partial u}{\partial x}$, and $U_{0j} \frac{\partial U_{0j}}{\partial x}$: are assumed to be neglected since these terms are arising from the extreme difference in length and velocity scales in axial and transverse directions, and also all approximated works treated such problems neglected them to simplify the linearized equations into a mathematically tractable form.

- $w \frac{\partial u}{\partial z}$: is neglected (2-D problem).

By taking into account last assumptions, substituting equation (6.2) and by rearranging equation (6.6b) yields

$$r_{0j} \left[\frac{\partial u_{xj}}{\partial t} + u_{xj} \frac{\partial U_{0j}}{\partial x} + v_{yj} \frac{\partial U_{0j}}{\partial y} \right] + r_{0j} U_{0j} \frac{\partial u_{xj}}{\partial x} = -\frac{\partial P_j}{\partial x} + m_j \left(\frac{\partial^2 u_{xj}}{\partial x^2} + \frac{\partial^2 u_{xj}}{\partial y^2} + \frac{\partial^2 u_{xj}}{\partial z^2} \right) \quad (6.7)$$

where

$r_{0j} \frac{\partial u_{xj}}{\partial t}$: represents the local inertial term.

$r_{0j} \frac{\partial u}{\partial x}$: represents the axial variation of particle velocity.

$m \frac{\partial^2 u}{\partial x^2}$: represents the viscous forces effects.

$\frac{\partial P}{\partial x}$: represents the axial pressure drop.

Expanding equation (6.5) in y – direction and assuming that ($v=v_{yj}+V_{0j}$) and taking into accounts the same assumptions in x-direction leads to:

$$r_{0j} \left[\frac{\partial v_{yj}}{\partial t} + u_{xj} \frac{\partial V_{0j}}{\partial x} + v_{yj} \frac{\partial V_{0j}}{\partial y} + w_{zj} \frac{\partial V_{0j}}{\partial z} \right] + r_{0j} V_{0j} \frac{\partial v_{yj}}{\partial y} = - \frac{\partial P_j}{\partial y} + m_j \left(\frac{\partial^2 v_{yj}}{\partial x^2} + \frac{\partial^2 v_{yj}}{\partial y^2} + \frac{\partial^2 v_{yj}}{\partial z^2} \right) \quad (6.8)$$

-in this case and under the last mentioned assumptions Continuity equation can be written as(Dokumaci (2001) and Allam(2006)):

$$\frac{\partial r_j}{\partial t} + u_{xj} \frac{\partial r_{0j}}{\partial x} + U_{0j} \frac{\partial r_j}{\partial x} + r_j \frac{\partial U_{0j}}{\partial x} + r_{0j} \nabla \cdot u_j = 0 \quad (6.9)$$

Energy equation can be written as

$$r_{0j} C_{pj} \left[\frac{\partial T_j}{\partial t} + U_{0j} \frac{\partial T_j}{\partial x} + u_{xj} \frac{\partial T_{0j}}{\partial x} \right] + r_j C_{pj} U_{0j} \frac{\partial T_{0j}}{\partial x} = - \frac{\partial P_j}{\partial t} + U_{0j} \frac{\partial P_j}{\partial x} + \frac{\partial P_{0j}}{\partial x} u_{xj} + K_{thj} \nabla_s^2 T_j \quad (6.10)$$

where:

T_j : represents the temperature fluctuations;

T_{0j} : is the ambient temperature.

State equation:

The gasses emission upon the exhaust pipe will be considered as an ideal gas, so

$$r_j = \left(\frac{p_j}{R_j T_{0j}} \right) - \left(\frac{r_{0j} T_j}{T_{0j}} \right), \quad r_j = r_j(x, y, z, t). \quad (6.11)$$

where

$$\begin{aligned}
r_j &= r_j(x, y, t) \\
T_j &= T_j(x, y, z, t) \\
P_j &= P_j(x, y, t)
\end{aligned}
\tag{6.12}$$

In all last equations, x, y denotes the channel axis, u_{xj}, v_{yj} are the acoustic particle velocities, $j = 1, 2$ represent the inlet and outlet pipes, respectively, p, T and ρ are the acoustic pressure, temperature and density, respectively, μ is the shear viscosity coefficient, k_{th} is the thermal conductivity of the fluid, R is the gas constant, C_p is the specific heat coefficient at constant pressure, P_0, T_0 and ρ_0 denote the ambient pressure, temperature and density, respectively, U_0, V_0 denotes the axial mean flow velocity and transverse velocity respectively, and ∇_s^2 denotes the Laplacian over the channel cross-section.

To describe the coupling between neighboring channels (which describes the porosity of diesel particulate filter) Darcy's law is applied to the fluctuating fields(in y-direction):

$$p_1 - p_2 = R_w u_w \tag{6.13}$$

where

u_w : is the acoustic velocity through the wall ;
 R_w is the wall resistance, which is given by $R_w = \mu_w h_t / \sigma_w$,
 μ_w is the dynamic viscosity,
 h_t is the wall thickness and
 σ_w is the wall permeability.

In this case Darcy's equation is applied since the DPF is considered partially porous media. Brinkman's relation (see ch.3) can be applied here, but for simplicity and since DPF is partially porous as mentioned above Darcy's relation is suitable.

The problem will be treated as a 2D problem i.e.

$$\frac{\partial U_{0j}}{\partial z} = \frac{\partial^2 U_{0j}}{\partial z^2} = \frac{\partial V_{0j}}{\partial z^2} = \frac{\partial^2 V_{0j}}{\partial z^2} = 0 \tag{6.14}$$

In order to find a solution for the acoustic model $u_{xj}, v_{yj}, P_j, \rho_j, T_j$ are considered to be varying with time only i.e. (time- harmonic variation). Such that

$$u_{xj} = A_0 e^{i\omega t} \tag{6.15}$$

$$v_j = B_0 e^{i\omega t} \tag{6.16}$$

Similarly

$$\begin{aligned} r_j &= r_0 e^{i\omega t}, \quad \text{and} \\ P_j &= P_0 e^{i\omega t}, \quad \text{and} \\ T_j &= T_0 e^{i\omega t} \end{aligned} \quad (6.17)$$

where

A_0, B_0 are some constants depend on x and y directions..

$$i = \sqrt{-1};$$

$\rho_0, P_0,$ and T_0 are ambient values of density, pressure, and temperature respectively. Also

t: is the time[s].

By differentiating all equations in (6.15), (6.16) and (6.17) with respect to time and substituting them in equations (6.4) to (6.8) yields

-Navier- Stokes equation in x-direction

$$r_{0j} \left[i\omega + U_{0j} \frac{\partial}{\partial x} \right] u_{xj} + r_{0j} \frac{\partial U_{0j}}{\partial x} u_{xj} + r_{0j} \frac{\partial U_{0j}}{\partial y} v_{yj} = - \frac{\partial P_j}{\partial x} + m_j \left(\frac{\partial^2 u_{xj}}{\partial x^2} + \frac{\partial^2 u_{xj}}{\partial y^2} + \frac{\partial^2 u_{xj}}{\partial z^2} \right) \quad (6.18)$$

-Similarly equation (6.8) becomes:

$$r_{0j} \left[i\omega + V_{0j} \frac{\partial}{\partial y} \right] v_{yj} + r_{0j} \frac{\partial V_{0j}}{\partial y} v_{yj} + r_{0j} \frac{\partial V_{0j}}{\partial x} u_{xj} = - \frac{\partial P_j}{\partial y} + m_j \left(\frac{\partial^2 v_{yj}}{\partial x^2} + \frac{\partial^2 v_{yj}}{\partial y^2} + \frac{\partial^2 v_{yj}}{\partial z^2} \right) \quad (6.19)$$

-Similarly equation (6.10) becomes:

$$\begin{aligned} r_{0j} C p_j \left[i\omega + U_{0j} \frac{\partial}{\partial x} \right] T_j + r_j C p_j \frac{\partial T_{0j}}{\partial x} u_{xj} + U_{0j} C p_j \frac{\partial T_{0j}}{\partial x} r_j = (U_{0j} \frac{\partial}{\partial x} + i\omega) P_j + \frac{\partial P_{0j}}{\partial x} u_{xj} \\ + K_{thj} \nabla_s^2 T_j \end{aligned} \quad (6.20)$$

For verification if the problem is back treated as a 1-D linear problem the equations (6.18) to (6.20) will reduces as given by Allam (2006).

To get a full description to the acoustic model of DPF unit, and then to find impedance, transmission losses, and other parameters needed, equations ((6.18) to (6.20) must be solved.

By using the following perturbations for ($T_j, P_j, u_{xj},$ and v_{yj}):

$$\begin{aligned}
P_j &= A_0 \exp(-i\Gamma k_1 x), \\
u_{xj} &= H_j(x, y, z)P_j, \\
T_j &= F_j(x, y, z)P_j, \\
v_{yj} &= H_j(x, y, z)P_j,
\end{aligned} \tag{6.21}$$

where

H_j, F_j are called dispersive functions in space.

By differentiating all terms in equation (6.21) and substituting them in equation (6.18) and (6.19) yields:

$$\begin{aligned}
r_{0j} i\omega H_j P_j + r_{0j} iU_{0j} H_j \Gamma k_1 P_j + r_{0j} \frac{\partial U_{0j}}{\partial x} H_j P_j + r_{0j} \frac{\partial U_{0j}}{\partial y} H_j P_j = i\Gamma k_1 P_j \\
+ m_j \left(\frac{\partial^2 H_j}{\partial x^2} + \frac{\partial^2 H_j}{\partial y^2} + \frac{\partial^2 H_j}{\partial z^2} \right)
\end{aligned} \tag{6.22}$$

By dividing by P_j and using the fact that:

$$\begin{aligned}
S_j^2 &= \frac{r_{0j} \omega}{m_j} \\
M_j &= \frac{U_{0j}}{C}
\end{aligned} \tag{6.23}$$

where

S_j is the shear wave number

M_j is Mach number

And by rearranging and substituting equation (6.23) in equation (6.22) the resultant becomes:

$$\frac{\partial^2 H_j}{\partial x^2} + \frac{\partial^2 H_j}{\partial y^2} + \frac{\partial^2 H_j}{\partial z^2} - i(1 - \Gamma M_j + \frac{1}{i\omega} \frac{\partial U_{0j}}{\partial x} + \frac{\partial U_{0j}}{\partial y}) S_j^2 H_j = \frac{-i\Gamma k_1}{m_j} \tag{6.24}$$

By assuming that

$$b_{xj}^2 = (1 - \Gamma M_{jx} + \frac{1}{i\omega} \frac{\partial U_{0j}}{\partial x} + \frac{\partial U_{0j}}{\partial y}) S_j^2 \tag{6.25}$$

It yields:

$$\frac{\partial^2 H_j}{\partial x^2} + \frac{\partial^2 H_j}{\partial y^2} + \frac{\partial^2 H_j}{\partial z^2} - i b_{xj}^2 H_j = \frac{-i \Gamma k_1}{m_j} \quad (6.26)$$

Similarly in y-direction equation (6.19) becomes:

$$\frac{\partial^2 H_j}{\partial x^2} + \frac{\partial^2 H_j}{\partial y^2} + \frac{\partial^2 H_j}{\partial z^2} - i b_{yj}^2 H_j = \frac{-i \Gamma k_1}{m_j} \quad (6.27)$$

where

$$b_{yj}^2 = (1 - \Gamma M_{jy} + \frac{1}{iw} \frac{\partial V_{0j}}{\partial y} + \frac{\partial V_{0j}}{\partial x}) S_j^2 \quad (6.28)$$

$M_{jy} = \frac{V_0}{C}$: is the Mach number, and

$k_1 = \frac{w}{C}$: is the wave number.

Γ : is the wave propagation constant.

Equation (6.27) is called the dispersion equation and both $H(x, y, z)$, and $F(x, y, z)$ are called dispersive functions and to be determined later in the average form.

By substituting derivation of equation (6.21) in equation (6.20) yields

$$\begin{aligned} r_{0j} C p_j i w F_j P_j - r_{0j} C p_j i U_{0j} F_j \Gamma k_1 P_j + r_{0j} C p_j \frac{\partial T_{0j}}{\partial x} H_j P_j + r_j C p_j \frac{\partial T_{0j}}{\partial x} P_j = i w P_j \\ - i U_{0j} \Gamma k_1 P_j \frac{\partial r_{0j}}{\partial x} H_j P_j + K_{thj} \left(\frac{\partial^2 F_j}{\partial x^2} + \frac{\partial^2 F_j}{\partial y^2} + \frac{\partial^2 F_j}{\partial z^2} \right) P_j \end{aligned} \quad (6.29)$$

By substituting state equation (6.11) in equation (6.29), rearranging and divided by P_j , and K_{thj} yields

$$\frac{\partial^2 F_j}{\partial x^2} + \frac{\partial^2 F_j}{\partial y^2} + \frac{\partial^2 F_j}{\partial z^2} - s_{jx}^2 F_j = s_{0jx}^2 + s_{1jx}^2 H_j \quad (6.30)$$

where

$$\begin{aligned} s_{jx}^2 &= i S_j^2 \text{Pr} \left(1 - \Gamma M_{jx} - \frac{U_{0j}}{i w T_{0j}} \frac{\partial T_{0j}}{\partial x} \right), \\ s_{0jx}^2 &= \frac{-i w}{K_{thj}} \left(1 + \frac{C p_j U_{0j}}{i w R_j T_{0j}} \frac{\partial T_{0j}}{\partial x} - \Gamma M_{jx} \right), \\ s_{1jx}^2 &= \frac{1}{K_{thj}} \left(r_{0j} C p_j \frac{\partial T_{0j}}{\partial x} - \frac{\partial P_{0j}}{\partial x} \right), \\ \text{Pr}^2 &= \frac{m_j C p_j}{K_{thj}} \end{aligned} \quad (6.31)$$

Where

Pr: is the Prandtl number.

In order to find a solution to equation in a weak (Galerkian) sense which assumes that the field is expanded in a double Fourier Sinus series such that $H_{jx}(x, y, z)$ is assumed to be just varying in other directions i.e. in y and z directions which implies that

$$\frac{\partial H_j}{\partial x} = 0, \quad \text{and} \quad \frac{\partial^2 H_j}{\partial x^2} = 0 \quad (6.32)$$

Fourier sinus series in x -direction can be written as

$$H(0, y, z) = \sum_{m,n} a_{mn} \sin \frac{m\Pi y}{2a_j} \sin \frac{n\Pi z}{2a_j} \quad (6.33)$$

Similarly in y -direction Fourier sinus series takes the form

$$H(x, 0, z) = \sum_{l,n} a_{ln} \sin \frac{l\Pi x}{2a_j} \sin \frac{n\Pi z}{2a_j} \quad (6.34)$$

where

$m, l, n=1,3,5,7,\dots$

This series included only symmetric terms since the assumed pressure distribution is symmetric over the cross-section and no slip wall Boundary conditions is satisfied by all the terms, Allam(2006).

To calculate (a_{mn} and a_{ln}) substituting the series into equation (6.24), integrate the results over the C.S and by using the orthogonality property of the terms Allam (2006). Multiplying equation (6.34) by: $\sin \frac{m\Pi y}{2a_j} \sin \frac{n\Pi z}{2a_j}$ And integrating over the cross section yields:

$$\sum_{m,n} a_{mn} b_j^2 a_{mn} (b_j a_j) I_1 = \frac{-ik\Gamma_1}{m_j} I_2 \quad (6.35)$$

where

$$a_{mn} (b_j a_j) = 1 + \frac{-\Pi^2}{4(b_j a_j)^2 (m^2 + n^2)} \quad (6.36)$$

$$I_1 = \iint_{a_j * a_j} \sin \frac{m\Pi y}{2a_j} \sin \frac{n\Pi z}{2a_j} \sin \frac{m'\Pi y}{2a_j} \sin \frac{n'\Pi z}{2a_j} dydz \quad (6.37)$$

$$I_2 = \iint_{a_j * a_j} \sin \frac{m'\Pi y}{2a_j} \sin \frac{n'\Pi z}{2a_j} dydz \quad (6.38)$$

By making last integrations when $m=m'$, $n=n'$ and $m \neq m'$, $n \neq n'$ yields (Allam (2006):

$$I_1 = \begin{cases} a_j^2, & m = m', n = n' \\ 0 & m \neq m' \\ 0 & n \neq n' \end{cases} \quad (6.39)$$

$$I_2 = \frac{16a_j^2}{m'n'\Pi^2} \quad (6.40)$$

where

m, n and m', n' are odd integers = (1,3,5.....)

By Substituting equations (6.39) and (6.40) into equation (6.35) yields

$$a_{mn} b_j^2 a_{mn} (b_j a_j) a_j^2 = \frac{i\Gamma k_1}{m_j} \frac{16a_j^2}{mn\Pi^2} \quad (6.41)$$

From equation (6.41) a_{mn} can be determined such that

$$a_{mn} = \frac{16i\Gamma k_1}{mn\Pi^2 b_j^2 a_{mn} (b_j a_j) m_j} \quad (6.42)$$

Similarly in y-direction

$$a_{ln} = \frac{16i\Gamma k_1}{nl\Pi^2 b_{jy}^2 a_{mn} (b_{jy} a_j) m_j} \quad (6.43)$$

In the same way b_{mn} , a_{mn} can be determined by assume:

$$F(0, y, z) = \sum_{mn} b_{mn} \sin \frac{m\Pi y}{2a_j} \sin \frac{n\Pi z}{2a_j} \quad (6.44)$$

And by following same procedure in y-direction

$$F(x, 0, z) = \sum_{ln} b_{ln} \sin \frac{l\Pi x}{2a_j} \sin \frac{n\Pi z}{2a_j} \quad (6.45)$$

Following same procedure in calculator a_{mn} , a_{ln} yields

$$b_{mn} = \frac{-1}{s_j^2 a_{mn} (s_j a_j) m_j} \left(\frac{16s_{0j}^2}{\Pi^2 mn} + s_{1j}^2 a_{mn} \right) \quad (6.46)$$

While in y- direction b_{ln} will be undefined so the problem will be continued only in x- direction and the y- direction will be neglected. In order to get a complete solution for the acoustic problem, equation (6.9) must be solved, in order to do this, equation (6.9) is written in the average form such that

$$(iw + U_{0j} \frac{\partial}{\partial x}) \langle r_j \rangle + \langle u_{xj} \rangle \frac{\partial r_{0j}}{\partial x} + U_{0j} \frac{\partial r_j}{\partial x} + \langle r_j \rangle \frac{\partial U_{0j}}{\partial x} + \langle r_{0j} \nabla \cdot u_j \rangle = 0 \quad (6.47)$$

In general from mathematics any average value can be written as

$$\langle f \rangle = \frac{1}{4a_j^2} \iint_{2a_j * 2a_j} f dy dz \quad (6.48)$$

So by averaging state equation (6.11) yields

$$\langle r_j \rangle = \frac{P_j}{R_j T_j} (1 - r_{0j} R_j \langle F_j \rangle) \quad (6.49)$$

where

$$\langle F_j \rangle = \sum_{m,n} \frac{4b_{mn}}{mn \Pi^2} \quad (6.50)$$

$$\langle u_{xj} \rangle = P_j \langle H_j \rangle, \text{ and}$$

$$\langle H_j \rangle = \sum_{m,n} \frac{4a_{mn}}{mn \Pi^2}, \quad (6.51)$$

In order to find $\langle \nabla \cdot u_j \rangle$

$$\begin{aligned} \langle \nabla \cdot u_j \rangle &= \frac{1}{4a_j^2} \iint_{2a_j * 2a_j} \left(\frac{\partial u_{xj}}{\partial x} + \frac{\partial v_{yj}}{\partial y} + \nabla_s \cdot u_j \right) dy dz \\ &= \frac{\partial \langle u_{xj} \rangle}{\partial x} + \frac{\partial \langle v_{yj} \rangle}{\partial y} + \frac{1}{4a_j^2} \oint_{c_j} u_j \cdot n_j ds \end{aligned} \quad (6.52)$$

But the last term in equation (6.52) can be written as

$$\oint_{c_j} u_j \cdot n_j ds = (-1)^{j-1} \oint_{c_j} \bar{u}_w ds \quad (6.53)$$

And the partial derivative of both u, v can be written as

$$\begin{aligned}\frac{\partial \langle u_{xj} \rangle}{\partial x} &= -ik_1 \Gamma P_j \langle H_j \rangle, \text{ and} \\ \frac{\partial \langle v_{xj} \rangle}{\partial y} &= -ik_1 \Gamma P_j \langle H_j \rangle,\end{aligned}\tag{6.54}$$

where

c_j is the curve around the channel perimeter.

u_w is the acoustic wall velocity.

By using Darcy's law (equation (6.13)).

$$\bar{u}_w = \frac{P_1 - P_2}{R_w}\tag{6.55}$$

Substitute equations (6.54) and (6.55) in equation (6.53) leads to

$$\oint_{c_j} u_j \cdot n_j ds = (-1)^{j-1} \frac{8a_j(P_1 - P_2)}{R_w}\tag{6.56}$$

By substituting equations (6.56) and (6.54) in equation (6.47) to get

$$\begin{aligned}(i\omega + U_{0j} \frac{\partial}{\partial x}) \left(\frac{P_j}{R_j T_{0j}} (1 - r_{0j} R_j \langle F_j \rangle) + \frac{\partial r_{0j}}{\partial x} P_j \langle H_j \rangle + r_{0j} (-2i\Gamma k_1 \langle H_j \rangle P_j) \right) \\ + \frac{\partial U_{0j}}{\partial x} \left(\frac{P_j}{R_j T_{0j}} (1 - r_{0j} R_j \langle F_j \rangle) + \langle r_{0j} \nabla u_j \rangle + (-1)^{j-1} \frac{r_{0j} * 8a_j (P_1 - P_2)}{4a_j^2 R_w} \right) = 0\end{aligned}\tag{6.57}$$

Rearrange equation (6.57) and substitute the value of P_j (given in equation (6.21)) leads to

$$\begin{aligned}\left[\frac{1}{R_j T_{0j}} (i\omega - \Gamma k_1 U_{0j} + \frac{\partial U_{0j}}{\partial x}) (1 - r_{0j} R_j \langle F_j \rangle) + \left(\frac{\partial r_{0j}}{\partial x} - 2ik_1 \Gamma r_{0j} \right) \langle H_j \rangle \right] A_j \\ + (-1)^{j-1} * \frac{2r_{0j} (A_1 - A_2)}{a_j R_w} = 0\end{aligned}\tag{6.58}$$

Multiplying equation (6.58) by $(\frac{R_w a_j}{2r_{0j}})$, yields

$$\begin{aligned}\left[\frac{R_w a_j}{2r_{0j} R_j T_{0j}} (i\omega - \Gamma k_1 U_{0j} + \frac{\partial U_{0j}}{\partial x}) (1 - r_{0j} R_j \langle F_j \rangle) + \frac{R_w a_j}{2r_{0j}} \left(\frac{\partial r_{0j}}{\partial x} - 2ik_1 \Gamma r_{0j} \right) \langle H_j \rangle \right] A_j \\ + (-1)^{j-1} (A_1 - A_2) = 0\end{aligned}\tag{6.59}$$

This equation represents a linear homogeneous equation system for the amplitudes of pressure waves A_1, A_2 in neighboring channels 1 and 2 which can be written as

$$\begin{bmatrix} K_{11} + K_{21} & -K_{12} \\ K_{21} & K_{12} - K_{22} \end{bmatrix} \begin{bmatrix} A_1 \\ A_2 \end{bmatrix} = \begin{bmatrix} 0 \\ 0 \end{bmatrix} \quad (6.60)$$

where

$$K_{1j} = \left[\frac{R_w a_j}{2r_{0j} R_j T_{0j}} (i\omega - \Gamma k_1 U_{0j} + \frac{\partial U_{0j}}{\partial x}) (1 - r_{0j} R_j < F_j >) + \frac{R_w a_j}{2r_{0j}} \left(\frac{\partial r_{0j}}{\partial x} - 2ik_1 \Gamma r_{0j} \right) < H_j > \right] \quad (6.61)$$

and

$$K_{2j} = (-1)^{j-1} \quad (6.62)$$

For non trivial solution the determinant

$$\begin{vmatrix} K_{11} + K_{21} & -K_{12} \\ K_{21} & K_{12} - K_{22} \end{vmatrix} \quad (6.63)$$

Should be equal to zero, and this leads to a transcendental equation for the propagation constant " Γ ". By substituting numerical values of different constants and physical quantities, and by using "Matlab" for the case of no-mean flow i.e. ($U_{0j} = V_{0j} = 0$). Wave propagation constants in such studies are usually calculated under two conditions; the first at operating conditions where $T = 500^\circ\text{C}$, Allam (2006), and secondly at $T = 1000^\circ\text{C}$. The final results for the values of the propagation constant are summarized below as follows;

-For hot conditions ($T = 773^\circ\text{K}$, $\omega = 400\text{-}1000\text{ Hz}$);

Table (2) propagation constants at hot conditions, four-port model

$\Gamma_1 = (0.2451 + 0.9873i) * 10^{-3}$;	$\Gamma_2 = (-0.2451 - 0.9873i) * 10^{-3}$
$\Gamma_3 = (-0.7035 + 0.3440i) * 10^{-3}$;	$\Gamma_4 = (0.7032 - 0.3440i) * 10^{-3}$

- Under the operating temperature $T = 1000^\circ\text{C}$:

Table (3) propagation constants at hot conditions, four-port model

$\Gamma_1 = (0.123 + 0.361i) * 10^{-3}$	$\Gamma_2 = (-0.123 - 0.361i) * 10^{-3}$
$\Gamma_3 = (-0.351 + 0.148i) * 10^{-3}$	$\Gamma_4 = (0.351 - 0.148i) * 10^{-3}$

Chapter 7

Six-Port DPF Acoustic Model

7.1 Introduction

Some previous studies built a four-port model for the sound propagation in porous DPF unit, Allam (2006), and Dokumaci (2001), but these models treated the problem as a 1-D model by neglecting the effects of transverse velocity. In last chapter a four-port 2-D model was built by taking into accounts the effects of transverse velocity and some improvements have been achieved, in this chapter a six-port model for the DPF unit will be built by taking into account that the parameters: pressure, temperature, densities, and velocities are considered to be harmonic in time and 2-D space. Following same procedure in last chapter, six roots which represent wave propagation constants are determined, and hence an invented six-port model is built, which will be used to find sound transmission losses, and other needed acoustic quantities.

7.2 Governing equations of six-port DPF model

To reach to the real case of the acoustic model for the DPF unit, u , v , P_j , ρ_j , and T_j are considered to be harmonic in time and 2-D space such that:

$$u_{xj} = -D_0(A_0 e^{\Gamma k_1 x} - B_0 e^{-\Gamma k_1 x}) + A_{00} e^{i\omega t} \quad (7.1)$$

$$v_{yj} = -D_0(A_0 e^{\Gamma k_1 y} - B_0 e^{-\Gamma k_1 y}) + B_{00} e^{i\omega t} \quad (7.2)$$

$$P_{jy} = A_0 e^{\Gamma k_1 y} + B_0 e^{-\Gamma k_1 y} + P_0 e^{-i\omega t} \quad (7.3)$$

$$P_{jx} = A_0 e^{\Gamma k_1 x} + B_0 e^{-\Gamma k_1 x} + P_0 e^{-i\omega t} \quad (7.4)$$

$$r_{jx} = A_0 e^{\Gamma k_1 x} + B_0 e^{-\Gamma k_1 x} + r_0 e^{i\omega t} \quad (7.5)$$

$$r_{jy} = A_0 e^{\Gamma k_1 y} + B_0 e^{-\Gamma k_1 y} + r_0 e^{i\omega t} \quad (7.6)$$

$$T_{jx} = A_0 e^{\Gamma k_1 x} + B_0 e^{-\Gamma k_1 x} + T_0 e^{i\omega t} \quad (7.7)$$

$$T_{jy} = A_0 e^{\Gamma k_1 y} + B_0 e^{-\Gamma k_1 y} + T_0 e^{i\omega t} \quad (7.8)$$

where

$$D_0 = \frac{ig_s}{\Gamma n r_0 C_0} \text{ and}$$

A_0, B_0, A_{00}, B_{00} are some constants.

So by differentiating all equations in (7.1) to (7.8) partially with respect to time and then with respect to x and y substituting them in equations (6.5) to (6.10) yields

$$\mathbf{r}_{0j} \left[i\omega + \frac{\partial U_{0j}}{\partial x} \right] u_{xj} + \mathbf{r}_{0j} \frac{\partial U_{0j}}{\partial y} v_{yj} + (D_{0j} U_{0j} + \frac{\partial}{\partial x}) P_{jx} = \mathbf{m}_j \left(\frac{\partial^2 u_{xj}}{\partial x^2} + \frac{\partial^2 u_{xj}}{\partial y^2} + \frac{\partial^2 u_{xj}}{\partial z^2} \right) \quad (7.9)$$

Similarly in y-direction

$$\mathbf{r}_{0j} \left[i\omega + \frac{\partial V_{0j}}{\partial y} \right] v_{yj} + \mathbf{r}_{0j} \frac{\partial V_{0j}}{\partial x} u_{xj} + (D_{0j} V_{0j} + \frac{\partial}{\partial x}) P_{jy} = \mathbf{m}_j \left(\frac{\partial^2 v_{yj}}{\partial x^2} + \frac{\partial^2 v_{yj}}{\partial y^2} + \frac{\partial^2 v_{yj}}{\partial z^2} \right) \quad (7.10)$$

While continuity equation becomes

$$\left(i\omega + \frac{\partial U_{0j}}{\partial x} \right) \mathbf{r}_j + \left(\frac{\partial \mathbf{r}_{0j}}{\partial x} + D_{0j} U_{0j} \right) u_{xj} + \mathbf{r}_{0j} \nabla \cdot \mathbf{u}_j = 0 \quad (7.11)$$

Also energy equation becomes

$$\begin{aligned} (\mathbf{r}_{0j} C p_j i\omega - K_{thj} \nabla_s^2) T_j + \mathbf{r}_{0j} C p_j u_{xj} \frac{\partial T_{0j}}{\partial x} + C p_j U_{0j} \frac{\partial T_{0j}}{\partial x} \mathbf{r}_{0j} = \\ (i\omega + U_{0j} \frac{\partial}{\partial x}) P_j + \left(\frac{\partial P_{0j}}{\partial x} - U_{0j} D_{0j} \mathbf{r}_{0j} \right) u_{xj} \end{aligned} \quad (7.12)$$

Using the same procedure in solving time harmonic variation equations in chapter 6 the new harmonic in time and 2-D space obtained equations will be solved to give the following partial differential equations.

- Navier-Stokes equation in x-direction becomes

$$\frac{\partial^2 H_j}{\partial x^2} + \frac{\partial^2 H_j}{\partial y^2} + \frac{\partial^2 H_j}{\partial z^2} - i b_{xj}^2 H_j = \frac{D_{0j} C M_j}{m_j} - \frac{-i \Gamma k_1}{m_j} \quad (7.13)$$

where

$$\begin{aligned} b_{xj}^2 &= (-\Gamma k_1 + \frac{1}{w} \frac{\partial U_{0j}}{\partial x} + \frac{1}{w} \frac{\partial U_{0j}}{\partial y}) S_j^2 \\ S_j^2 &= \frac{\mathbf{r}_{0j} w}{m_j} \end{aligned} \quad (7.14)$$

-in y-direction, Navier-Stokes equation can be written as

$$\frac{\partial^2 H_j}{\partial x^2} + \frac{\partial^2 H_j}{\partial y^2} + \frac{\partial^2 H_j}{\partial z^2} - i b_{xy}^2 H_j = \frac{D_{0j} C M_j}{m_j} - \frac{-i \Gamma k_1}{m_j} \quad (7.15)$$

where

$$b_{xy}^2 = (-\Gamma k_1 + \frac{1}{w} \frac{\partial V_{0j}}{\partial x} + \frac{1}{w} \frac{\partial V_{0j}}{\partial y}) S_j^2$$

$$D_{0j} = \frac{i g_s k_1}{n C_0}$$

$$D_{0ij} = \frac{-\Gamma^2 k_1 n r_0 C_0}{i g_s} \quad (7.16)$$

Energy equation also solved by the same method (in chapter 6) and yields

$$\frac{\partial^2 F_j}{\partial x^2} + \frac{\partial^2 F_j}{\partial y^2} + \frac{\partial^2 F_j}{\partial z^2} - s_{jk}^2 F_j = s_{0j}^2 + s_{1j}^2 H_j \quad (7.17)$$

where

$$s_{jk}^2 = S_j^2 \text{Pr} \left(i - \frac{U_{0j}}{w T_{0j}} \frac{\partial T_{0j}}{\partial x} \right),$$

$$s_{0jk}^2 = \left(\frac{\text{Pr} S_j^2}{w} \frac{\partial T_{0j}}{\partial x} - \frac{1}{K_{thj}} \frac{\partial P_{0j}}{\partial x} + \frac{S_j^2 M U_{0j}}{w K_{thj}} D_0 \right),$$

$$s_{jk}^2 = \frac{1}{K_{thj}} \left(i w - i U_{0j} \Gamma M w - \frac{C p_j U_{0j}}{R_j T_{0j}} \frac{\partial T_{0j}}{\partial x} \right), \quad (7.18)$$

$$\text{Pr}^2 = \frac{m_j C p_j}{K_{thj}}$$

To solve equation (7.13), and (7.17) the field is expanded by using Fourier sinus series

$$H(0, y, z) = \sum_{m,n} a_{mn} \sin \frac{m \Pi y}{2 a_j} \sin \frac{n \Pi z}{2 a_j} \quad (7.19)$$

Differentiate equation (7.19) then substitute in equation (7.15) and making the same

Procedures as in chapter (6) yields

$$a_{mn} = \frac{16ik_1}{mn \Pi^2 b_j^2 a_{mn} (b_j a_j) m_j} \left(\frac{g_s M_j}{n_1} - \Gamma \right) \quad (7.20)$$

Followed the same procedure

$$a_{ln} = \frac{16ik_1}{n \Pi^2 b_{jy}^2 a_{mn} (b_{jy} a_j) m_j} \left(\frac{g_s M_j}{n_1} - \Gamma \right) \quad (7.21)$$

Same procedure used for equation (6.20) to find b_{mn} yields

$$b_{mn} = \frac{-1}{s_j^2 a_{mn} (s_j a_j)} \left(\frac{16s_{0j}^2}{\Pi^2 mn} + s_{1j}^2 a_{mn} \right) \quad (7.22)$$

To complete the solution energy equation should be solved, by averaging this equation yields

$$(iw + \frac{\partial U_{0j}}{\partial x}) \langle r_j \rangle + \langle u_{xj} \rangle \left(\frac{\partial r_{0j}}{\partial x} + D_0 U_{0j} \right) + r_{0j} \langle \nabla u_j \rangle = 0 \quad (7.23)$$

By substituting equations (6.48) to (6.55) in equation (7.23) this leads to

$$\begin{aligned} (iw + \frac{\partial U_{0j}}{\partial x}) \left(\frac{P_j}{R_j T_{0j}} (1 - r_{0j} R_j \langle F_j \rangle) + \frac{\partial r_{0j}}{\partial x} \langle u_{xj} \rangle + D_0 U_{0j} \langle u_{xj} \rangle \right) \\ + r_{0j} (-2ik_1 \Gamma \langle H_j \rangle + P_j) + (-1)^{j-1} \frac{r_{0j} * 8a_j (P_1 - P_2)}{4a_j^2 R_w} = 0 \end{aligned} \quad (7.24)$$

Rearrange equation (7.24) gives

$$\begin{aligned} \left[\frac{1}{R_j T_{0j}} (iw + \frac{\partial U_{0j}}{\partial x}) (1 - r_{0j} R_j \langle F_j \rangle) + \left(\frac{\partial r_{0j}}{\partial x} + D_0 U_{0j} - 2ik_1 \Gamma r_{0j} \right) \langle H_j \rangle \right] A_j \\ + (-1)^{j-1} * \frac{2r_{0j} (A_1 - A_2)}{a_j R_w} = 0 \end{aligned} \quad (7.25)$$

where $\langle F_j \rangle$ and $\langle H_j \rangle$: are called average dispersive functions given in equation (6.50) and (6.51).

Equation (7.25) can be written in matrix form as follows

$$\begin{bmatrix} K11 + K21 & -K12 \\ K21 & K12 - K22 \end{bmatrix} \begin{bmatrix} A_1 \\ A_2 \end{bmatrix} = \begin{bmatrix} 0 \\ 0 \end{bmatrix} \quad (7.26)$$

where

$$K_{1j} = \left[\frac{R_w a_j}{2r_{0j} R_j T_{0j}} (iw + \frac{\partial U_{0j}}{\partial x})(1 - r_{0j} R_j < F_j >) + \frac{R_w a_j}{2r_{0j}} (\frac{\partial r_{0j}}{\partial x} + D_0 U_{0j} - 2ik_1 \Gamma r_{0j}) < H_j > \right] \quad (7.27)$$

and

$$K_{2j} = (-1)^{j-1} \quad (7.28)$$

For non trivial solution the determinant

$$\begin{vmatrix} K_{11} + K_{21} & -K_{12} \\ K_{21} & K_{12} - K_{22} \end{vmatrix} \quad (7.29)$$

should be equal to zero. And this leads to a transcendental equation for the propagation constant "Γ".

By substituting numerical values of different constants and physical quantities, and by using "Matlab" for the case of no-mean flow i.e. ($U_{0j} = V_{0j} = 0$). The final results for the values of the propagation constant are summarized below as follows;

-For hot conditions: ($T=773^\circ\text{K}$, $w=400-1000\text{ Hz}$);

Table (4) propagation constants at hot conditions, six-port model

$\Gamma_1 = -0.3407 - 0.1522i;$	$\Gamma_2 = 0.3407 + 0.1522i;$
$\Gamma_3 = 0.2719 + 0.2250i;$	$\Gamma_4 = -0.2719 - 0.2250i;$
$\Gamma_5 = 0.0688 - 0.0391i;$	$\Gamma_6 = -0.0688 + 0.0391i;$

- At hot condition : $T=1000^\circ\text{C}$, $w=400-1000\text{ Hz}$.

Table (5) propagation constants at hot conditions, six-port model

$\Gamma_1 = -0.170 - 0.0423i;$	$\Gamma_2 = 0.170 + 0.0423i;$
$\Gamma_3 = 0.1195 + 0.4261i;$	$\Gamma_4 = -0.1195 - 0.4261i;$
$\Gamma_5 = 0.0759 - 0.0204i;$	$\Gamma_6 = -0.0759 + 0.0204i;$

Chapter 8

Acoustic Impedance and Transmission Losses of DPF Unit

8.1 Introduction

In order to find sound transmission losses for the DPF unit, the results of chapter 6 and 7 are used. In this chapter the eigenvalues for the propagation constant are used to find eigenvectors which are at the end contribute in building the transfer matrix , S, which used to find transmission losses and noise reduction factor. These two quantities represent the capability of DPF units in treating the extremely noise problem of diesel engines, the transmission losses increase the more efficient DPF unit, and same for the noise reduction.

8.2 Finding the T_2 matrix

For each root of eigenvalues of Γ there is a corresponding 2D mode (eigenvector) e_n . Using these eigenvectors and mode the general expression of these eigenvectors can be given as:

For the time harmonic variation

$$\begin{pmatrix} p_1(x) \\ p_2(x) \end{pmatrix} = \sum_{n=1}^4 a_n e^{-ik_1 \Gamma_n x} e_{j,n} \quad (8.1)$$

Where

a_n is the modal amplitude

$p(x)$ is the acoustics pressure.

For each acoustics pressure there is an acoustics volume velocity $q_j(x)$ such that

$$\begin{pmatrix} q_1(x) \\ q_2(x) \end{pmatrix} = \sum_{n=1}^4 a_n e^{-ik_1 \Gamma_n x} e'_{j,n} \quad (8.2)$$

where $e'_{j,n} = 4a_j^2 < H_{j,n} > e_{j,n}$.

So by using last equations the total four-port matrix can be written as

$$\begin{pmatrix} p_1(x) \\ p_2(x) \\ q_1(x) \\ q_2(x) \end{pmatrix} = \begin{pmatrix} e^{-ik_1 \Gamma_1 x} e_1 & e^{-ik_1 \Gamma_2 x} e_2 & e^{-ik_1 \Gamma_3 x} e_3 & e^{-ik_1 \Gamma_4 x} e_4 \\ e^{ik_1 \Gamma_1 x} e_1 & e^{ik_1 \Gamma_2 x} e_2 & e^{ik_1 \Gamma_3 x} e_3 & e^{ik_1 \Gamma_4 x} e_4 \\ e^{-ik_2 \Gamma_1 x} e_1 & e^{-ik_2 \Gamma_2 x} e_2 & e^{-ik_2 \Gamma_3 x} e_3 & e^{-ik_2 \Gamma_4 x} e_4 \\ e^{ik_2 \Gamma_1 x} e_1 & e^{ik_2 \Gamma_2 x} e_2 & e^{ik_2 \Gamma_3 x} e_3 & e^{ik_2 \Gamma_4 x} e_4 \end{pmatrix} \begin{pmatrix} a_1 \\ a_2 \\ a_3 \\ a_4 \end{pmatrix} \quad (8.3)$$

Where

$$\begin{aligned} k_2 &= k_1 \sqrt{1 - 8ib/k_1} \\ b &= C_j r_w / dh_j R_w, \text{ Allam (2005).} \\ \langle H_j \rangle &= 4a_{11}/\Gamma^2 \end{aligned} \quad (8.4)$$

By applying boundary conditions at $x=0$, $x=L$, to get

$$\begin{pmatrix} p_1(0) \\ p_2(0) \\ q_1(0) \\ q_2(0) \end{pmatrix} = H(0) \begin{pmatrix} a_1 \\ a_2 \\ a_3 \\ a_4 \end{pmatrix} \quad (8.5)$$

And at $x=L$

$$\begin{pmatrix} p_1(L) \\ p_2(L) \\ q_1(L) \\ q_2(L) \end{pmatrix} = H(L) \begin{pmatrix} a_1 \\ a_2 \\ a_3 \\ a_4 \end{pmatrix} \quad (8.6)$$

From equation (8.6) it can be shown that

$$\begin{pmatrix} a_1 \\ a_2 \\ a_3 \\ a_4 \end{pmatrix} = H^{-1}(L) \begin{pmatrix} p_1(L) \\ p_2(L) \\ q_1(L) \\ q_2(L) \end{pmatrix} \quad (8.7)$$

and

$$\begin{pmatrix} p_1(0) \\ p_2(0) \\ q_1(0) \\ q_2(0) \end{pmatrix} = H(0) H^{-1}(L) * \begin{pmatrix} p_1(L) \\ p_2(L) \\ q_1(L) \\ q_2(L) \end{pmatrix} \quad (8.8)$$

Let the value $H(0)H^{-1}(L)$ be called as S-matrix.

The four-port matrix S can be used to find the two-port matrix T_2 by using rigid wall boundary conditions in channel 1 and 2 i.e.

$$\begin{aligned} \dot{q}_2(0) &= 0 \\ \text{and} \\ \dot{q}_1(L) &= 0 \end{aligned}$$

Also the relation can be written as

$$\begin{pmatrix} \dot{p}_1(0) \\ \dot{p}_2(0) \\ \dot{q}_1(0) \\ \dot{q}_2(0) \end{pmatrix} = \begin{pmatrix} S11 & S12 & S13 & S14 \\ S21 & S22 & S23 & S24 \\ S31 & S32 & S33 & S34 \\ S41 & S42 & S43 & S44 \end{pmatrix} \begin{pmatrix} \dot{p}_1(L) \\ \dot{p}_2(L) \\ \dot{q}_1(L) \\ \dot{q}_2(L) \end{pmatrix} \quad (8.9)$$

By applying last B.C yields

$$\begin{aligned} \dot{p}_1(0) &= S11 \left(\frac{-S44\dot{q}_2(L) - S42\dot{p}_2(L)}{S41} \right) + S12\dot{p}_2(L) + S14\dot{q}_2(L) \\ &= (S12 - S11S42/S41)\dot{p}_2(L) + (S14 - S11S44/S41)\dot{q}_2(L) \end{aligned} \quad (8.10)$$

And

$$\begin{aligned} \dot{q}_1(0) &= S31 \left(\frac{-S44\dot{q}_2(L) - S42\dot{p}_2(L)}{S41} \right) + S32\dot{p}_2(L) \\ &= (S32 - S31S42/S41)\dot{p}_2(L) + (S34 - S31S44/S41)\dot{q}_2(L) \end{aligned} \quad (8.11)$$

So the two-port matrix can be written as

$$\begin{pmatrix} \dot{p}_1(0) \\ \dot{q}_2(0) \end{pmatrix} = T_2 \begin{pmatrix} \dot{p}_2(L) \\ \dot{q}_2(L) \end{pmatrix} \quad (8.12)$$

where

$$T_2 = \begin{pmatrix} T11 & T12 \\ T21 & T22 \end{pmatrix}$$

If the number of channels at inlet ($x=0$) and outlet ($x=L$) is N, then the total volume flow in all the open channels should be added, such that

$$T_2 = \begin{pmatrix} T11 & T12/N \\ NT21 & T22 \end{pmatrix} \quad (8.13)$$

where

$$T11 = S12 - S42S11/S41$$

$$T12 = S14 - S44S11/S41$$

$$T21 = S32 - S42S31/S41$$

$$T22 = S34 - S44S31/S41 \quad (8.14)$$

By substituting numerical values the S matrix can be given as

$$S_{at T=500 C=1} * e^3 \begin{pmatrix} 2.2079 + 0.3830i & -1.4236 - 0.1530i & -3.6978 - 0.9379i & -2.3229 - 0.7576i \\ 2.2079 + 0.3830i & -1.4236 - 0.1530i & -3.6978 - 0.9379i & -2.3229 - 0.7576i \\ (0.0009 - 0.0000i & -0.0005 + 0.0008i & 0.0003 + 0.0001i & 0.0002 + 0.0001i) * 10^{-2} \\ (-0.0009 + 0.0000i & 0.0005 - 0.0008i & -0.0003 - 0.0001i & -0.0002 - 0.0001i) * 10^{-2} \end{pmatrix} \quad (8.15)$$

$$S_{HOT, T=1000 C=1} * e^2 \begin{pmatrix} 9.4804 + 6.0904i & -5.9253 - 3.8065i & 3.4061 - 7.1114i & -2.6799 - 9.8755i \\ 9.4804 + 6.0904i & -5.9253 - 3.8065i & 3.4061 - 7.1114i & -2.6799 - 9.8755i \\ (-0.0012 + 0.0045i & 0.0011 + 0.0033i & 0.0064 + .0002i & 0.0039 - 0.0001i) * 10^{-2} \\ (0.0012 - 0.0045i & -0.0011 - 0.0033i & -0.0064 - .0002i & -0.0039 + 0.0001i) * 10^{-2} \end{pmatrix} \quad (8.16)$$

8.2 The Lumped Impedance Model for the DPF unit

To obtain the acoustic resistance of the DPF, it is assumed that the acoustic field acts as a quasi-stationary disturbance of the steady state pressure drop (ΔP) over the filter unit.

This pressure drop is modeled using Darcy's law with a quadratic Forcheimer extension - equation (5.6).

By differentiating this equation with respect to U yields

$$\frac{d(\Delta P)}{dU} = \left(\frac{R_1 + 2R_2U}{A_f} \right) * A_f$$

$$d(\Delta P) = \left(\frac{R_1 + 2R_2U}{A_f} \right) * A_f dU \quad (8.17)$$

But since $dQ = A_f * dU$ yields

$$d(\Delta P) = R_{ac} dQ \quad (8.18)$$

where

$$R_{ac} = \frac{R_1 + 2R_2U}{A_f} \quad (8.19)$$

R_{ac} is the acoustics resistance

A_f is the filter cross-sectional area.

The lumped impedance model can be used for the in and outlet sections including the adjacent short pipes, see Allam (2002), and Allam (2005). This implies that (for two-port model)

$$T_x = \begin{pmatrix} 1 & Z_x \\ 0 & 1 \end{pmatrix} \quad (8.20)$$

where

$x=IN+1$, or $3+OUT$ sections of the DPF.

$$Z_x = r_x + \frac{ir_xwl_x}{d_{hj}^2}, \text{ Allam (2005)} \quad (8.21)$$

r is the acoustic resistance of the filter section.

l is the end correction length

d_{hj} is the hydraulic radius.

From Allam (2005)

$$r_{1+IN} = r_{3+OUT} = \frac{R_2U_0}{A} \quad (8.22)$$

Where R_2 can be given as

$$R_2 = \begin{cases} r_{IN}(1-1/m_{IN})^2/4 \\ r_{OUT}(1-1/m_{OUT})^2/2 \end{cases} \quad (8.23)$$

m_{IN} , m_{OUT} are the open area ratios at inlet and outlet respectively.

So by multiplying equation (8.22) by (C_j/C_j) and substitute equations (8.23) in equation (8.20) yields

$$Z_x = \begin{cases} Z_{IN}M_{IN}(1/m_{IN}^2 - 1) + \frac{irwl_1}{d_{hj}^2N} \\ 2Z_{OUT}M_{IOUT}(1-1/m_{OUT}) + \frac{irwl_3}{d_{hj}^2N} \end{cases} \quad (8.24)$$

Depending in last equations and derivations the full transforming matrices for different sections of the DPF can be written as follows

$$T_{IN} = \frac{1}{2} \begin{pmatrix} 1 & 2Z_{IN}M_{IN}(1/m_{IN}^2 - 1) \\ 0 & 1 \end{pmatrix} \quad (8.25)$$

-for section number 1 of the DPF

$$T_1 = \frac{1}{2} \begin{pmatrix} 1 & \frac{irwl_1}{d_{hj}^2 N} \\ 0 & 1 \end{pmatrix} \quad (8.26)$$

- For the outlet section of the DPF unit

$$T_{OUT} = \frac{1}{2} \begin{pmatrix} 1 & 4Z_{OUT}M_{OUT}(1 - 1/m_{OUT}) \\ 0 & 1 \end{pmatrix} \quad (8.27)$$

-for section number 3 of the DPF

$$T_3 = \frac{1}{2} \begin{pmatrix} 1 & \frac{irwl_3}{d_{hj}^2 N} \\ 0 & 1 \end{pmatrix} \quad (8.28)$$

While for section 2 it was given in equation (8.13).

where

$$Z_{IN} = \frac{r_{IN}C_{IN}}{A_{IN}}, \text{ and} \quad (8.29)$$

$$Z_{out} = \frac{r_{out}C_{out}}{A_{out}}$$

By applying equation (6.1) and then take all terms of the matrix T_{DPF} in series and then applying equation (5.39) the resulted quantity is known as the transmission losses, which can be given as

$$\begin{aligned} TL_{DPF} = 10 \log_{10} & \left((1/16)T_{11} + (1/8)iY_1NT_{21} + (1/8)NT_{21}Z_{IN}M_{IN}(1/m_{IN}^2 - 1) + \right. \\ & (1/4)T_{11}Z_{OUT}M_{OUT}(1 - 1/m_{OUT}) + (1/2)iY_1NT_{21} + 0.5NT_{21}Z_{IN}M_{IN}(1/m_{IN}^2 - 1) + \\ & Z_{OUT}M_{OUT}(1 - 1/m_{OUT}) + (1/8)iY_3T_{11} - 0.25Y_3Y_1NT_{21} + 0.25iY_3NT_{21}Z_{IN}M_{IN}(1/m_{IN}^2 - 1) + \\ & (1/16)T_{12}NiY_3 - (1/8)Y_1Y_3T_{22} + (1/8)iY_3T_{22}Z_{IN}M_{IN}(1/m_{IN}^2 - 1) + (1/16)NT_{21} + \\ & \left. 0.25NT_{21}Z_{OUT}M_{OUT}(1 - 1/m_{OUT}) + (1/8)NT_{21}iY_3 + (1/16)T_{22} \right) \end{aligned} \quad (8.30)$$

where

$$Y_1: \text{ is the plug mass impedance of section 1 } (Y_1 = \frac{irwl_1}{d_{hj}^2 N})$$

$$Y_3: \text{ is the plug mass impedance of section 3 } (Y_3 = \frac{irwl_3}{d_{hj}^2 N})$$

For be harmonic in time and 2-D space case, six roots have been found, and for each root (eigenvalue), there is an eigenvector, so equation (8.1) becomes

$$\begin{pmatrix} p_1(x) \\ p_2(x) \\ p_3(x) \end{pmatrix} = \sum_{n=1}^6 a_n e^{-ik_1 \Gamma_n x} e_{j,n} \quad (8.31)$$

And so equation (8.2) becomes

$$\begin{pmatrix} q_1(x) \\ q_2(x) \\ q_3(x) \end{pmatrix} = \sum_{n=1}^6 a_n e^{-ik_1 \Gamma_n x} e'_{j,n} \quad (8.32)$$

By following same procedure outlined in section 8.1 the S matrix becomes of 6x6 order matrix, i.e. a sixth-port model is invented here. This new model describes the pressure flow and velocity of gasses emission at inlet($x=0$), outlet ($x=L$), and between porous walls. So equations (8.31) and (8.32) can be rewritten as

$$\begin{pmatrix} p_1(x) \\ p_2(x) \\ p_3(x) \\ q_1(x) \\ q_2(x) \\ q_3(x) \end{pmatrix} = \begin{pmatrix} e^{-ik_1 \Gamma_1 x} e_1 & e^{-ik_1 \Gamma_2 x} e_2 & e^{-ik_1 \Gamma_3 x} e_3 & e^{-ik_1 \Gamma_4 x} e_4 & e^{-ik_1 \Gamma_5 x} e_5 & e^{-ik_1 \Gamma_6 x} e_6 \\ e^{ik_1 \Gamma_1 x} e_1 & e^{ik_1 \Gamma_2 x} e_2 & e^{ik_1 \Gamma_3 x} e_3 & e^{ik_1 \Gamma_4 x} e_4 & e^{ik_1 \Gamma_5 x} e_5 & e^{ik_1 \Gamma_6 x} e_6 \\ e^{ik_1 \Gamma_1 x} e_1 & e^{ik_1 \Gamma_2 x} e_2 & e^{ik_1 \Gamma_3 x} e_3 & e^{-ik_1 \Gamma_4 x} e_4 & e^{-ik_1 \Gamma_5 x} e_5 & e^{-ik_1 \Gamma_6 x} e_6 \\ e^{-ik_2 \Gamma_1 x} e_1 & e^{-ik_2 \Gamma_2 x} e_2 & e^{-ik_2 \Gamma_3 x} e_3 & e^{-ik_2 \Gamma_4 x} e_4 & e^{-ik_2 \Gamma_5 x} e_5 & e^{-ik_2 \Gamma_6 x} e_6 \\ e^{ik_2 \Gamma_1 x} e_1 & e^{ik_2 \Gamma_2 x} e_2 & e^{ik_2 \Gamma_3 x} e_3 & e^{ik_2 \Gamma_4 x} e_4 & e^{ik_2 \Gamma_5 x} e_5 & e^{ik_2 \Gamma_6 x} e_6 \\ e^{ik_2 \Gamma_1 x} e_1 & e^{ik_2 \Gamma_2 x} e_2 & e^{ik_2 \Gamma_3 x} e_3 & e^{-ik_2 \Gamma_4 x} e_4 & e^{-ik_2 \Gamma_5 x} e_5 & e^{-ik_2 \Gamma_6 x} e_6 \end{pmatrix} \begin{pmatrix} a_1 \\ a_2 \\ a_3 \\ a_4 \\ a_5 \\ a_6 \end{pmatrix} \quad (8.33)$$

S-matrix given in equation (8.8) can be given as:

$$S = H(0) H^{-1}(L) = \begin{pmatrix} S11 & S12 & S13 & S14 & S15 & S16 \\ S21 & S22 & S23 & S24 & S25 & S26 \\ S31 & S32 & S33 & S34 & S35 & S36 \\ S41 & S42 & S43 & S44 & S45 & S46 \\ S51 & S52 & S53 & S54 & S55 & S56 \\ S61 & S62 & S63 & S64 & S65 & S66 \end{pmatrix} \quad (8.34)$$

But it is obvious from last equations that

$$\begin{pmatrix} p_1(0) \\ p_2(0) \\ p_3(0) \\ q_1(0) \\ q_2(0) \\ q_3(0) \end{pmatrix} = H(0) \begin{pmatrix} a_1 \\ a_2 \\ a_3 \\ a_4 \\ a_5 \\ a_6 \end{pmatrix} \quad (8.35)$$

And in the same way at $x=L$

$$\begin{pmatrix} p_1(L) \\ p_2(L) \\ p_3(L) \\ q_1(L) \\ q_2(L) \\ q_3(L) \end{pmatrix} = H(L) \begin{pmatrix} a_1 \\ a_2 \\ a_3 \\ a_4 \\ a_5 \\ a_6 \end{pmatrix} \quad (8.36)$$

The six-port matrix S can be used to find the two-port matrix (T_2) by using boundary conditions in channel one and two.

$$\begin{array}{lll} q_2(0) = 0 & q_3(0) = 0 & p_3(0) = 0 \\ \text{and} & \text{and} & \text{and} \\ q_1(L) = 0 & q_3(L) = 0 & p_3(L) = 0 \end{array}$$

Now by applying these B.C. yields

$$\begin{pmatrix} p_1(0) \\ q_2(0) \end{pmatrix} = T_2 \begin{pmatrix} p_2(L) \\ q_2(L) \end{pmatrix} \quad (8.37)$$

where

$$T_2 = \begin{pmatrix} T_{11} & T_{12}/N \\ NT_{21} & T_{22} \end{pmatrix} \quad (8.38)$$

Each term in the last matrix can be determined by using B.C.s such that

$$\begin{aligned} T_{11} &= S_{12} \\ T_{12} &= S_{15} - (S_{22} + S_{55})S_{11}/S_{51} \\ T_{21} &= S_{42} \\ T_{22} &= S_{45} - (S_{55} + S_{52})S_{41}/S_{51} \end{aligned} \quad (8.39)$$

By substituting numerical values given in appendix 2 in equation (8.33) the following S matrices for both hot and cold conditions

$S_{\text{at } T=500 \text{ C}} =$

$1.0e^{16} *$

Columns 1 through 4

-0.0003 + 0.0004i -0.0001 - 0.0002i -0.0005 - 0.0002i -0.3585 + 1.7305i
 -0.0003 + 0.0004i -0.0001 - 0.0002i -0.0005 - 0.0002i -0.3585 + 1.7305i
 -0.0003 + 0.0004i -0.0001 - 0.0002i -0.0005 - 0.0002i -0.3585 + 1.7305i
 -0.0000 + 0.0002i -0.0001 - 0.0000i -0.0002 + 0.0000i 0.2386 + 0.5908i
 -0.0001 + 0.0004i -0.0002 - 0.0001i -0.0005 + 0.0000i 0.4054 + 1.5278i
 0.0001 - 0.0003i 0.0000 + 0.0003i 0.0001 + 0.0001i 0.4521 - 0.3587i

Columns 5 through 6

-0.2815 - 1.8014i -0.4736 + 0.0477i
 -0.2815 - 1.8014i -0.4736 + 0.0477i
 -0.2815 - 1.8014i -0.4736 + 0.0477i
 -0.4447 - 0.4841i -0.1325 + 0.1090i
 -0.9458 - 1.3286i -0.3598 + 0.2276i
 -0.2758 + 0.5067i 0.0689 + 0.0504i

$S_{\text{hot } T=1000 \text{ C}} =$

$1.0e^{15} *$

Columns 1 through 4

-0.0005 - 0.0021i 0.0036 - 0.0008i -0.0026 - 0.0020i -0.1289 - 4.3701i
 -0.0005 - 0.0021i 0.0036 - 0.0008i -0.0026 - 0.0020i -0.1289 - 4.3701i
 -0.0005 - 0.0021i 0.0036 - 0.0008i -0.0026 - 0.0020i -0.1289 - 4.3701i
 -0.0004 + 0.0004i -0.0029 - 0.0009i 0.0021 + 0.0012i -1.6481 + 0.4864i
 -0.0014 - 0.0012i 0.0021 - 0.0024i -0.0028 - 0.0001i -2.2753 - 2.9946i
 -0.0004 + 0.0004i -0.0029 - 0.0009i 0.0021 + 0.0012i -1.6481 + 0.4864i

Columns 5 through 6

2.0042 - 4.7261i 0.0000 + 4.5036i
 2.0042 - 4.7261i 0.0000 + 4.5036i
 2.0042 - 4.7261i 0.0000 + 4.5036i
 -0.8709 - 0.1965i 0.9007 - 0.4504i
 -0.9601 - 4.3104i 2.2518 + 3.1525i
 -0.8709 - 0.1965i 0.9007 - 0.4504i

To find the values of transmission losses for different cases and for different types of DPF, numerical values for different physical quantities will be substituted in equation (8.30), the results will be shown and discussed later in the following next chapters.

Chapter 9

Results and Discussion

9.1 Introduction

In this chapter the obtained results are presented including wave propagation constants in both conditions: hot and cold conditions and for both models: four-port, and six-port models. Also transmission losses, noise reduction factor for typical DPF unit, and other DPFs type are plotted against frequency, pressure drop model, and other relations between transmission losses and porosity, permeability, number of channels, and other quantities are also plotted. These results are followed by a discussion to explain some points, and relations. A comparison between different types of DPF units is demonstrated in this chapter depending on both transmission losses and noise reduction factor.

9.2 Results

The following figures represent the obtained results from the two mentioned approaches (four-port and six-port models) under the two conditions; hot and cold.

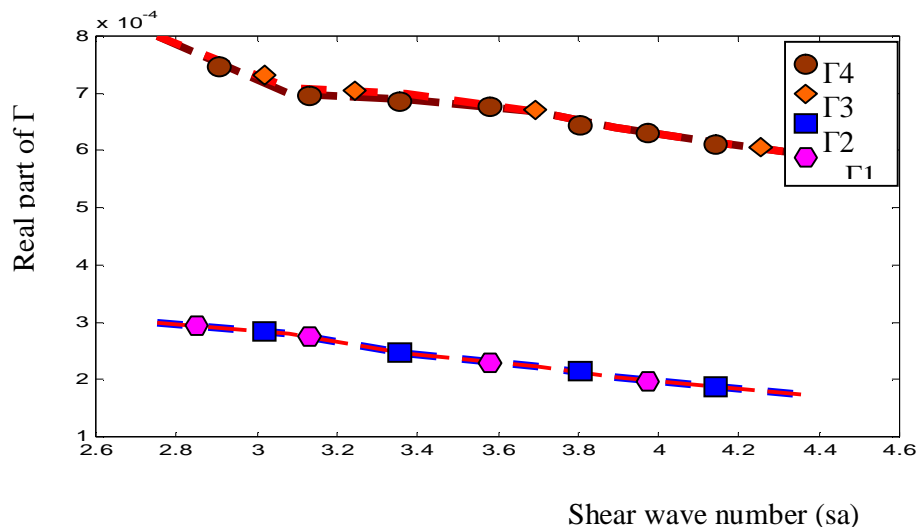


Figure (10): Real part of Γ (attenuation) against shear wave number, Γ_1 , and Γ_2 propagation constants for uncoupled waves, Γ_3 , and Γ_4 propagation constants for coupled waves, time harmonic variation only, and under hot conditions ($T=500^\circ\text{C}$).

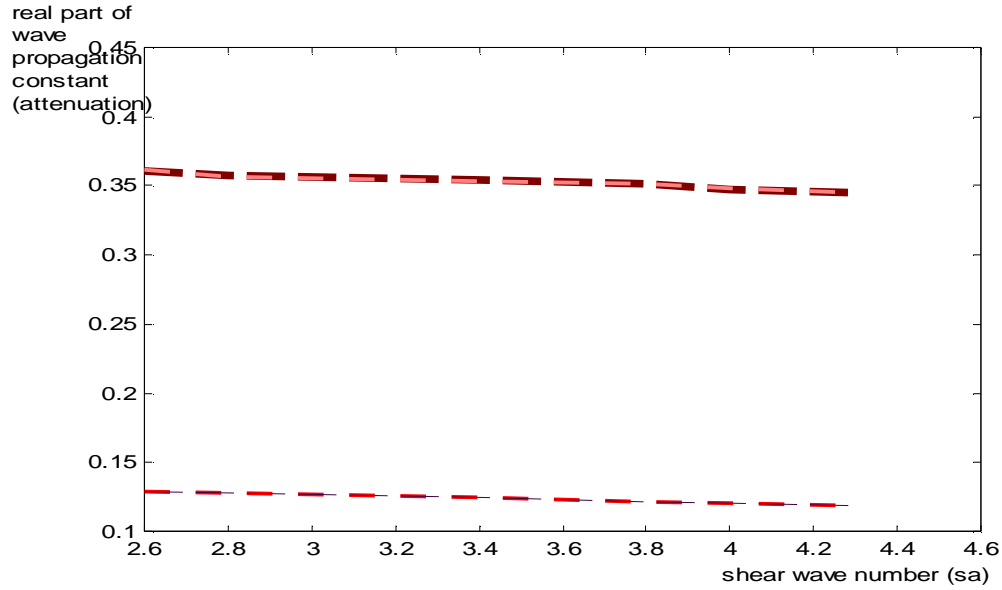


Figure (11): Real part of Γ vs. shear wave number, \dots Γ_1 , and $---$ Γ_2 are propagation constants represent uncoupled waves, \dots Γ_3 , and $---$ Γ_4 propagation constants for coupled waves, time harmonic variation only, and under hot conditions ($T=1000^\circ\text{C}$).

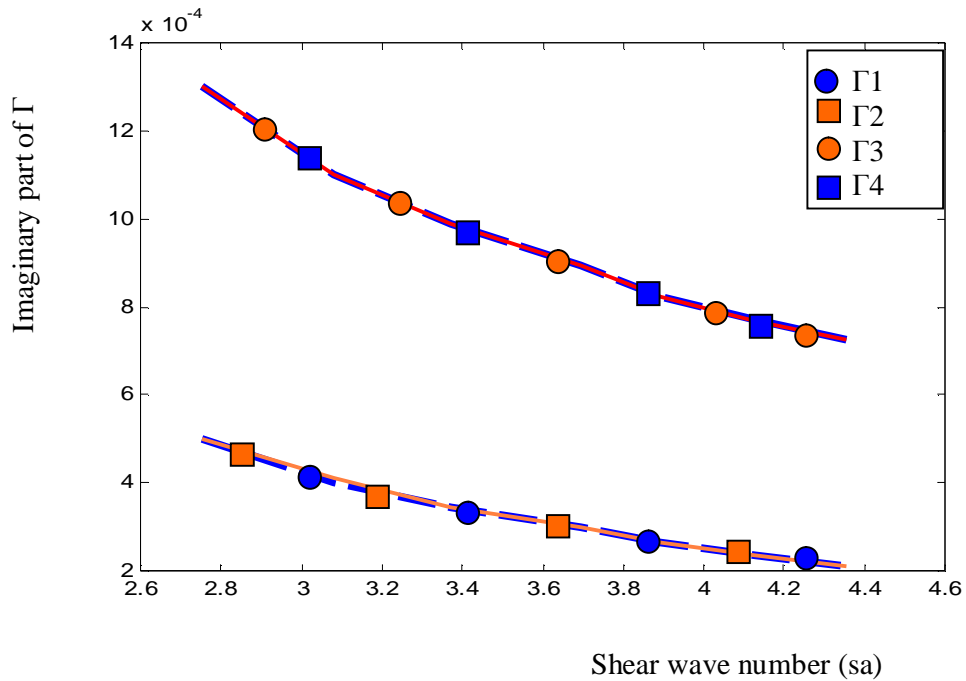


Figure (12): Imaginary part of Γ (phase shift) against shear wave number, Γ_1 , and Γ_2 propagation constants for uncoupled waves, Γ_3 and Γ_4 propagation constants for coupled waves, time harmonic variation only, and under hot conditions ($T=500^\circ\text{C}$).

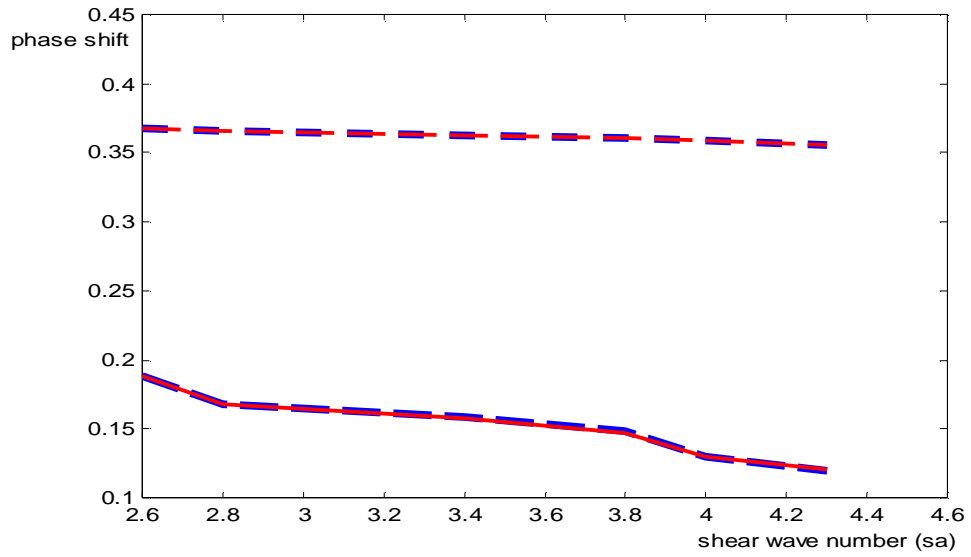


Figure (13): Imaginary part of Γ (phase shift) against shear wave number,..... Γ_1 , and ----- Γ_2 propagation constants for uncoupled waves, ——— Γ_3 and ---- Γ_4 propagation constants for coupled waves, under hot conditions ($T=1000^\circ\text{C}$).

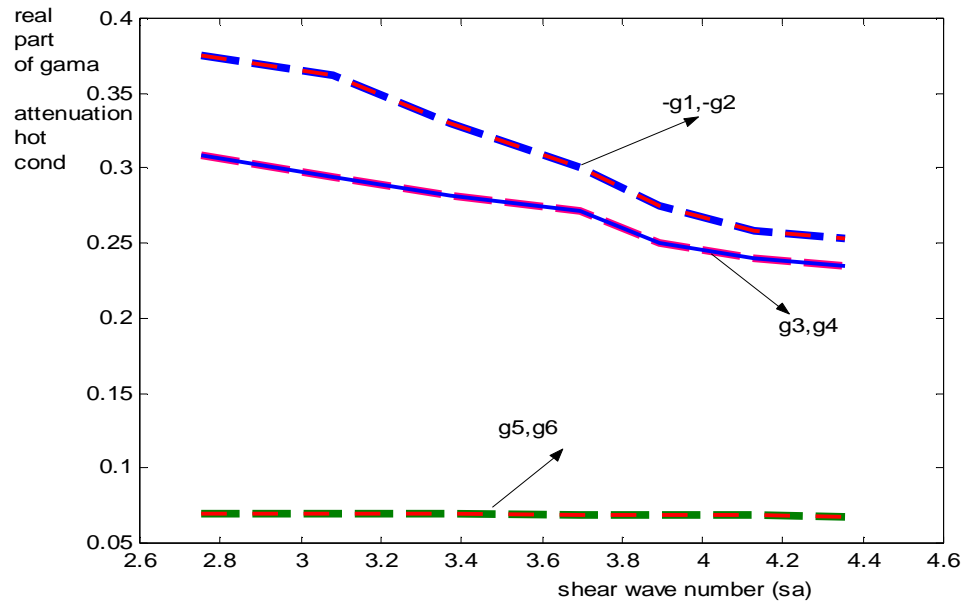


Figure (14): Real part of Γ vs. shear wave number (phase shift), Γ_1 and Γ_2 propagation constants for uncoupled waves, Γ_3 and Γ_4 propagation constants for coupled waves, Γ_5 and Γ_6 represent the interfering parts, time and 2-D space harmonic variation, and under hot conditions($T=500^\circ\text{C}$).

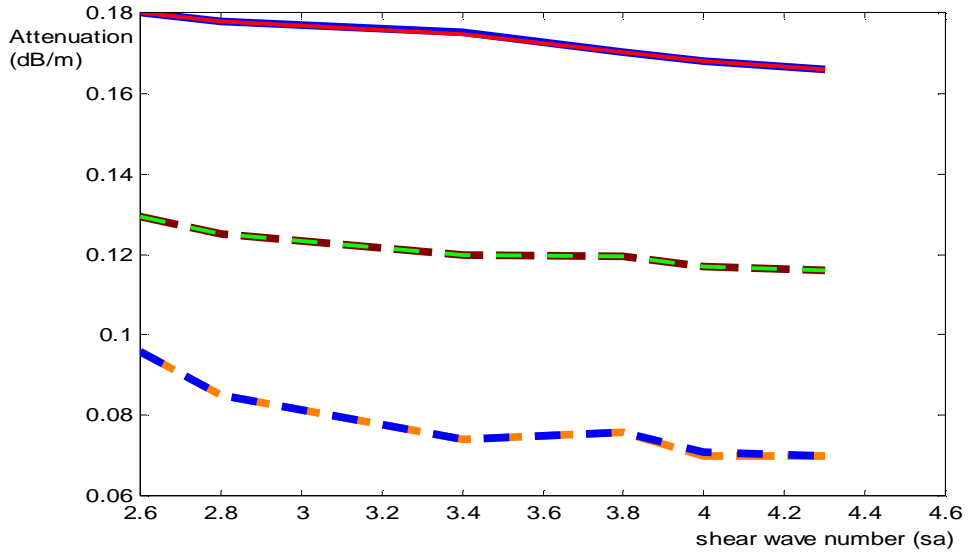


Figure (15): Real part of Γ vs. shear wave number, $\dots\Gamma1$, and $---\Gamma2$ are propagation constants represent uncoupled waves, $\dots\Gamma3$, and $---\Gamma4$ propagation constants for coupled waves, $\dots\Gamma5$, and $---\Gamma6$ under hot conditions ($T=1000^{\circ}\text{C}$).

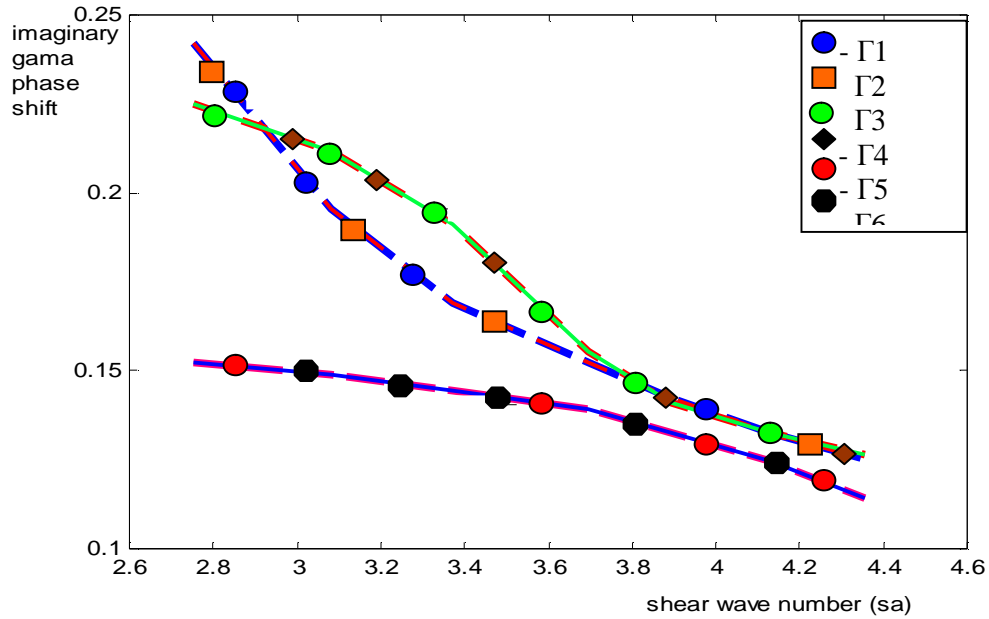


Figure (16): Imaginary part of Γ vs. shear wave number (phase shift), $\Gamma1$ and $\Gamma2$ propagation constants for uncoupled waves, $\Gamma3$ and $\Gamma4$ propagation constants for coupled waves, $\Gamma5$ and $\Gamma6$ represent the interfering parts, under hot conditions ($T=500^{\circ}\text{C}$).

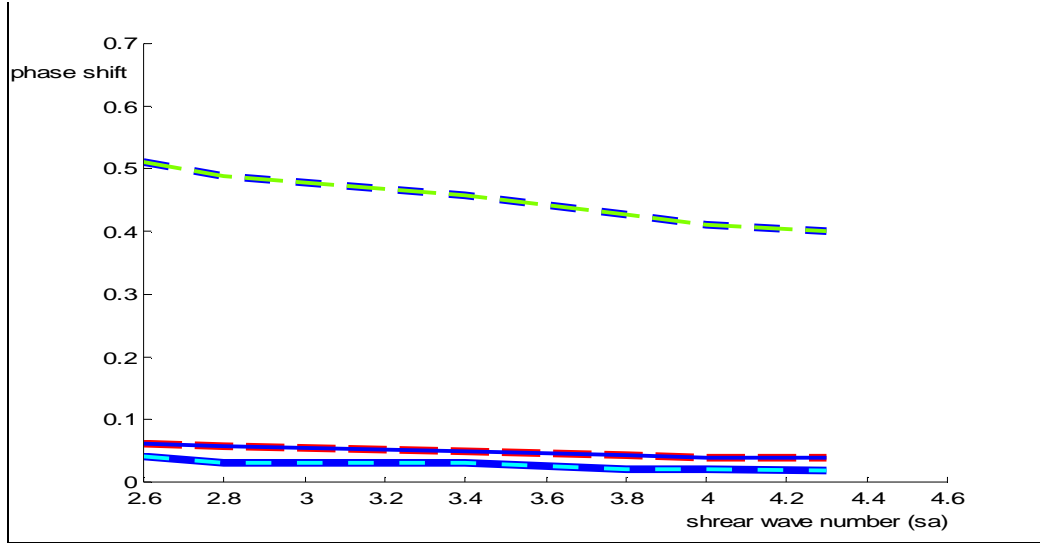


Figure (17): Imaginary part of Γ against shear wave number, --- Γ_1 , and--- Γ_2 are propagation constants represent uncoupled waves, Γ_3 , and -.-.- Γ_4 propagation constants for coupled waves, Γ_5 , and Γ_6 , under hot conditions ($T=1000^\circ\text{C}$).

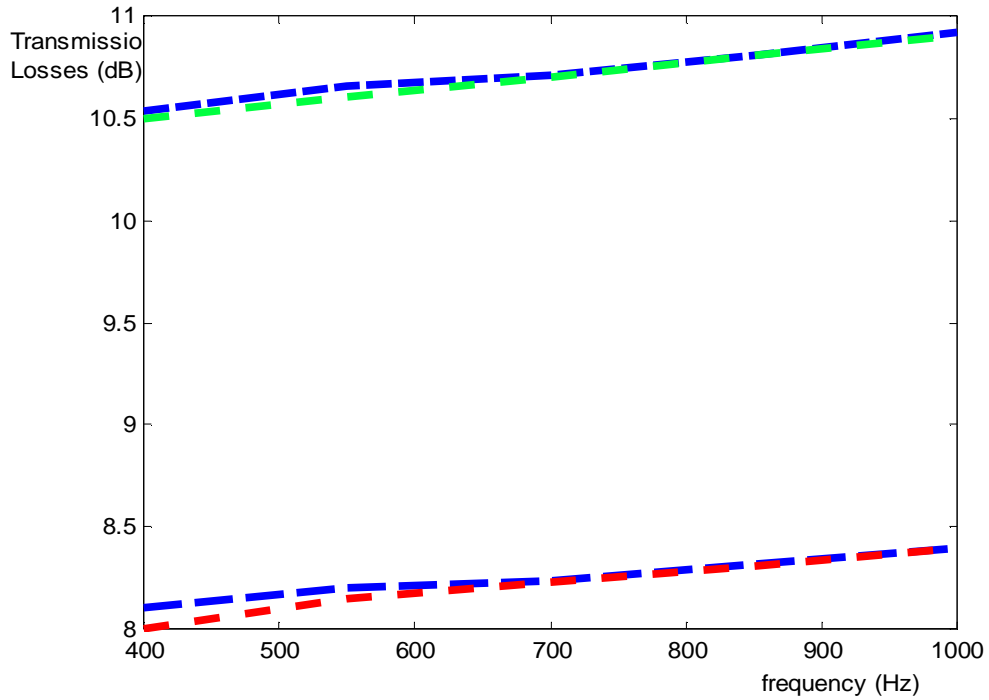


Figure (18): transmission losses against frequency under the case of hot conditions ($T=500\text{ C}$) compared with the recent study by Allam(2006), -.-.- (With no soot layer) present study, Allam,Allam (with soot layer), and -.-.-.present study with soot layer. Mach=0.02, for typical filter, and time harmonic variation only.

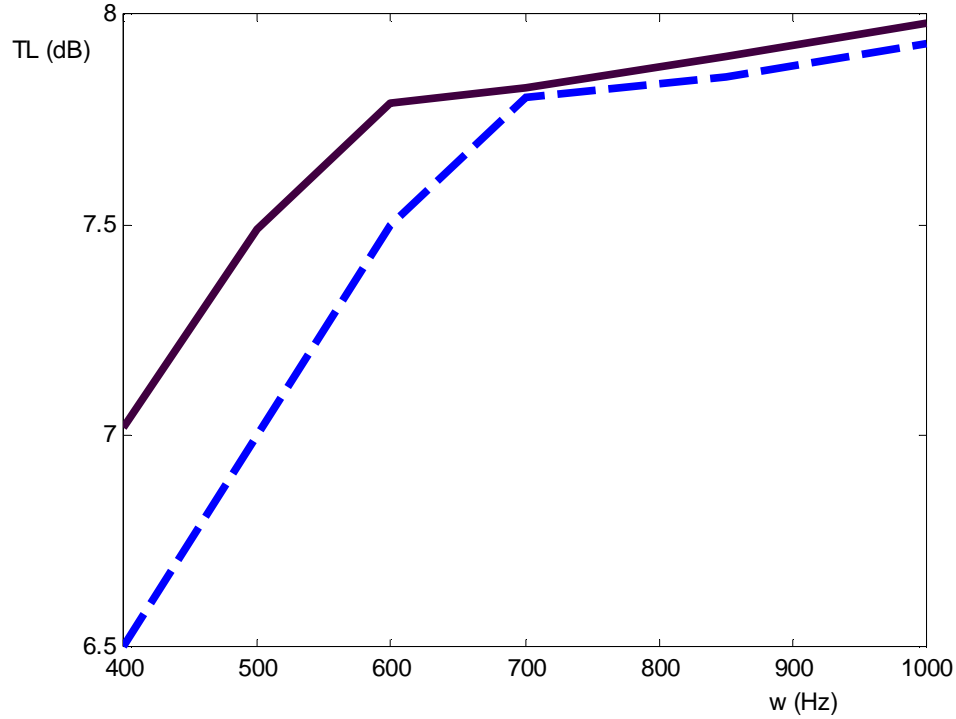


Figure (19): transmission losses against frequency for RC:200/12 DPF unit type under the case of hot conditions ($T=500\text{C}$) compared with last recent study [Allam], --- for Allam, while — is for the proposed study, (With no soot layer), and Mach=0.02.

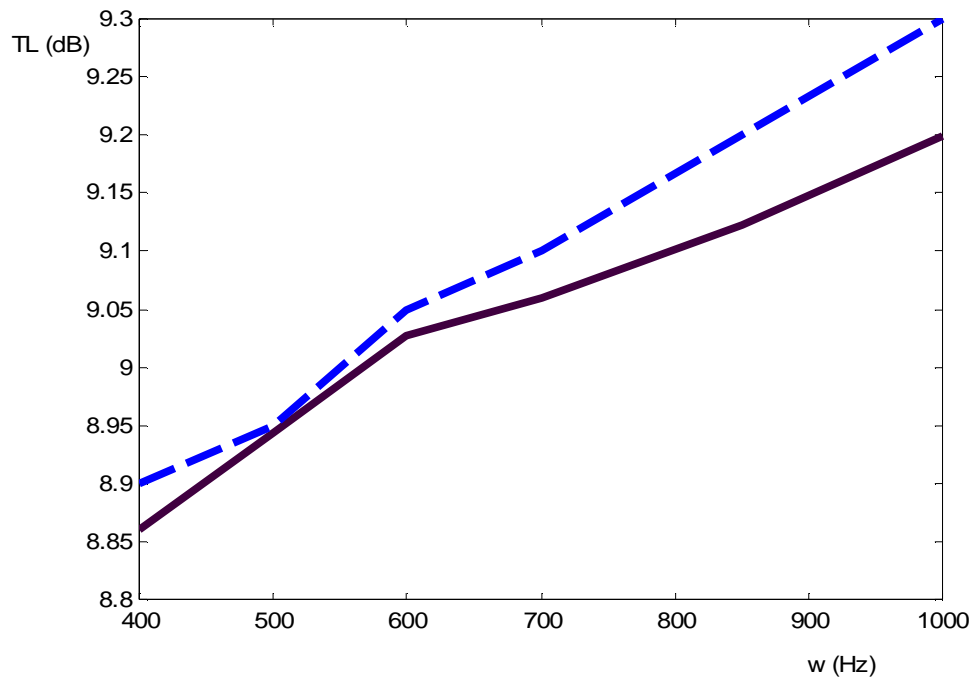


Figure (20): transmission losses against frequency for RC: 200/20 DPF unit type under the case of hot conditions ($T=500\text{C}$) compared with last recent study [Allam], --- for Allam, while — is for the proposed study, (With no soot layer), and Mach=0.02.

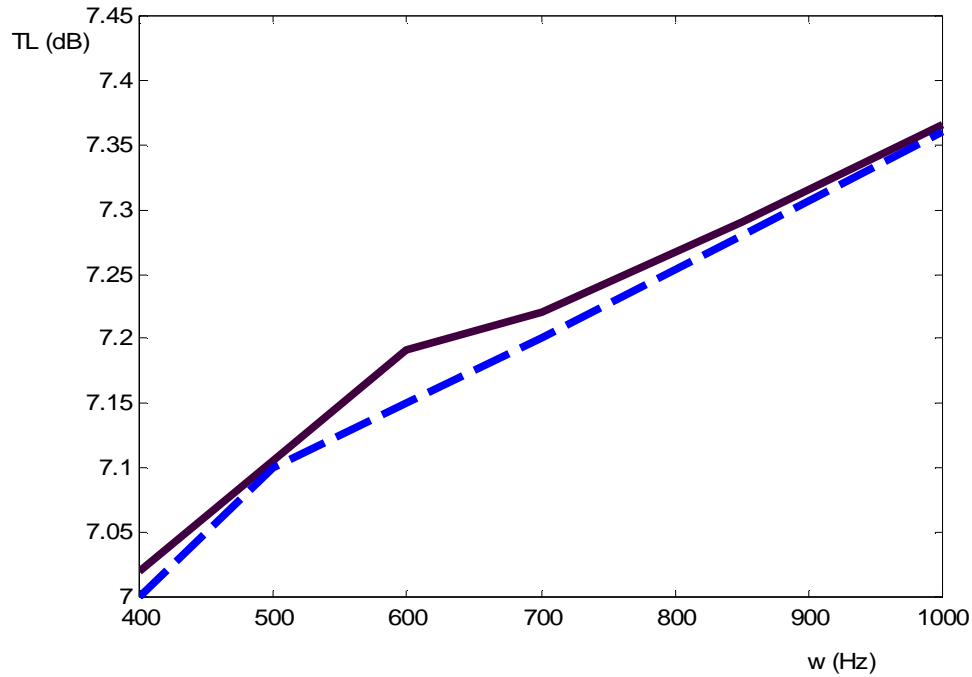


Figure (21): transmission losses against frequency for EX80:100/17 DPF unit type under the case of hot conditions ($T=500\text{C}$) compared with last recent study [Allam], ---- for Allam, — for the proposed study, (With no soot layer), and Mach=0.02.

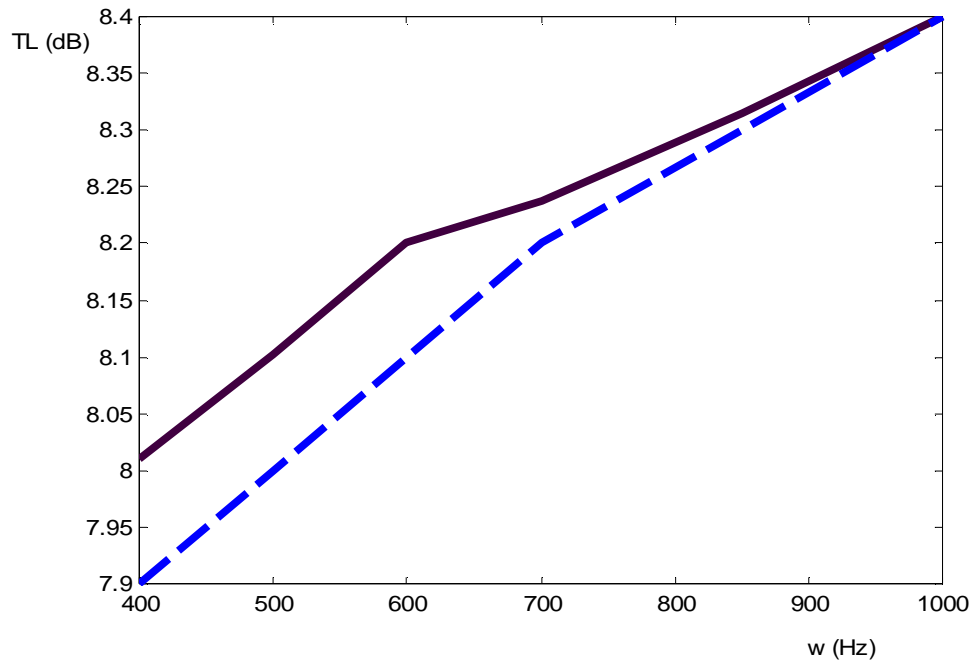


Figure (22): transmission losses against frequency for EX80:200/14 DPF unit type under the case of hot conditions ($T=500\text{ C}$) compared with last recent study [Allam], ---- for Allam, — is for the proposed study, (With no soot layer), and Mach=0.02

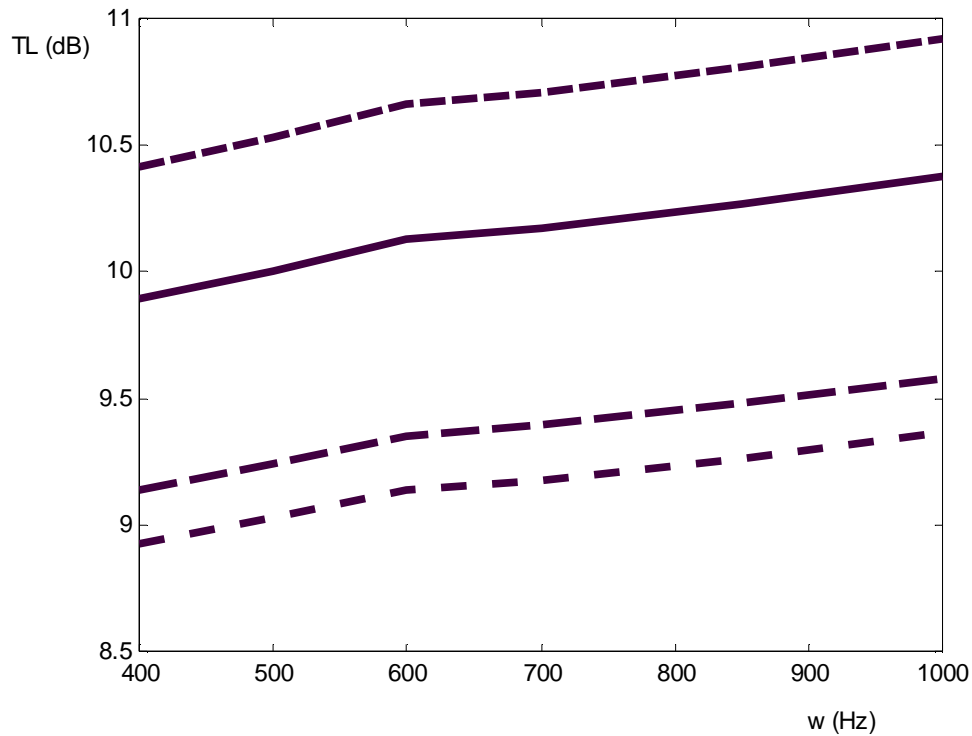


Figure (23): transmission losses against frequency, — for RC:200/12, -.-.-for EX80:200/14, ----for EX80:100/17, and.....for RC:200/20 DPF unit type under the case of hot conditions ($T=500$ C), (With soot layer), and Mach=0.02.

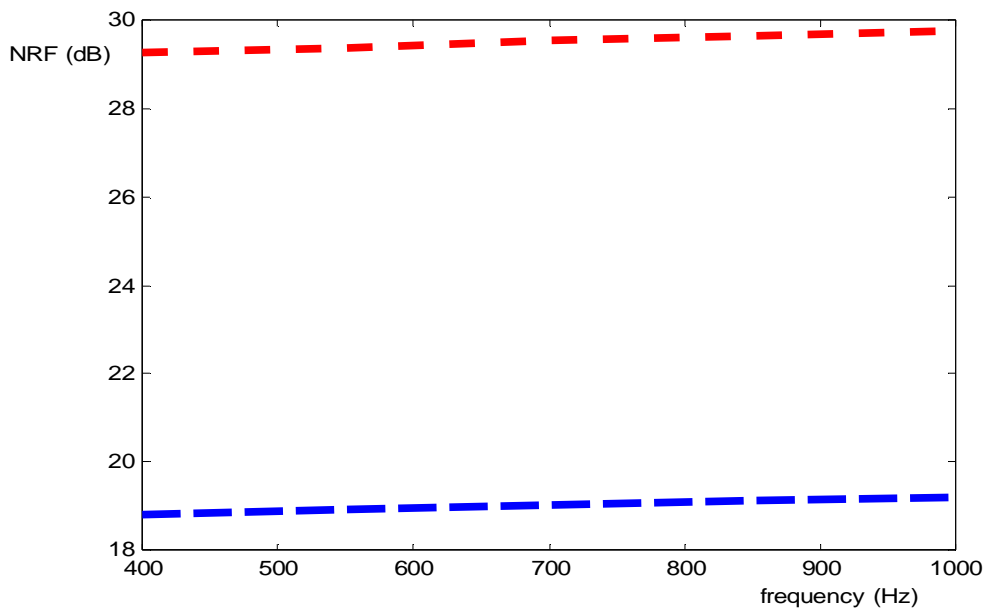


Figure (24): NRF against frequency for typical DPF under the case of hot conditions,(With soot layer), and -.-.- with no soot layer, and at Mach=0.02.

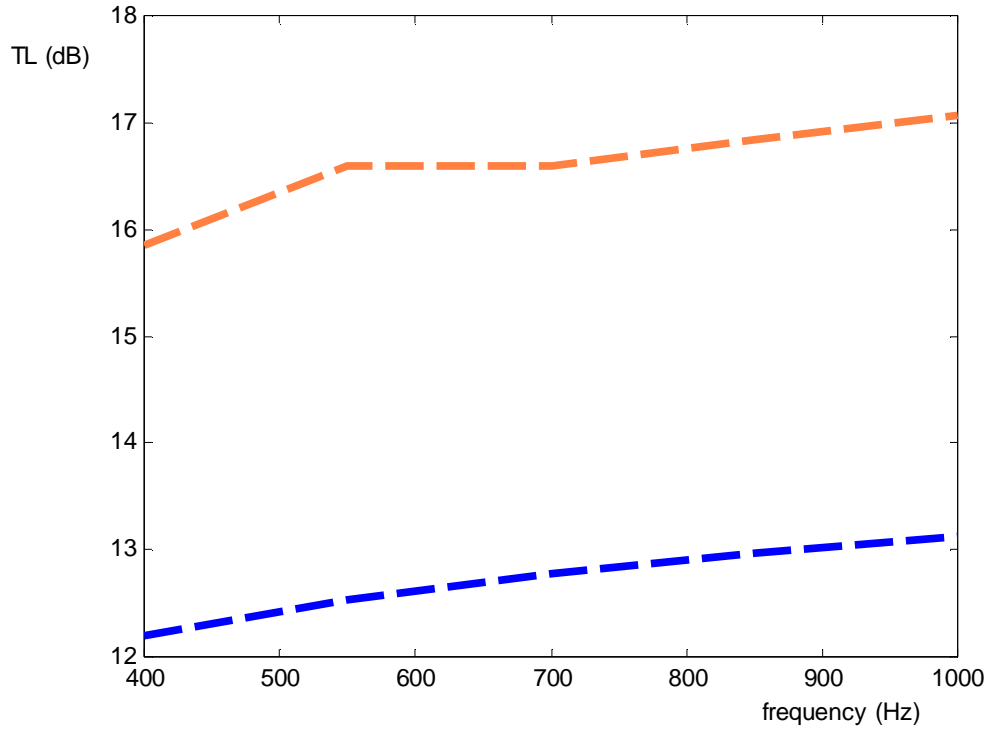


Figure (25): transmission losses against frequency under the case of hot conditions ($T=1000$ C), --- (With no soot layer), and --- with soot layer, and $Mach=0.02$.

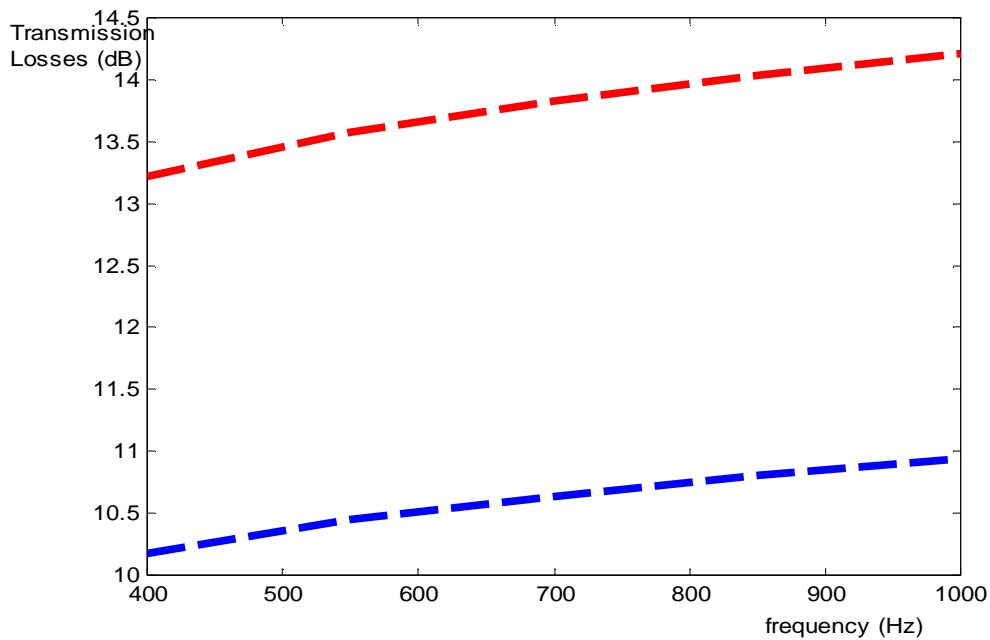


Figure (26): Transmission losses against frequency under the case of hot conditions ($T=500$ C) for typical filter --- for the case of no soot layer, --- for the case with soot layer. $Mach=0.02$, and harmonic in time and 2-D space case.

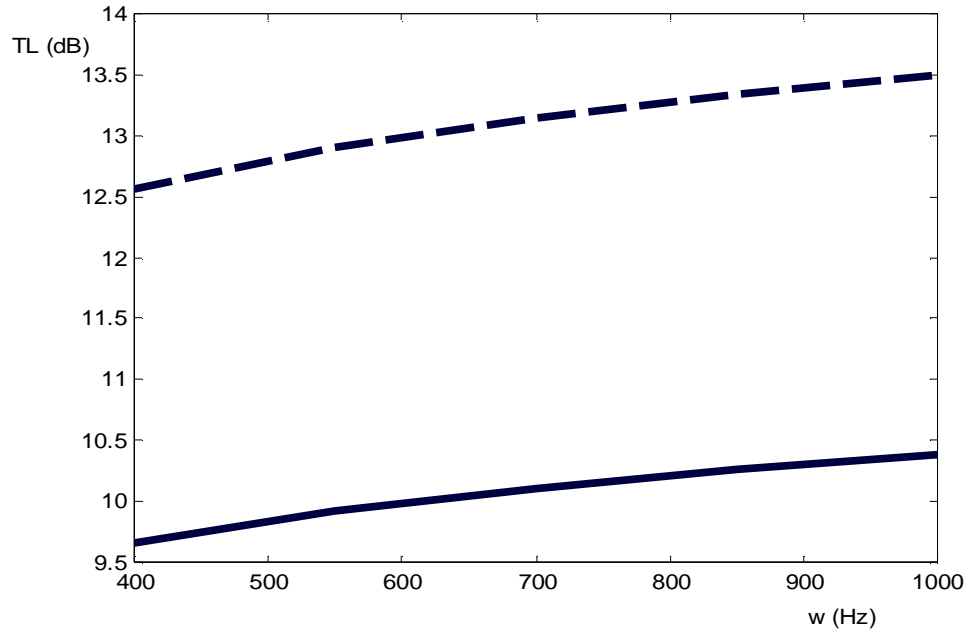


Figure (27): transmission losses against frequency under the case of hot conditions ($T=500\text{ C}$) for RC 200/12 filter type, ---- is for with soot layer, — is for the case of no soot layer, Mach=0.02, and harmonic in time and 2-D space case.

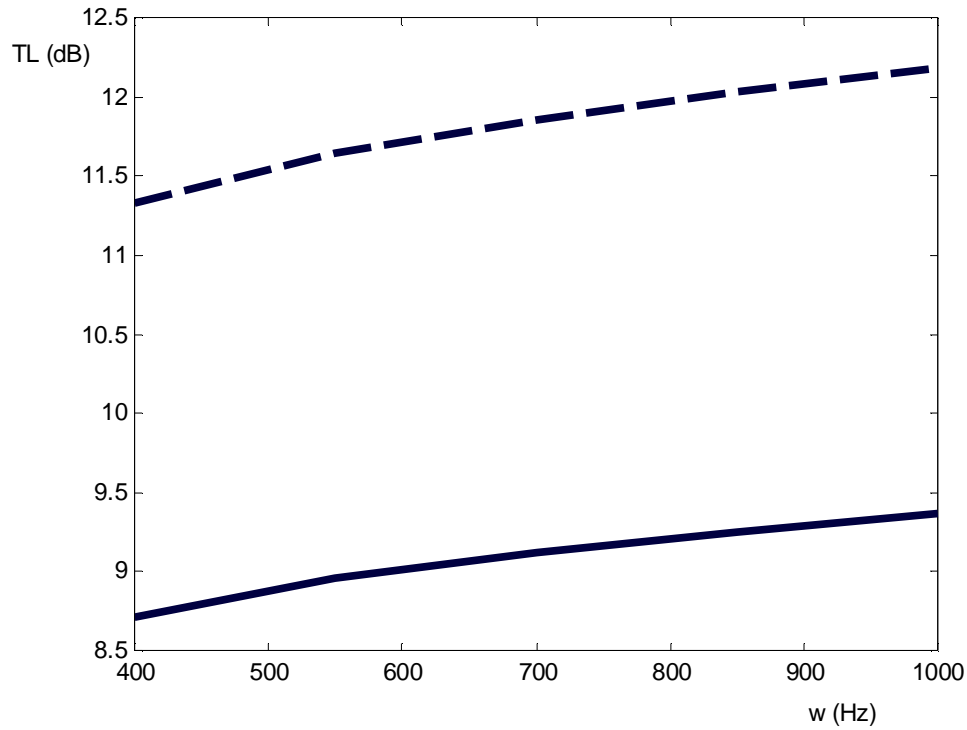


Figure (28): transmission losses against frequency under the case of hot conditions for RC 200/20 filter type, ---- for with soot layer, — is for the case of no soot layer, Mach=0.02, and harmonic in time and 2-D space case, ($T=500^{\circ}\text{ C}$).

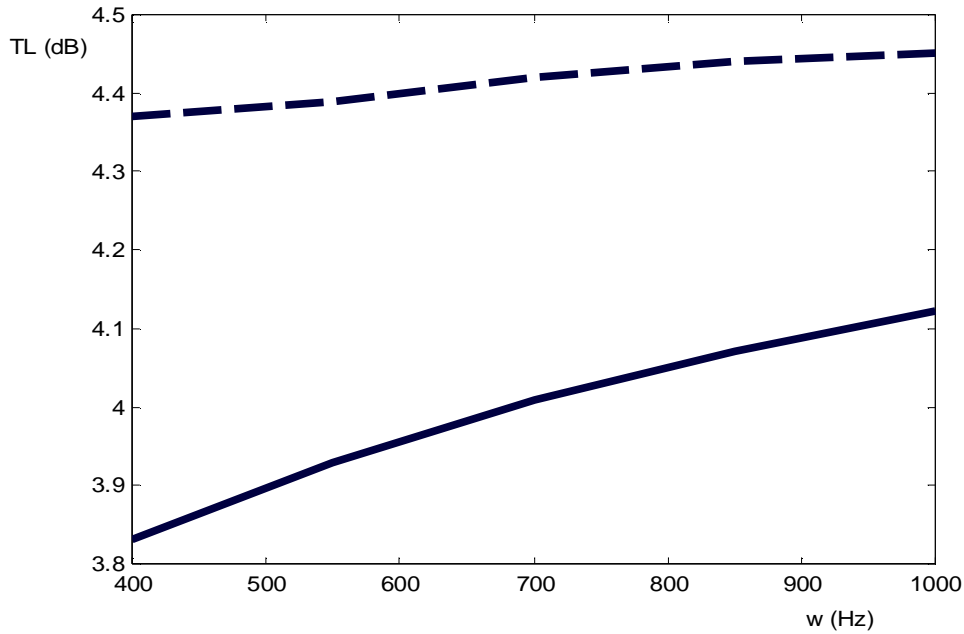


Figure (29): transmission losses against frequency under the case of hot conditions for EX: 100/17 filter type, ----- for with soot layer, — is for the case of no soot layer, Mach=0.02, and harmonic in time and 2-D space case, ($T=500^{\circ}\text{C}$).

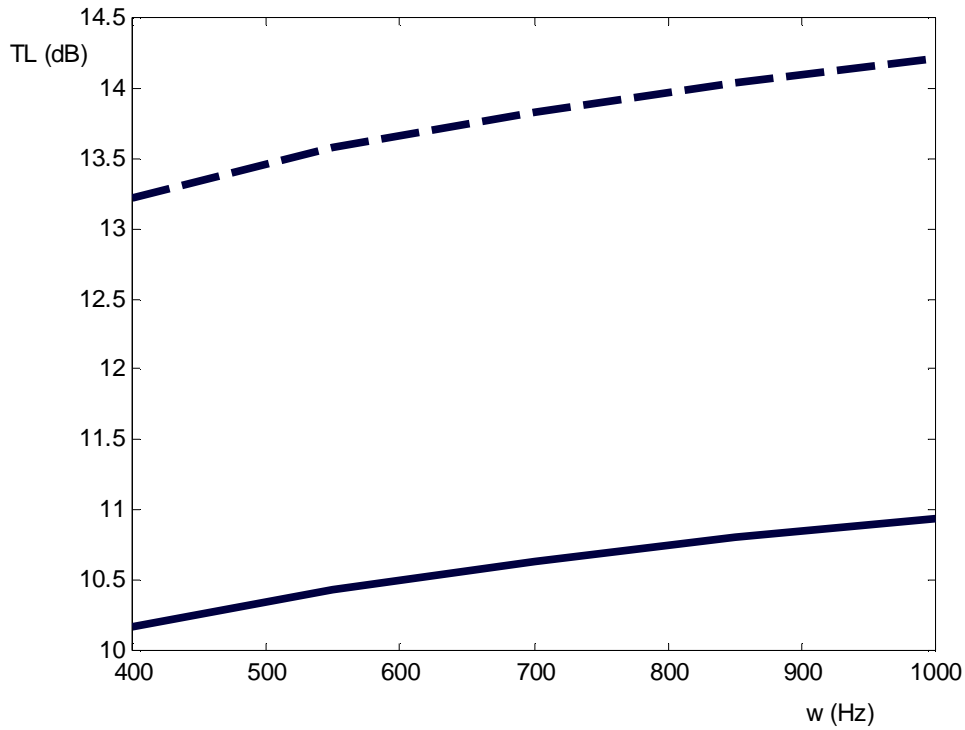


Figure (30): transmission losses against frequency under the case of hot conditions for EX: 200/14 filter type, ----- for with soot layer, — is for the case of no soot layer, Mach=0.02, and harmonic in time and 2-D space case, ($T=500^{\circ}\text{C}$).

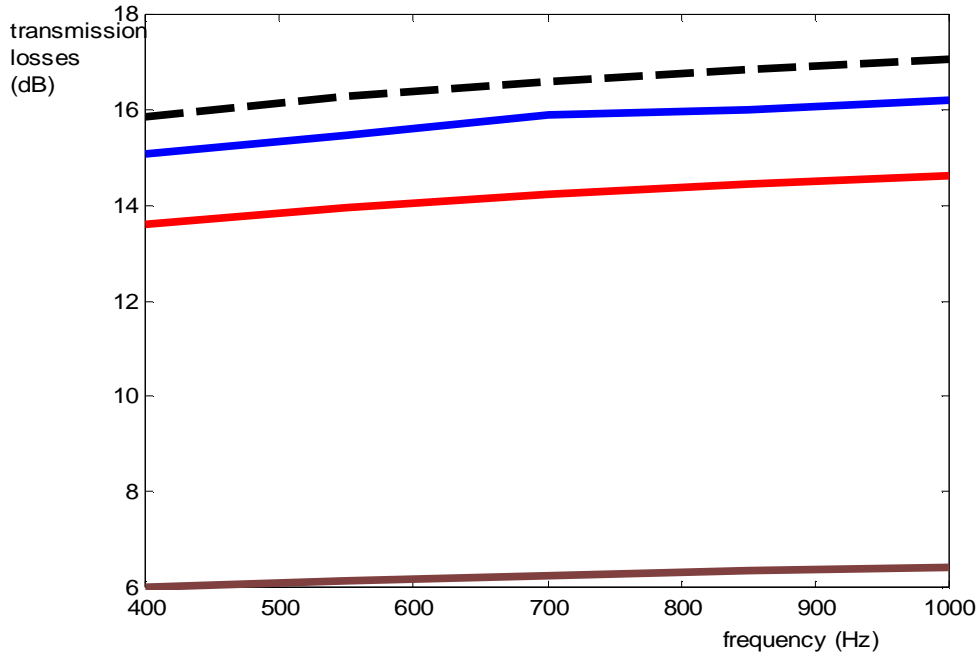


Figure (31): transmission losses against frequency, — for RC:200/12,-----for EX80:200/14,—— for EX80:100/17, and — for RC:200/20 DPF unit type under the case of cold conditions $T=1000$ C, (With soot layer), and $Mach=0.02$.

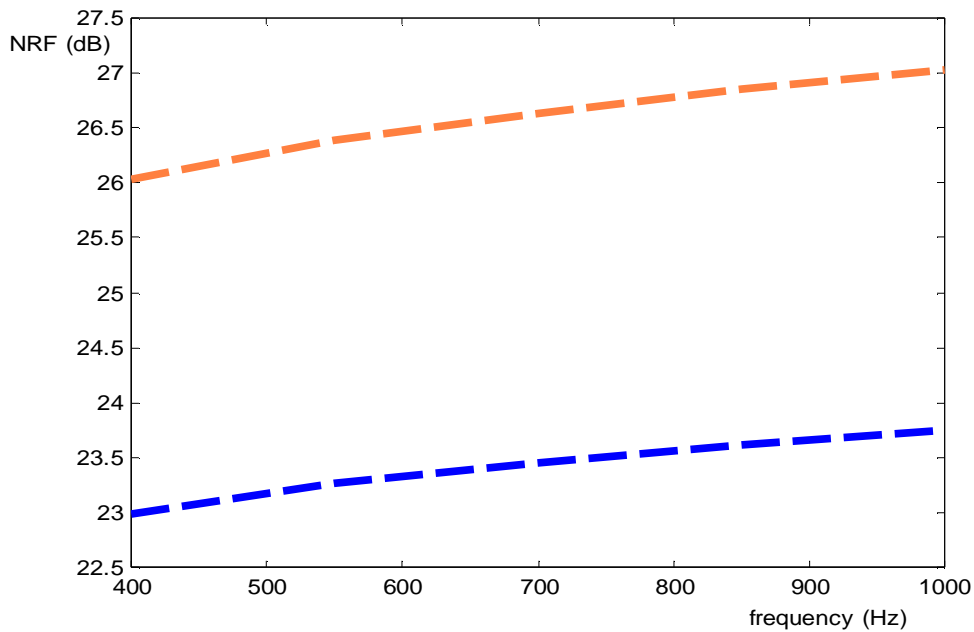


Figure (32): NRF against frequency for typical DPF under the case of hot conditions ($T=500$ C),----- (With no soot layer), and -----for the case with soot layer. $Mach=0.02$, under the case of harmonic in time and 2-D space.

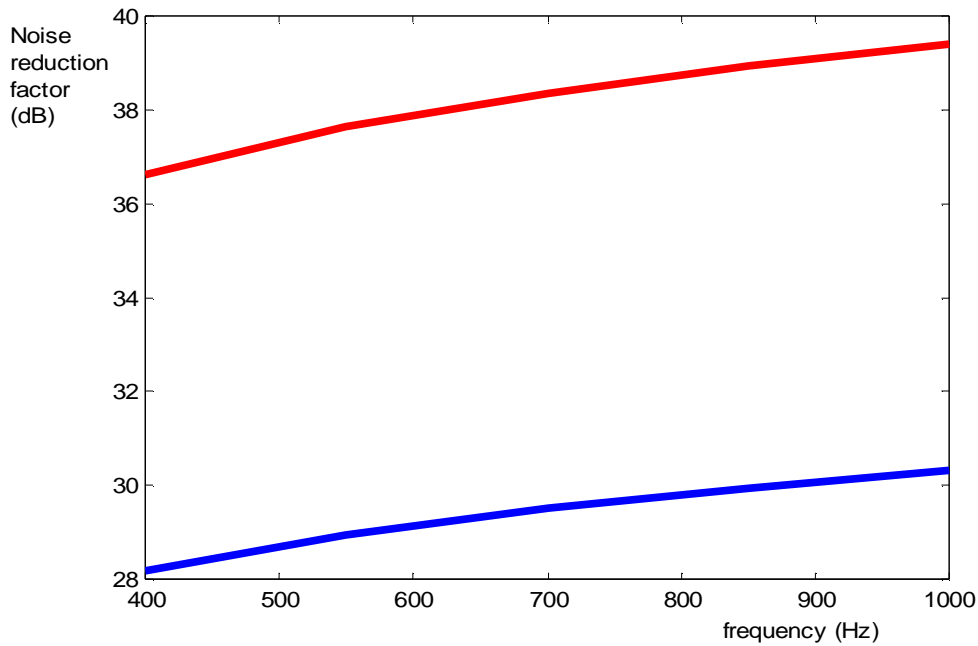


Figure (33): Noise reduction factor against frequency for typical DPF under the case of hot conditions ($T=1000$ C), — with soot layer, and — with no soot, Mach=0.02.

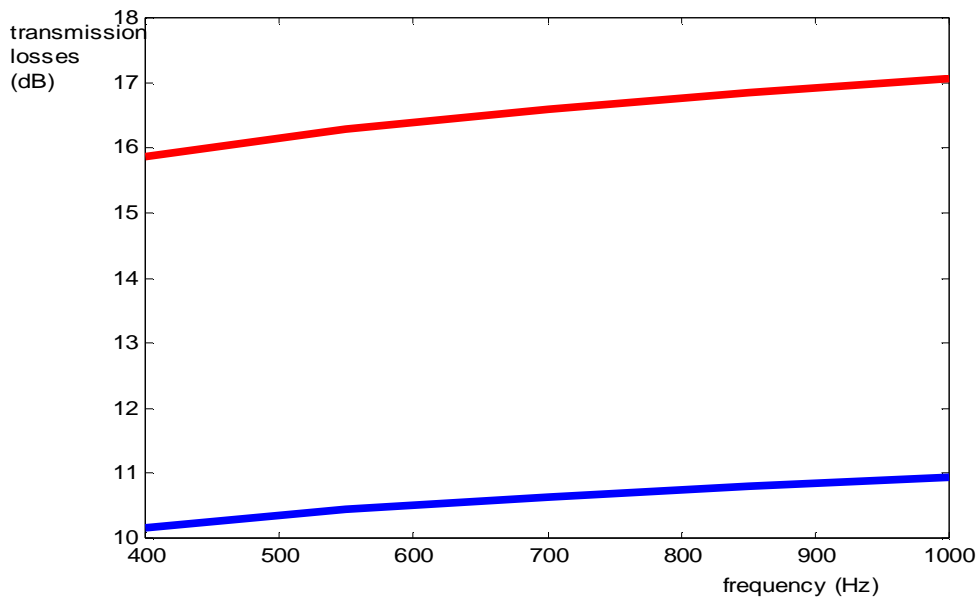


Figure (34): Transmission losses against frequency for typical DPF under the case of hot conditions : — for $T=1000$ C, and — for $T=500$ C, with soot, Mach=0.02.

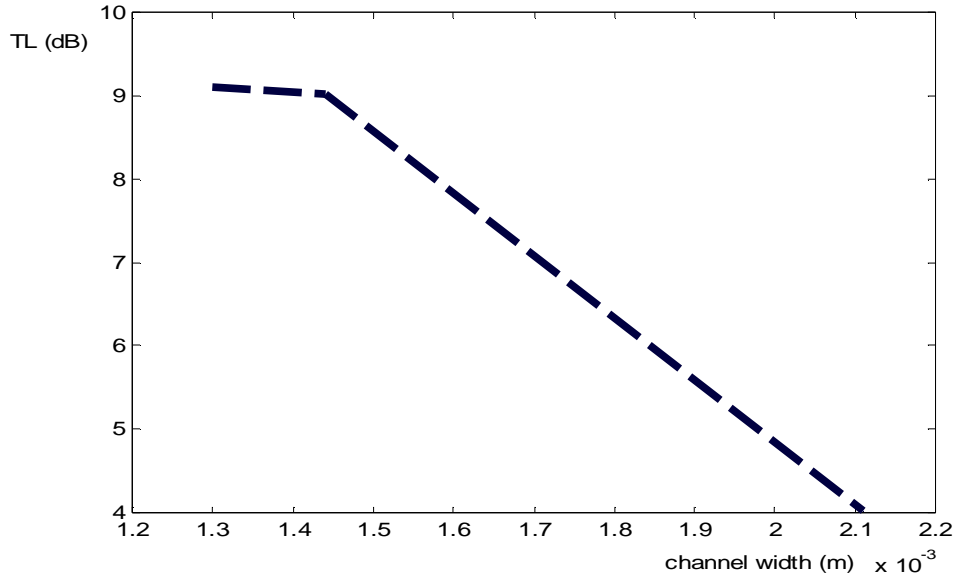


Figure (35): TL against channel width at $w=700$ Hz, with soot layer, harmonic in time and 2-D space case, and under hot conditions.

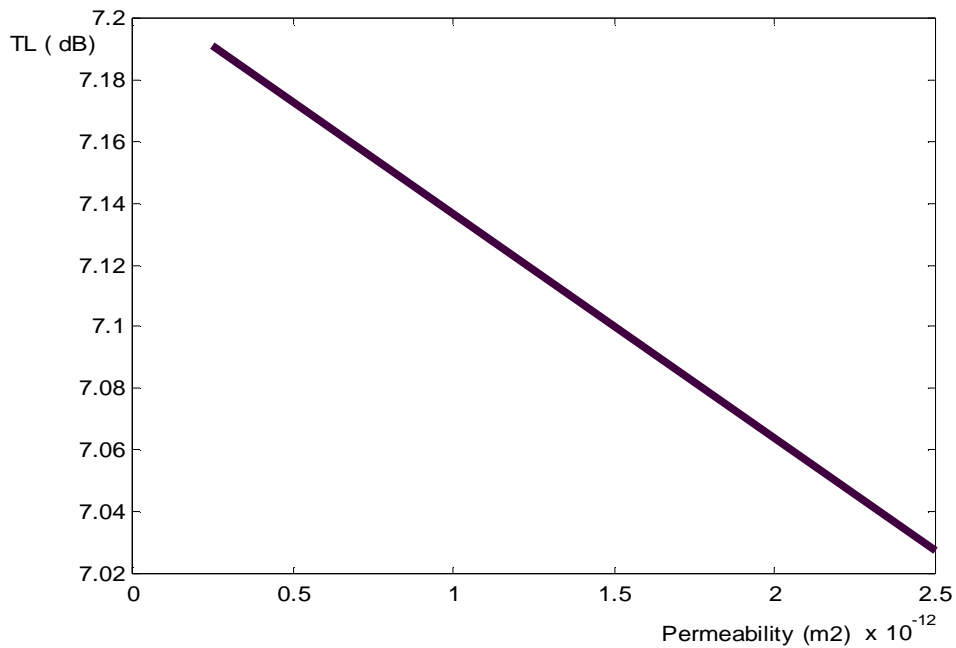


Figure (36): TL against permeability at $w=700$ Hz, with no soot layer, time harmonic variation, and under hot conditions.

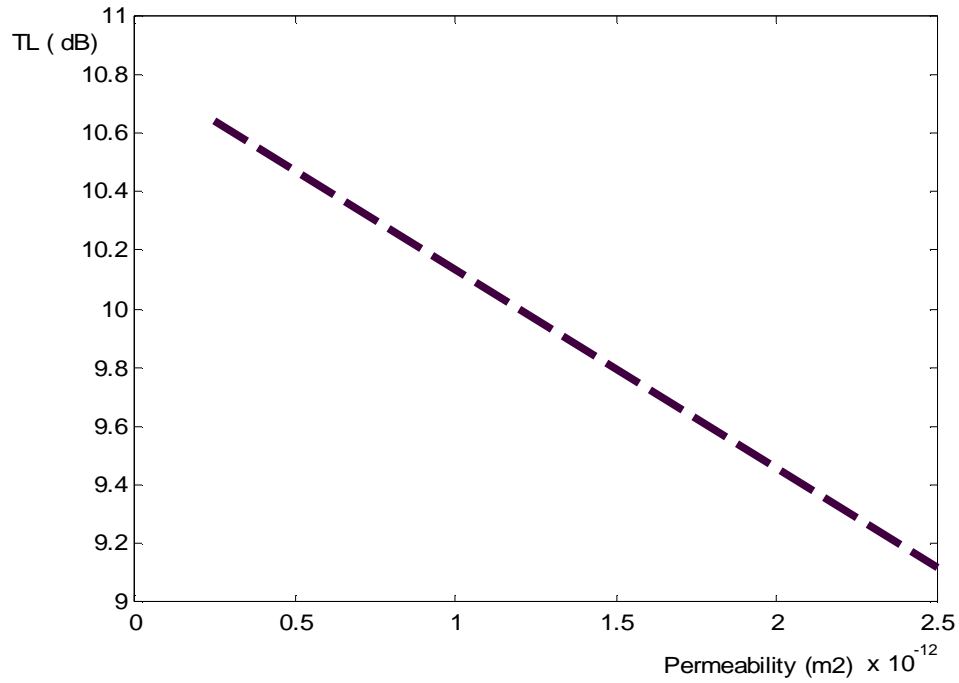


Figure (37): TL against permeability at $w=700$ Hz, with no soot layer, harmonic in time and 2-D space case, and under hot conditions.

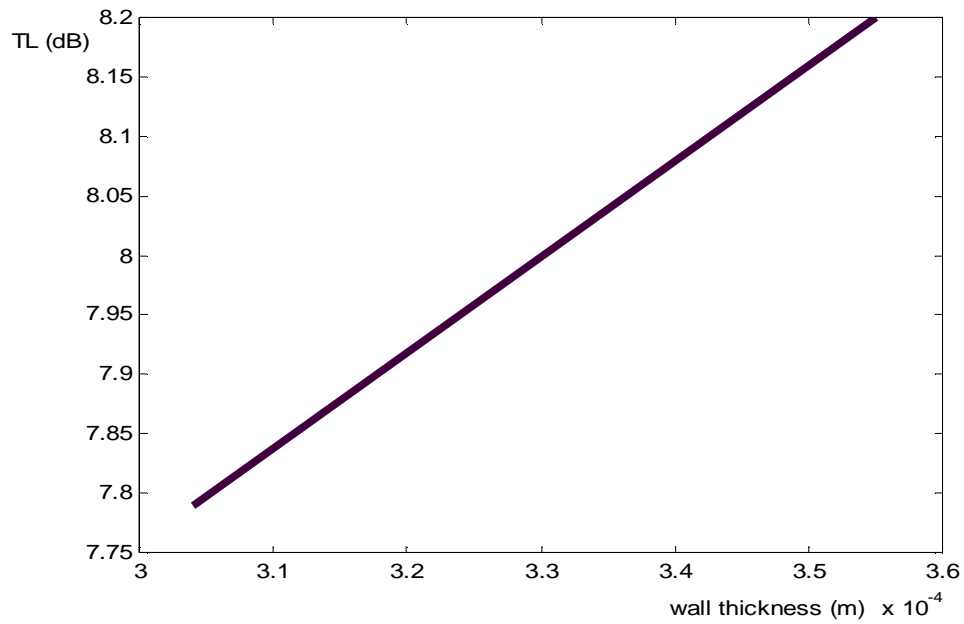


Figure (38): TL against Wall thickness at $w=700$ Hz, with no soot layer, time harmonic variation, and under hot conditions.

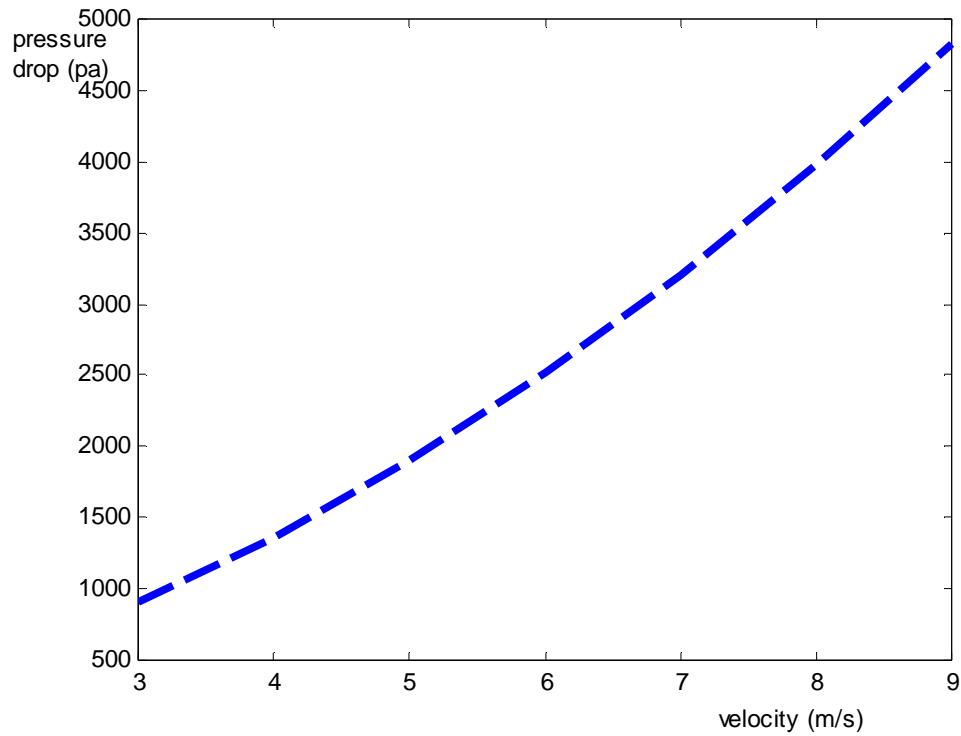


Figure (39): pressure drop against axial velocity for typical filter.

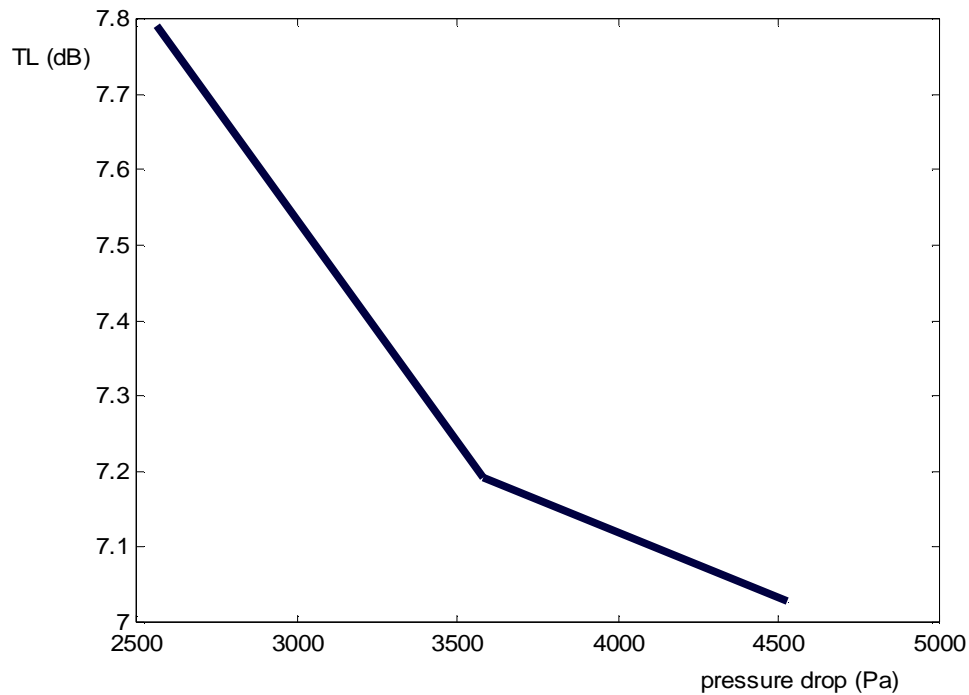


Figure (40): TL against Pressure drop at $w=700$ Hz, with no soot layer, time variation, and under hot conditions.

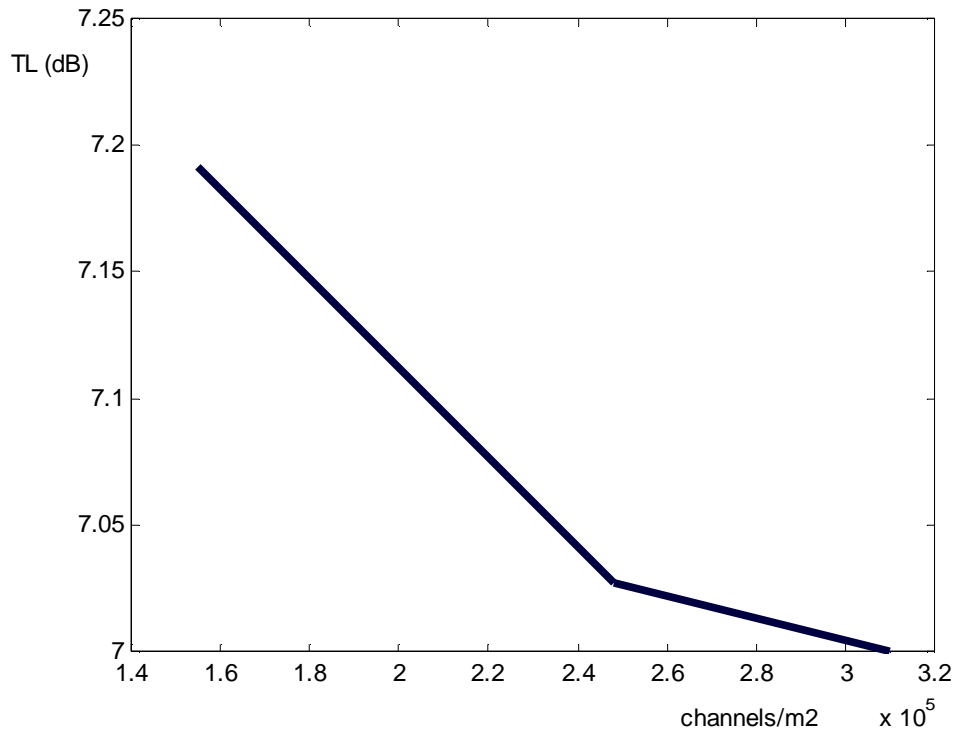


Figure (41): TL against Channel/ m² at w=700 Hz, with no soot layer, harmonic in time and 2-D space case, and under hot conditions.

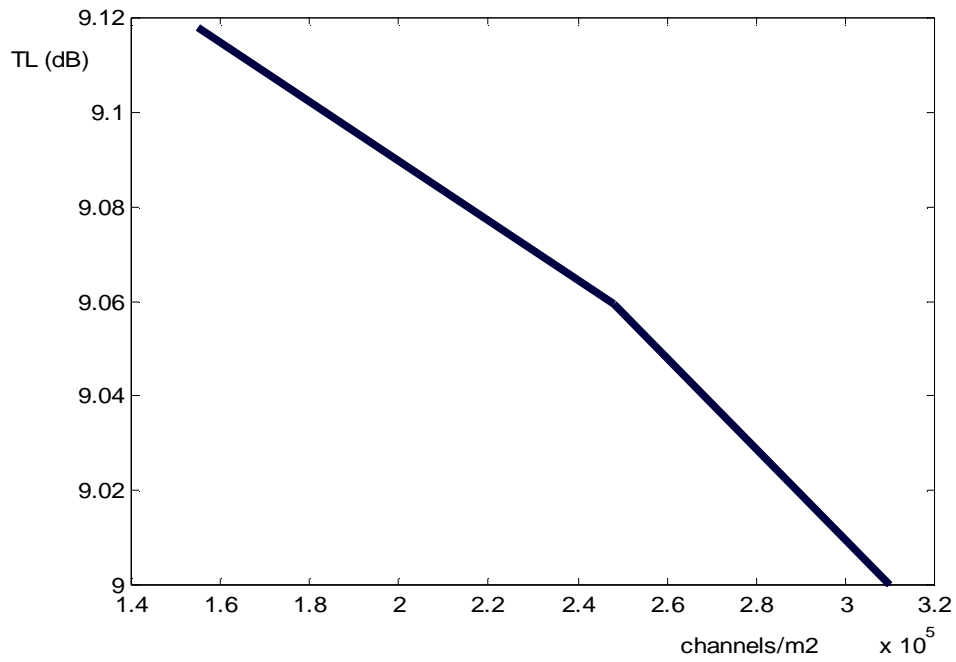


Figure (42): TL against Channel/ m² at w=700 Hz, with no soot layer, time variation, and under hot conditions.

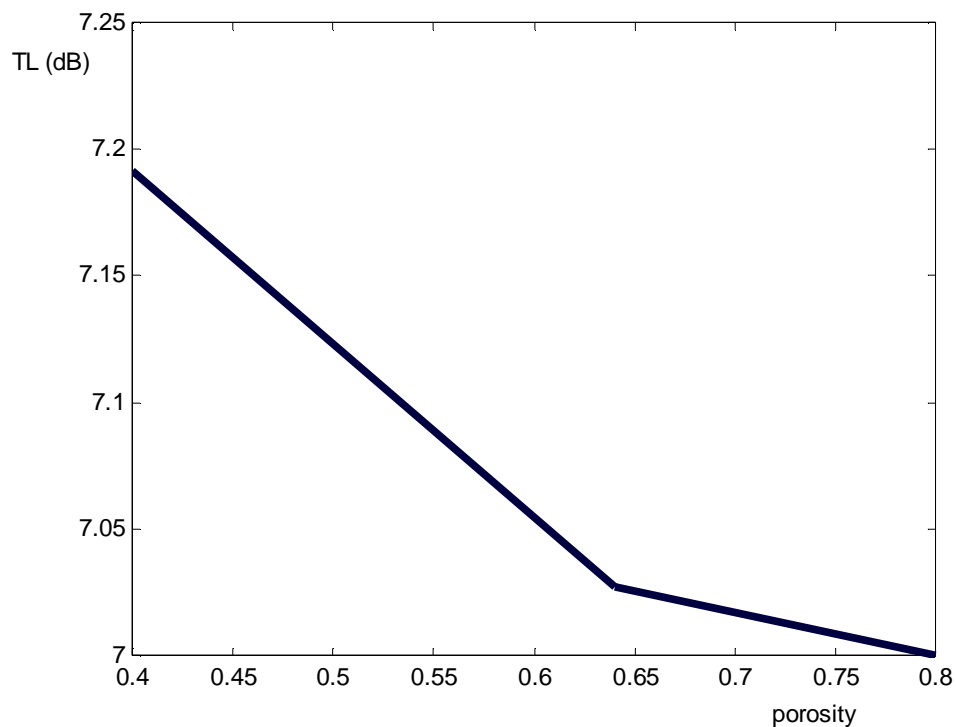


Figure (43): TL against porosity at $w=700$ Hz, with no soot layer, time variation, and under hot conditions.

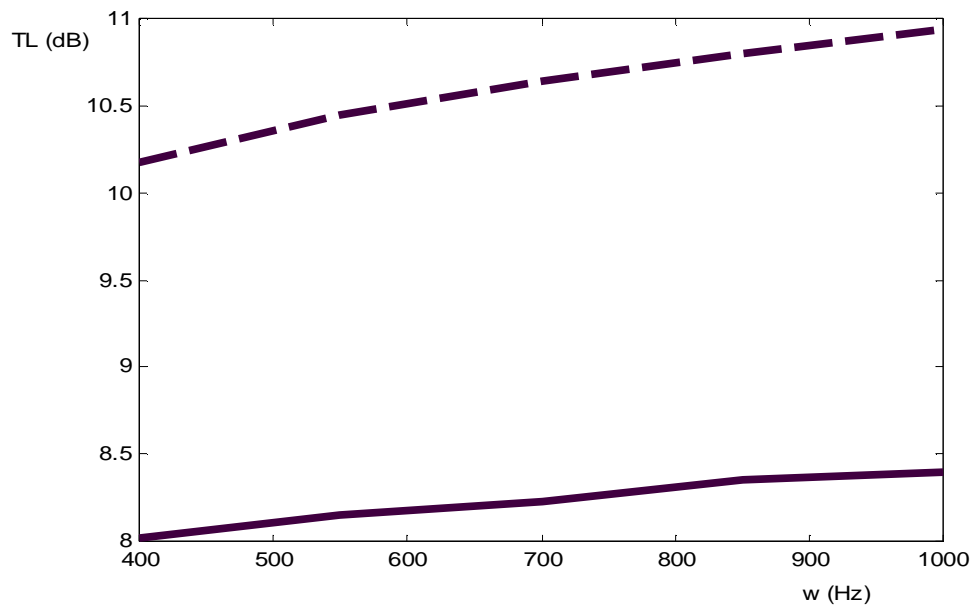


Figure (44): TL against frequency, for typical filter with no soot layer, ----- for the case of harmonic in time and 2-D space case, ——— for time harmonic variation, $M=0.02$, and under hot conditions.

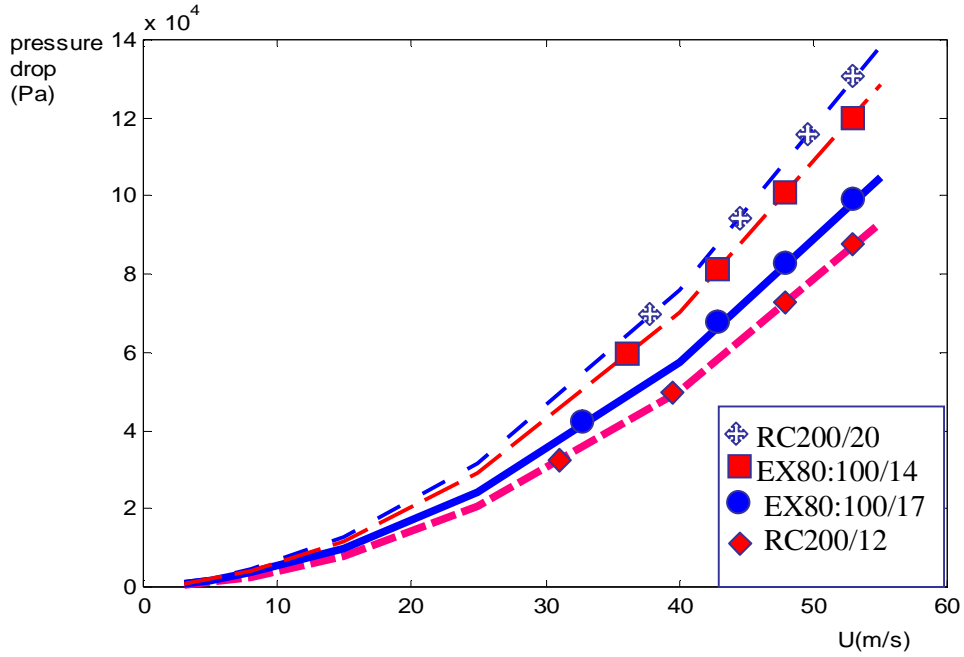


Figure (45): pressure drop for different types of DPF against velocity.

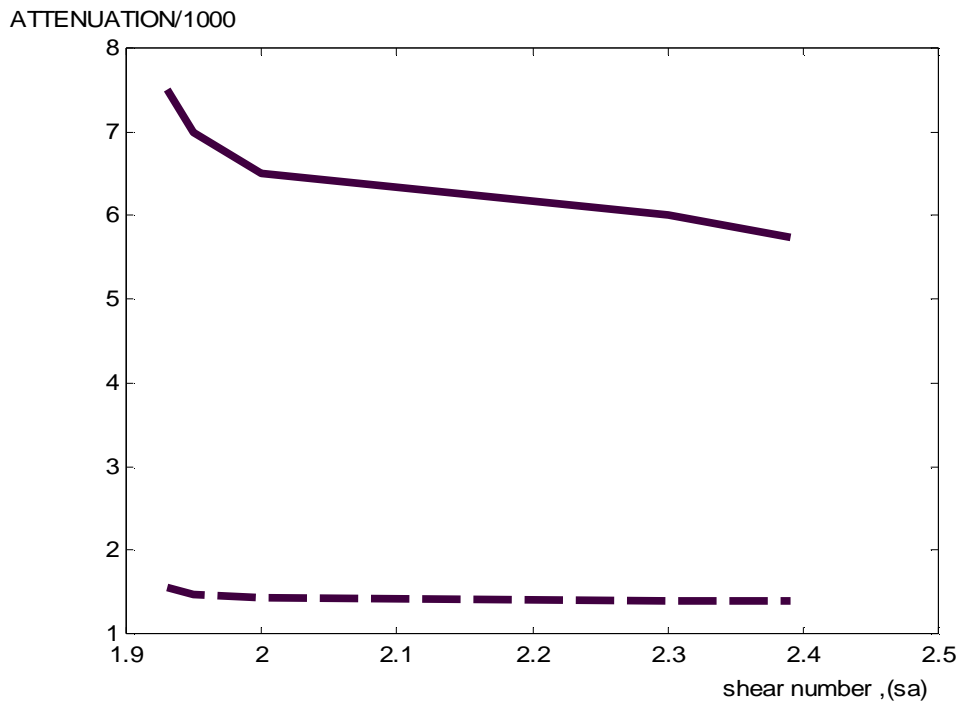


Figure (46): Attenuation against shear number comparison ----- for the present study, ——— for Allam, under hot conditions.

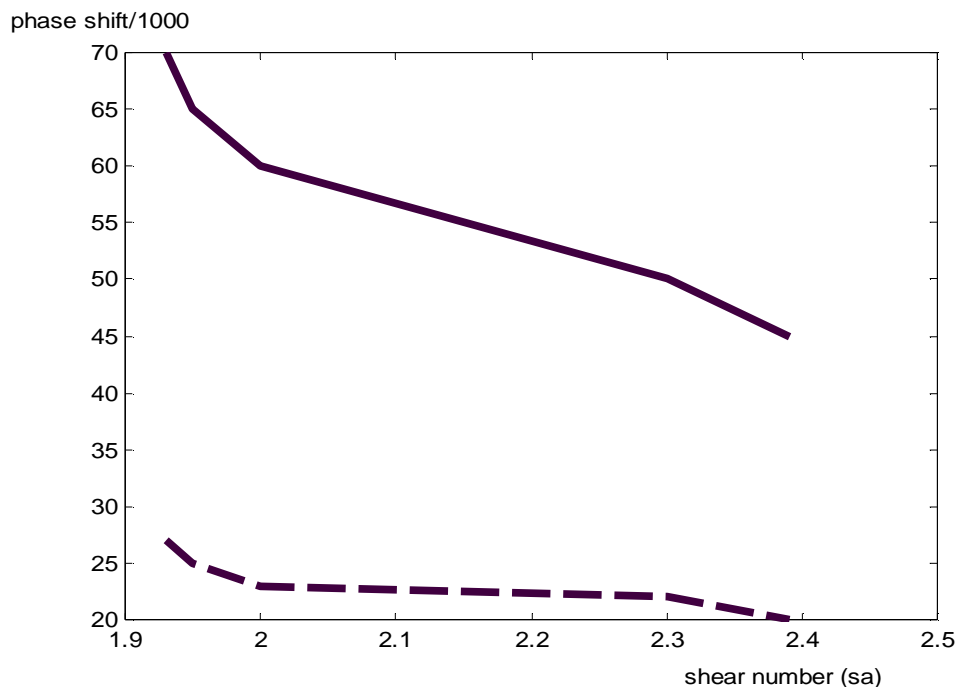


Figure (47): phase shift against shear number comparison ----- for the present study, ——— for Allam, under hot conditions.

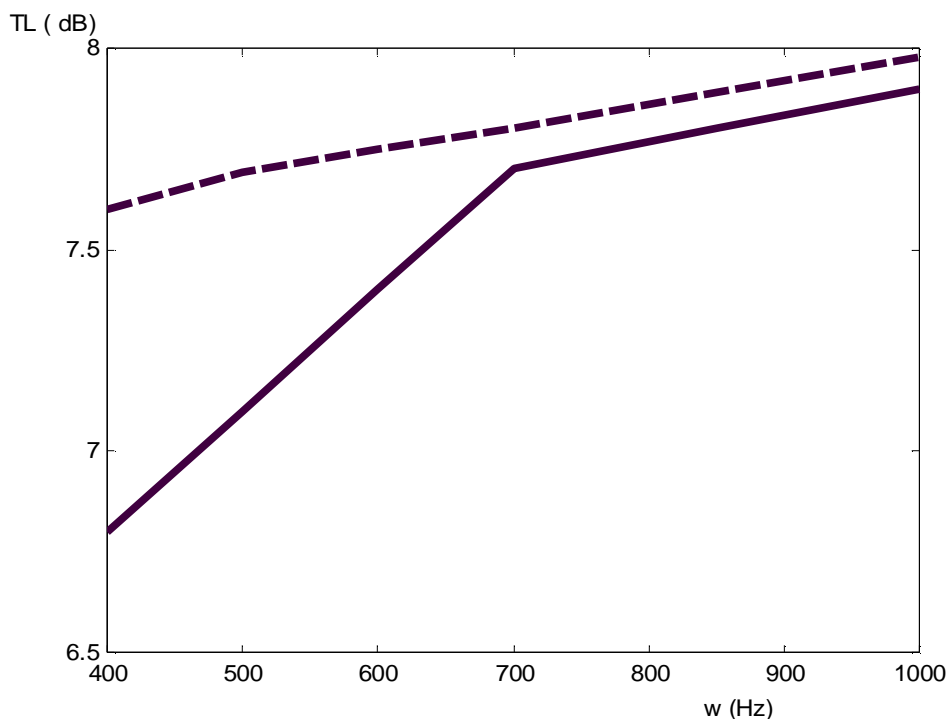


Figure (48): transmission losses against frequency for RC: 200/12 DPF unit type under the case of hot conditions compared with experimental studies by Allam (2006), ----for present study, ——— is for the measured values, (With no soot layer), and Mach=0.02.

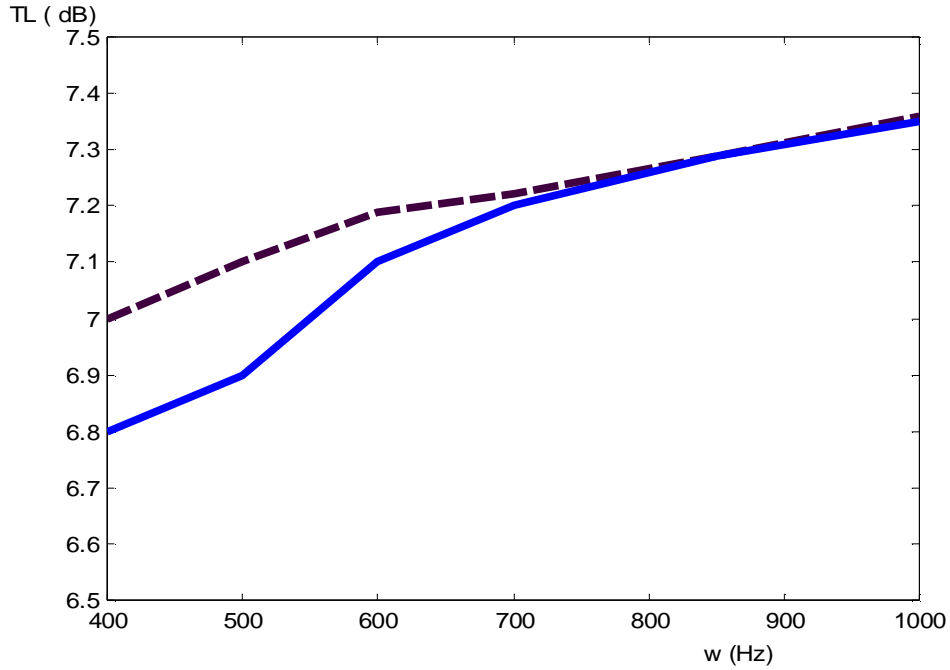


Figure (49): transmission losses against frequency for EX: 100/17 DPF unit type under the case of hot conditions compared with experimental studies[Allam (2006)], ---for present study, , and — is for the measured values, (With no soot layer), and Mach=0.02.

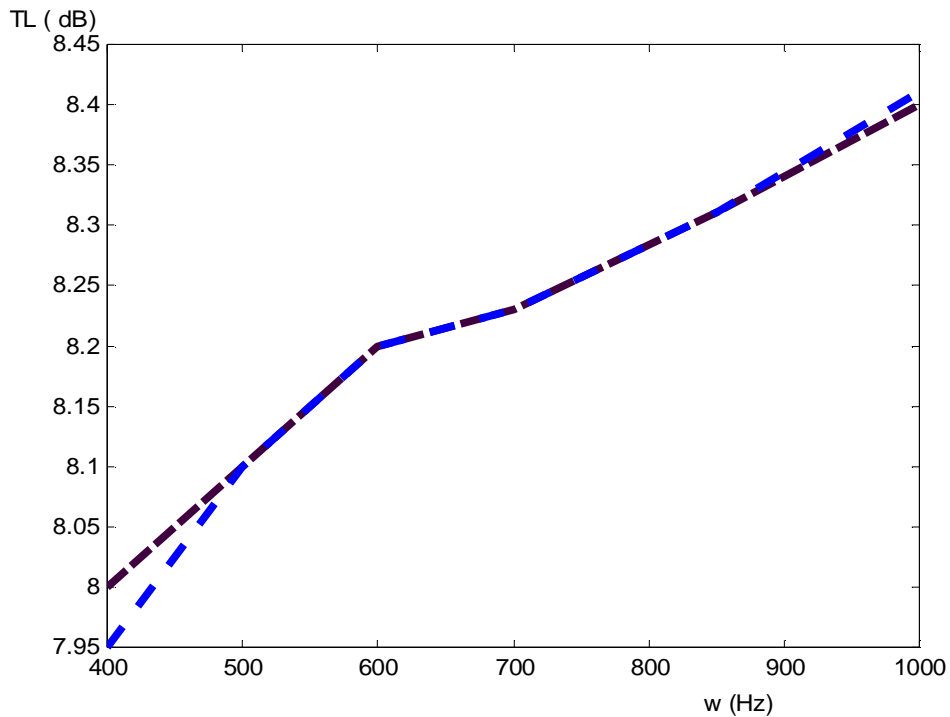


Figure (50): transmission losses against frequency for EX80: 200/14 DPF unit type under the case of hot conditions compared with experimental studies[Allam (2006)], --- for present study, -----is for the measured values by Allam(2006), (With no soot layer), and Mach=0.02

9.3 Discussion

Figures 10 through 17 show the wave propagation constants for the two mentioned approaches or models: the four-port model (time harmonic variation only) and the six-port model (harmonic in time and 2-D space variations) and under both cold and hot conditions.

Figure (10) and (11) represent the real part of the wave propagation constant; Γ_1 , Γ_2 , Γ_3 , and Γ_4 (which represent the attenuation) against the shear wavenumber for the case of time harmonic variation only (four-port model), and under the hot conditions; $T=500$ °C and $T=1000$ °C respectively. These real parts of the roots corresponding to uncoupled waves. From last two figures it can be noticed that as the shear wavenumber increases these real parts are decreased; because as the shear wavenumber increases the shear forces increase and the reactive and dissipative processes are increased too, because of the interactions between the acoustic field and the entropy (diffusion of heat) and the vorticity field (diffusion of shear waves); these effects are created on the boundary walls and that extracts energy from the acoustic waves. Due to the same reason the attenuation (real part of the wave propagation constant) is decreasing with the increase in shear wave number in figures (14) and (15) which represent the attenuation against the shear wavenumber; for the case of harmonic in time and 2-D space variation and under hot conditions $T=500$ °C and $T=1000$ °C respectively.

Figures (12) and (13) represent the imaginary parts of these roots (phase shift) against the shear wavenumber for the case of time harmonic variation only under the hot conditions; $T=500$ °C and $T=1000$ °C respectively. It can be noticed that the phase shift decreases as the shear wavenumber increase because as the shear wavenumber increase more shear forces appear and this will affect by decreasing the values of wave propagation constant, i.e. the phase shift. These parts correspond to the coupled waves

that are significantly more damped than the uncoupled waves because they are coupled and hence the resultant is their sum while for the uncoupled roots the resultant is their difference. Due to the same reason the phase shift is decreasing with the increase in shear wavenumber in figures (16) and (17) which represents the imaginary parts of these roots (phase shift) against the shear wavenumber for the case of harmonic in time and 2-D space variation under the hot conditions ($T=500\text{ }^{\circ}\text{C}$) and $T=1000\text{ }^{\circ}\text{C}$ respectively.

Figure (18) describes the transmission losses (TL) against the frequency under the case of time harmonic variation only for the typical filter with soot layer and with no soot layer compared with Allam(2006) under the hot conditions $T=500\text{ }^{\circ}\text{C}$ and $T=1000\text{ }^{\circ}\text{C}$. As shown in this figure the transmission losses are increased with frequency because transmission losses are proportional to frequency, this is obvious from the final mathematical relationship – equation (8.30), and as the frequency increases it means more disturbance and hence, the capacity of the DPF filter is increasing and so more acoustic energy absorption and more transmission losses. By comparing TL of the proposed study with that presented by Allam (2006): it can be noticed that there is an improvement in the proposed study. The reason that TL values for the proposed study are higher than those presented in Allam (2006) is that the proposed study deals with the flow of gases emission as a 2-D flow and so the flow in the transverse direction (y-direction) is not negligible as in last studies, hence TL can be of a noticeable value in the transverse direction. At high frequencies it can be noticed that there is a good agreement between the two studies and the behaviour is the same and the values are converged; this is because the systems at high frequencies become more stable.

Figures (19) through (22) describes TL for the typical filter with soot layer compared with that of Allam (2006) at $\text{Mach}=0.02$. It can be noticed from the figure that there is a

good agreement in the behavior of the two studies, but the TL for the proposed study is higher than that of Allam (2006) because it takes into accounts the effect of transverse velocity, but a more agreement at high frequencies is achieved because the systems at high frequencies become more stable and the sound propagation becomes isothermal at high frequencies.

Figures (19) through (22) represent TL of different types of DPF unit with no soot layer, compared with results given by Allam (2006), under the case of hot condition and time harmonic variation only, and it can be noticed from these figures that there is a good agreement in the behavior of TL against the frequency between the two studies; the present and that of Allam, but there is some improvement for the proposed study because the present study is taking into account the effect of transverse velocity. Hence, more acoustic transmission losses and more noise reduction.

Figure (23) represents the TL of different types of DPF against frequency with soot layer, it can be noticed that EX80:200/14 DPF type has a good property in transmission losses, but EX80:100/17 DPF type has less ability to do this. Because EX80: 200/14 has a good properties and suitable dimensions compared with other DPF types; include low channel width, low permeability, high wall thickness, low porosity, and making high pressure drop.

Figure (24) shows noise reduction factor (NRF) against frequency for typical DPF unit, with soot and with no soot layer, it can be noticed from the figure that the noise reduction is proportional to frequency since it is proportional to transmission losses as shown in equation (5.41). From last figure it can be noticed that the values of noise reduction factor in the case of soot layer is higher than those of with no soot layer because the soot layer represents a new absorber for sound waves and hence, more transmission losses and noise reduction.

Figures (25) through (30) show the TL versus frequency for the typical DPF unit and other types under hot condition, time harmonic variation only and harmonic in time and 2-D space cases; with soot layer and with no soot layer, and $M=0.02$. From last figures it can be noticed that the transmission losses with the existence of soot layer are higher than those with no soot layer for the above mentioned reasons.

Figure (31) represents the transmission losses for different types of DPF unit against frequency, at $T=1000\text{ }^{\circ}\text{C}$, from figure it can be noticed that EX80:200/14 DPF type has the best property to make transmission losses, but EX80:100/17 DPF type has the lowest property to do this, because EX80:200/14 DPF unit has a good specifications and diminssions (properties) which give it the ability to make more transmission losses and noise reduction.

Figure (32) and (33) represent the relation between noise reduction factot and the frequency under the case of hot conditions $T=500\text{ C}$, and $T=1000\text{ C}$ respectively, with soot layer and with no soot layer, from figures it can be seen that noise reduction values for the case of with soot layer are higher than that of with no soot layer for the reasons mentioned above.

Figure (34) comparing between values of transmission losses at two operating temperatures: $500\text{ }^{\circ}\text{C}$ and $1000\text{ }^{\circ}\text{C}$, it can be noticed that the temperature plays a significant role which affecting transmission loss and hence, noise reduction. The figure shows that transmission losses increase as the temperature increases, since values of these two quantities (TL and NRF) are increasing as the temperature becomes higher. The reason for this is that as the temperature increase the regeneration of the filter becomes fast and more efficient. Hence, a new soot layer is loaded, therefore more transmission losses in sound waves and more noise reduction is occurred.

Figure (35) relate TL to channel width of the DPF unit for the case of harmonic in time and in 2-D space (under hot condition), it can be noticed that as the channel width increases the TL decreases, because space inside the DPF unit becomes larger, so sound absorption by channels decreases and hence TL decreases.

Figure (36) and (37) relate TL to permeability of the DPF unit in both cases time variation only (under hot conditions) and for the case of harmonic in time and in 2-D space (under hot condition, $w=700$ Hz) respectively, it can be noticed that as the permeability increases the TL decreases, because as the permeability increases sound absorption by walls between channels decreases but more gases reduction.

Figure (38) shows that as the wall thickness of the channel increases TL increase because the filter becomes more solid and hence it absorbs or prevents more sound waves and so TL increase.

Figure (39) represents the relation between pressure drop along the typical DPF unit and the axial velocity, and it can be noticed that as the velocity increases pressure drop also increase (as the velocity increase pressure decrease). At the same time, as the pressure drop increases TL for the typical filter decreases, as shown in figure (40) the reason beyond this is that as the pressure drop increases –hence velocity of gases emission flow increase- time for flow to be go through the porous walls decreases, so TL decrease.

Figure (41) and (42) represent the relation between TL and number of channels per square meter at no soot layer, under hot conditions ($w=700$ Hz), for the case of harmonic in time and in 2-D space and time harmonic variation only respectively. From last two figures TL decreases as channels/m² increases, because as the number of channels increases the DPF becomes as a hollow cylinder and so noise reduction becomes less so TL decreases. At the same time as the number of channels increases, the DPF unit porosity also increases and so TL will decrease as shown in figure (43).

Figure (44) comparing between values of TL for the typical filter under hot conditions in both cases time harmonic variation only and for the case of harmonic in time and in 2-D space. From this figure it can be noticed that TL for the case of harmonic in time and in 2-D space (six-port model) are higher than that of time harmonic variation (four-port model), i.e. an improvement at this stage is achieved. The reason behind this is that the six-port taking into account more the effects of the interfering between channels and hence, more losses for the acoustic transmission is appeared.

Figure (45) represents pressure drop versus the axial velocity of gases flow through the different types of DPF unit, from figure it can be noticed that ΔP for EX80: 200/14 DPF unit type is higher than other types, for RC: 200/14 it is the lowest. But at low velocities it can be noticed that EX80: 200/14 DPF unit type has the lowest pressure drop, hence it has a maximum values of transmission losses.

In figure (46) and (47) there are a comparison between values of attenuation and phase shift against shear wavenumber, under hot conditions with no soot layer for the presented study and previous study made by Allam (2006), from figures it can be noticed that both attenuation and phase shift values determined by Allam have higher values than the presented study, the main reason for this is that the last studies treated the problem as a 1-D model, by neglecting the transverse velocity so waves attenuation and phase shift are more than the presented study which takes into account the effect of transverse velocity (2-D model) since the presented studys transmission losses values are higher than that of Allam(2006). To make verification for the new model a comparison is made between values of TL for different types of DPF units of the presented study with those of the experimental values presented by Allam (2006) and Allam (2005).

Figure (48) through figure (50) represent a comparison between values of transmission losses of the new presented model (at the case of time harmonic variation only) and experimental values of TL presented by Allam(2006). It can be noticed that TL for the presented study is higher in some cases than the experimental by about 1-2.5 dB, in some other cases there is a good agreement between them (0.05 dB difference) as can be noticed from figure (50).

Figures (54) through (75) represent numerical solution or results for the laminar flow in porous media (DPF unit), the figures represent the model, temperature distributions and profiles, axial and transverse velocities distributions and profiles, pressure distributions and wall shear at both conditions cold ($T=293^{\circ}\text{K}$) and hot ($T=773^{\circ}\text{K}$, and $T=1000^{\circ}\text{C}$).

Figure (54) represents the 2-D finite element model for exhaust gasses flowing through porous media (the DPF unit), the figure shows a porous DPF unit as a meshing pipe.

Figure (55) shows the rate of change of VX, VY, and pressure for the gas flow through the DPF unit at cold conditions, from this figure it can be noticed that all of these quantities decrease with the accumulative iteration number, i. e. with time and flow progress. This is a natural result since pressure and velocity of gasses emission are decreasing as the flow go through the filter, hence a pressure drop will occur, and also the velocity of flow gases is decreased as the flow is in progress.

Figure (56) represents the axial velocity variation profile for gasses emission through the porous media in the radial coordinate under cold conditions, the figure shows that there are fluctuations in the axial velocity variation with the continuity of gasses flow, because the porous DPF unit has variable nature i.e. sometimes rigid edges, pores, and other variable situations, so the velocity will change from place to place and from time to time.

Figure (57) represents outlet temperature variation profile for gasses emission through the porous media in the radial coordinate under cold conditions, the figure shows that there are fluctuations in the outlet temperature with the continuity of gasses flow because of the nature of porous media.

The nodal solution for axial velocity distribution at cold conditions is shown in figure (58), from figure it can be noticed that the axial velocity increases transversly over the tube because gase flow through the pores which considered as nozzles which increases the outlet velocity, while the transverse velocity distribution, V_Y , under cold conditions, is shown in figure (59), and from this figure it can be noticed that the transverse velocity values are changed and not constant depending on the nature of porous material but the variation is very small. From last two figures it can be seen that these velocities has different values from place to another one inside the DPF unit, because as mentioned above that the DPF unit has a variable nature.

Figure (60) represents the pressure distribution through the porous media (DPF) unit under cold conditions, from this figure it can be noticed that the pressure decreases down the pipe from inlet to outlet and this creates the pressure drop, while the total pressure change across the porous media can be noticed in figure (61) axially and transversly, from last figure it can be noticed that the total pressure is increased transversly because the sound pressure increases by some perturbation values. From last two figures it can be seen that a pressure drop for the flow through porous media will occur because of the collisions and interactions between the flow gasses and DPF channels and other component, and a back pressure will develop.

Wall shear for DPF unit is represented in figure (62) under cold conditions. Wall shear has a high value beside the walls and this value decreases rapidly far away from these walls because the shear forces has a higher values near the walls. Temperature

distributions through the porous media under cold conditions are represented in figure (63). From last it is clear that the temperature decreases as the flow continued because the heat dissipated through the porous media and it will be either lose or dissipated by convection, radiation, or conduction. Figure (64) represents the rate of change of VX, VY, and Pressure for the gas flow through the porous media under hot conditions, and it can be noticed from figure that all these quantities suffer of depression with time of flow and this is a natural results because velocities, pressure and temperature decreases as the gasses flow through the porous media.

Figure (65) shows the axial velocity variation profile for gasses emission through the DPF unit under hot conditions, and a big fluctuations can be noticed for axial velocity for the flow through the porous media, this fluctuation is resulted from the variation in axial velocity values as the gases in flow because of the change in nature of the porous media. Figure (66) represents the outlet temperature profile for exhaust gasses emission at hot conditions. From last two figures it can be noticed that both axial velocity and outlet temperature are decreases as the gasses flow is continued, but axial velocity fluctuation is more.

Figure (67) shows the nodal solution for axial velocity distribution under hot conditions, from figure it can be noticed that the axial velocity increases transversly over the tube because gase flow through the pores which considered as nozzles which increses the outlet velocity. Figure (68) shows the nodal solution for transverse velocity distribution under hot conditions, and from this figure it can be noticed that the transverse velocity values are changed and not constant depending on the nature of porous material but the variation is very small. From last two figures it can be seen that these velocities has different values from place to another one inside the DPF unit, because as mentioned above that the DPF unit has a variable nature.

Figure (69) represents the pressure distribution through the porous media under hot conditions, from this figure it can be noticed that the pressure decreases down the pipe from inlet to outlet and this creates the pressure drop.

The nodal solution for temperature distribution under hot conditions can be noticed in figure (70), From last it is clear that the temperature decreases as the flow continued because the heat dissipated through the porous media and it will be either lose or dissipated by convection, radiation, or conduction. Figure (71) represents the total pressure change across the porous media at hot conditions, from last figure it can be noticed that the total pressure is increased transversly because the sound pressure increases by some perturbation values.

Figure (72) shows the vector solution for velocity of gases flow through porous media under hot conditions. From last figure it can be noticed that the velocity values are increased transversly through the porous pipe because the pores works as a nozzels which increases the velocity.

Figure (73) represented the wall shear stress distributions under hot conditions. From last figure it can be noticed that the wall shear values near the wall is higher than that farther than because shear forces near walls are higher. Figure (74) shows the axial velocity distributions under hot conditions. From figure it can be noticed that the axial velocity increases transversly over the tube because gasses flow through the pores which considered as nozzles which increses the outlet velocity.

Figure (75) represents the temperature distributions for gasses flow through porous media under hot conditions. It can be noticed that the temperature distribution decreases transversly because the heat dissipated through the porous media and it will be either lose or dissipated by convection, radiation, or conduction. and hence, the temperature decreases. As shown in last figures in which the results of the two acoustic models are

represented and under both hot and cold conditions, the new models are in a very good agreement with the previous theoretical and experimental data.

Chapter 10

Conclusions and Recommendations

10.1 Conclusions

Two-dimensional acoustic models have been built to study the sound propagation in DPF unit under two cases, under the first case, the parameters: pressure, temperature, density, and velocities were considered to be time harmonic variables, which gave a modified four-port (2-D) acoustic model. The solution of eigenvalue problem of this model gave four roots, then transmission losses have been calculated and a good agreement and an improvement were achieved over the preceding studies. Secondly the parameters are assumed to be harmonic in time and in 2-D space, at this stage a six-port acoustic model has been invented since six roots and six corresponding eigenvectors are resulted. The main conclusions of this work can be summarized as follows:

- Waves propagate through the DPF unit suffer from both attenuation and phase shift, and both of these factors damped as shear wave number increases.
- Both transmission losses and noise reduction factor for the diesel particulate filters are increasing as frequency increases.
- Transmission losses at the case of existing soot layer are higher than those with no soot layer.
- EX80:200/14 DPF unit type has the best capability of transmission losses, while EX80:100/17 DPF type has the lowest capability.
- Transmission losses and NRF are proportional to frequency, and wall thickness.
- Transmission losses and NRF are not proportional to porosity, number of channels per square meter, pressure drop, permeability, and channel width.
- Transmission losses for the case of six-port model have higher values than those of four-port model at the same conditions.

- There is a good agreement between theoretical values of TL of the present study with those available in the literature and also with experimental one.

-The temperature has a significant effect on both transmission losses and noise reduction factor, as the temperature increase both of these quantities are increase.

10.2 Recommendations

For future work it is recommended to extend the problem in 3-D problem, further taking into accounts the non-linearity of the problem, and chemical reactions. It's recommended to study experimentally the effect of DPF location on the reduction of both combustion products and noise.

References

- Allam, S., and Abom, M. (2006). Sound propagation in an array of narrow porous channels with application to diesel particulate filters, **Journal of Sound and vibration**, 291(3-5), 882-901.
- Allam, S., and Abom, M. (2005). Acoustic modeling and testing of diesel particulate filters, **Journal of Sound and Vibration** 288 (1/2), 255–273.
- Allam, S., and Abom, M. (2003). Acoustic modeling of an after treatment device (ATD). **Euronoise, Naples**, paper ID: 399/p.1.
- Allam, S., and Abom, M. (2002). On acoustic modeling and testing of diesel particulate filter. **The 2002 international congress and exposition on noise control engineering, M1, USA**, August 19-21.
- Arenans, J., Gerges, S., Vergara, E., and Aguayo, J. (2004). On the technique for measuring muffling devices with flow. **Acustica 2004**, paper ID: 98/P.1. Brazil.
- Astley, and Cummings, R.A. (1995). Wave propagation in catalytic converter: formulation of the problem and finite element scheme, **Journal of Sound and vibration** 188 (5), 635–657.
- Ballagh, K.O. (2004). Accuracy of prediction methods for sound transmission loss. **The 33rd international congress and exposition on noise control engineering, Prague. Czech.** August 22-25.
- Boden, H., and Abom, M. (1995). Maximum sound power from in-duct sources with applications to fans. **Journal of Sound and vibration**, 187 (3), 543--550.
- Boden, H., and Abom, M. (1990). Characteristics of acoustic two-port sources. **Proceedings- international conference of noise control engineering**, p 541.
- Boden, H., Abom, M., and Glav, R. (1988). Acoustic model for automobile catalytic converters. **Proceedings- international conference of noise control engineering**, p 1261.
- Boij, S., and Nilsson, B. (2001). Reflection of sound at area expansion in a flow duct. **Journal of Sound and Vibration** 260, 477-498.
- Cummings, A. (1993). Sound propagation in narrow tubes of arbitrary cross-section. **Journal of Sound and Vibration** 162 (1), 27-42.
- Chen, M., and Karen, S. (2003). A modeling approach to the design optimization of catalytic converters of I.C. engines. **ASME, ICEF03**.
- Davies, P.O. (1988). Practical flow duct acoustics, **Journal of Sound and Vibration** 124 , 91–115.

De wiest, R.J.M. (1969). **Flow through porous media**, Academic Press, INC, New York, USA.

Dokumaci, E. (1998). On transmission of sound in circular and rectangular narrow pipes with superimposed mean flow, **Journal of sound and vibration** 210 (3), 375–389.

Dokumaci, E. (2001). An approximate dispersion equation for sound waves in a narrow pipe with ambient gradients, **Journal of Sound and Vibration** 240 (4), 637–646.

Dokumaci, E. (1995). Sound transmission in narrow pipes with superimposed uniform mean flow and acoustic modeling of automobile catalytic converters, **Journal of Sound and vibration** 182, 799–808.

Eugen, S. (1971). **The foundations of acoustics**, Springer-verlag, Wien New York.

Fairbrother, R., and Tonsa, M. (2003). Acoustic simulation of after treatment devices using linear and nonlinear methods. **Tenth international sound and vibration**, 7-10 July 2003, Stockholm, Sweden.

Francisco, S., and Jaime, P. (2004). Guidelines for the acoustic design of absorptive devices. **Institute of acoustics (CSIC), C. Serrano**, 144, 28006 Madrid, Spain.

Greevesm, G. (1977). Origins of hydrocarbon emission from diesel engines. **SAE tans.** 86.

Hassall, J. R., and Zaveri, K. (1988). **Acoustics noise measurements**. 5th edition, 1st print, Sewden.

Holzbecher, E.O. (1998). **Modeling density-driven flow in porous media**. Springer-verlag Berlin, Germany.

Ih, J. G., Park, C.M., and Kim, H. J. (1996). A model for sound propagation in capillary ducts with mean flow, **Journal of Sound and Vibration** 190 (2), 163–175.

Jeong, K. W., and Ih, J. G. (1996). A numerical study on the propagation of sound through capillary tubes with mean flow, **Journal of Sound and Vibration** 198 (1), 67–79.

Konstandopoulos, A.G., and Johnson, J.H. (1989). Wall-flow diesel particulate filters their pressure drop and collection efficiency, **SAE paper** No. 890405.

Keefe, D.H. (1984). Acoustical wave propagation in cylindrical ducts: transmission line parameter approximations for isothermal and nonisothermal boundary conditions, **Journal of the Acoustical Society of America** 75 (1), 58–62.

Klinkenberg. (1995). **Petroleum Reservoir Engineering**, pp. 92-100.

- Kar, T., and Munjal, M. (2005). Generalized analysis of a muffler with any number of interacting ducts. **Journal of Sound and Vibration** 285, 585-596.
- Keith, A. (1982). Acoustical characteristics of porous materials. **Physics reports**, 82(3), 179-227.
- Lord, H., Gately, W., and Evensen, H. (1980). **Noise control for engineers**. McGraw Hill, USA.
- Martys, N. S. (2001). Improved approximation of the Brinkman equation using a lattice Boltzman method. **Physics of fluids**, volume 13, number 6.
- Mehdizadeh, O.Z., and Paraschivoiu, M. (2005). A three-dimensional finite elements approach for predicting the transmission losses in mufflers and silencers with no mean flow. **Applied acoustics** 66, 902-918.
- Munt, R. (1990). Acoustic transmission properties of a jet pipe with subsonic jet flow. **Journal of Sound and Vibration** 142 (3), 413-436.
- Muter, J. (1998). Predicting diesel particulate filters performance, **diesel controls limited**.
- Qh, S.K., Baik, D.S., and Han, Y.C. (2002). Performance and exhaust gas characteristics on DPF trap. **International journal of automotive technology**. Vol. 3, no.3, pp. 111-115.
- Pain, H. J. (1989). **The physics of vibration and waves**, 3rd edition, John Wiley, PP 100-160.
- Peat, K. (1994). A first approximation to the effects of mean flow on sound propagation in capillary tubes, **Journal of Sound and Vibration** 175, 475-489.
- Selamet, A., Lee, I., and Huff, N. (2003). Acoustic attenuation of hybrid silencers. **Journal of Sound and Vibration** 262, 509-527.
- Seto, W. W. (1971). **Schaum's outline of theory and problems of acoustics**, Schaum's outline series, McGraw-hill book company, USA.
- Sette, D. (1976). **New directions in physical acoustics**. North-Holland publishing company.
- Silin, D., Korneev, V., and Goloshibi, G. (2003). Pressure diffusion waves in porous media. **University of California, paper LBNL**, 52536-EXT-Abs.
- Stanley, H., Andrade, J., Almeida, M., Mendes, J., Havlin, S., and Suki, B. (1997). Fluid flow through porous media, **physical review letters**. Vol. 79, 21

Tao, Z., and Seybert, A. (2001). A review of Current techniques for measuring muffler transmission loss. **Society of automotive engineers, Inc. university of Kentucky.** 03NVC-38.

Tao, Z., Seybert, A., and Herrin, D. (2003). Measuring bulk properties of sound-absorbing materials using the two-source method. **Society of automotive engineers, Inc. university of Kentucky.** 03NVC-200.

To, C., and Doige, A. (1979). A transient testing technique for the determination of matrix parameters of acoustic systems, 1: theory and principles. **Journal of Sound and Vibration** 260 (2), 207-222.

Tudenan, H. (1975). On the propagation of sound waves in cylindrical tubes. **Journal of Sound and Vibration** 39 (1), 1-33.

Wijnant, Y.H., Hannink, M., and Boer, A. (2003). Application of viscothermal wave propagation theory for reduction of boundary layer induced noise. **Euronoise, Naples**, paper ID: 212/P.1.

Wu, T., Zhang, P., and Cheng, C.Y. (1998) Boundary element analysis of mufflers with an improved method for deriving the four-port parameters. **Journal of Sound and Vibration**, 217 (4) 767-779.

Yeh, L., Chang, Y., and Chiu, M. (2005). Shape optimal design on double-chamber mufflers using simulated annealing and a genetic algorithm. **Turkish J. Eng. Sci.**, 29, 207-224.

Yu, R., Shahed, S.M., (1981). Effects of injection timing and exhaust gas recirculation on emissions from a DI diesel engine. **SAE paper** no. 811234.

Zheng, H., and Keith, J. (2004). Ignition analysis of wall-flow monolith diesel particulate filters. **Journal of catalysis today**, 98, 403-412.

Appendix A



a



b

Figure (51a, b): some DPF types and designs, (source: DCL international Inc.)



Figure (52): DPF unit, (source: www.meca.com).

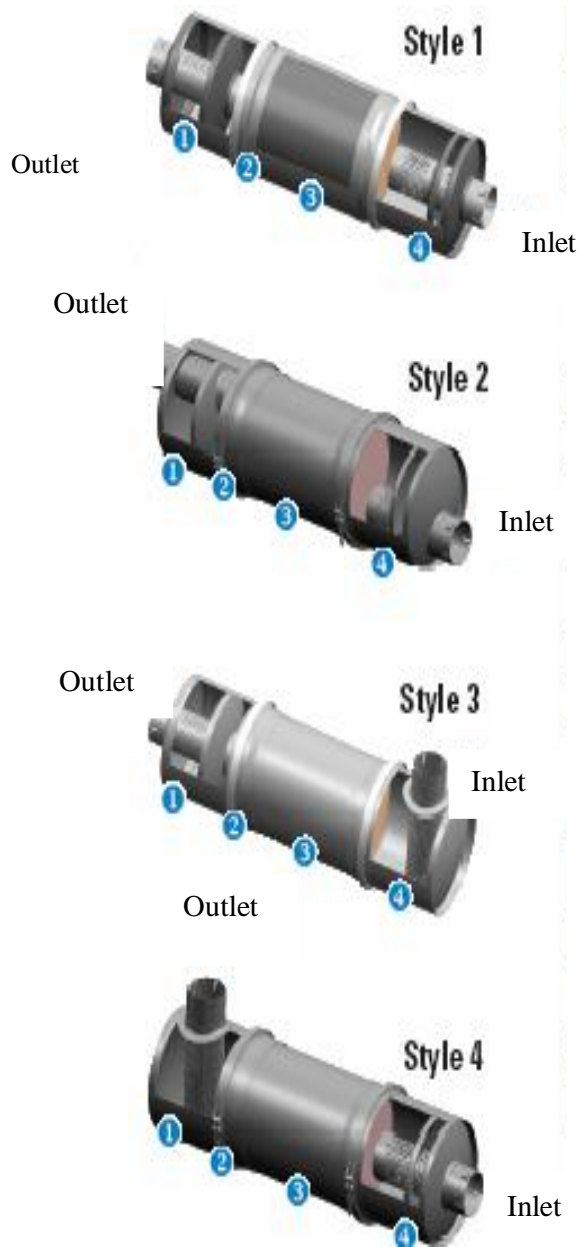


Figure (53): some DPF styles, (source: www.meca.com).

Appendix B

-Numerical values*

1) Typical filter

Table (B1) Numerical values for typical filter

Diameter/length mm	channels/m ² n x 10 ⁻⁵	channels width mm d _h x 10 ³ m	wall thickness mm h _t x 10 ⁴ m	wall permeability σ _w x 10 ¹³ m ²
150/250	3.10	1.44	3.55	2.5

2) For different types of filters

Table (B2) Numerical values for different types of DPF units

Filter name	channels/m ² n x 10 ⁻⁵	channels width d _h x 10 ³ m	wall thickness h _t x 10 ⁴ m	wall permeability σ _w x 10 ¹³ m ²	R1	R2
RC: 200/12	3.87	1.5	3.04	25	87.1	29.2
RC: 200/20	2.48	1.3	5.04	25	233.3	41.56
EX80: 100/17	1.55	2.11	4.3	2.5	199.8	30.92
EX80: 200/14	3.10	1.44	3.55	2.5	184.1	39.2

*Source: Dokumaci (2001), Allam (2002), Allam (2005), and Allam (2006).

3) Other constants*

Table (B3)

Quantity	value
γ	1.4
ρ_0	0.35 Kg/m ³
a_j	0.0015 m
R	287 J/Kg.K
l	0.11 m
K_{th}	0.0674 W/m. K
C_{pj}	1141J/Kg.K
C	343.3 m/s
$m_{in} = m_{out}$	0.51

*Source: Dokumaci (2001), Allam (2002), Allam (2005), and Allam (2006).

Appendix C

Numerical solution for laminar flow in porous media

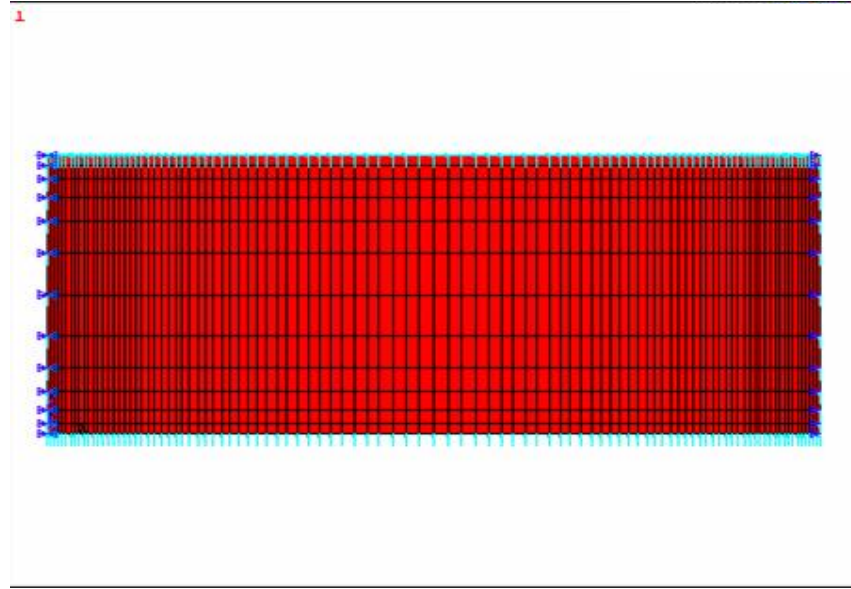


Figure (54): 2-D model for a porous media pipe under cold conditions.

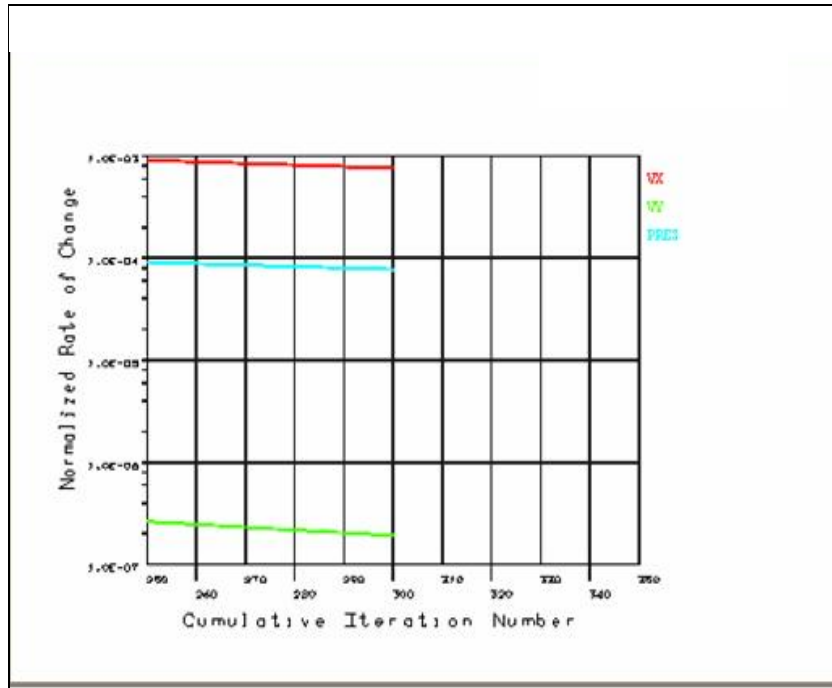


Figure (55): VX, VY, and Pressure rate of change for the gas flow through porous media under cold conditions.

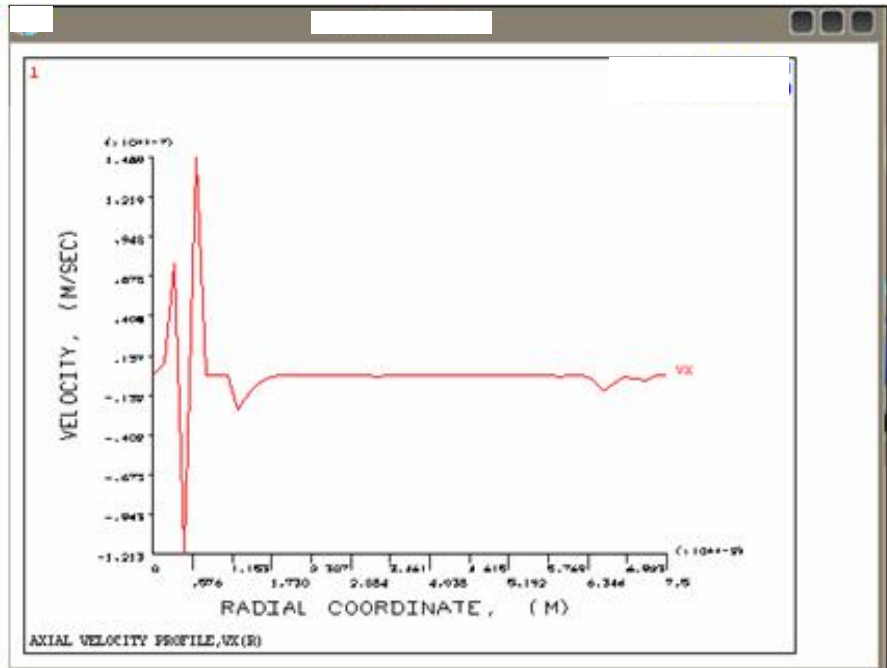


Figure (56): axial velocity profile for gases emission through the porous media under cold conditions.

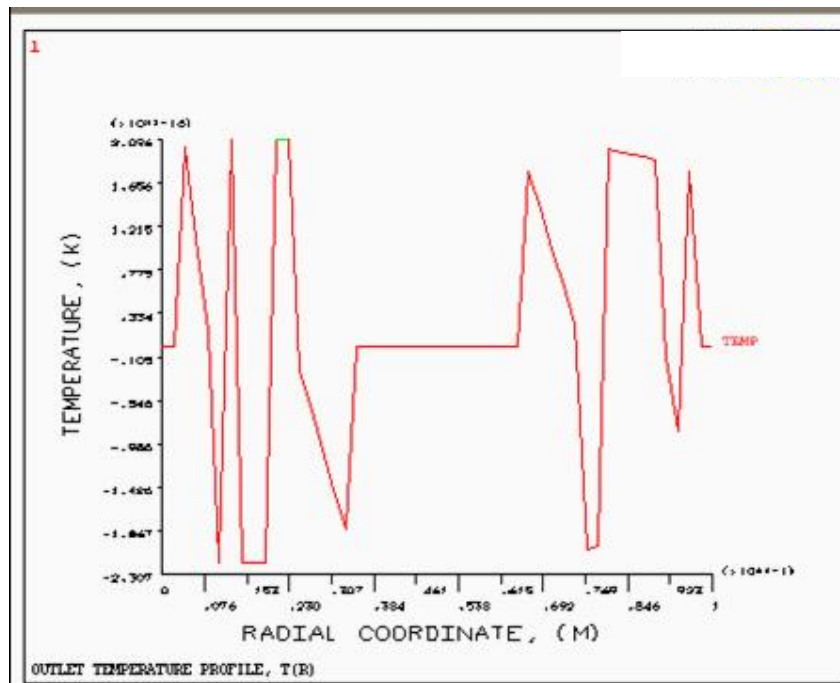


Figure (57): temperature variation profile for gases emission through the porous media under cold conditions.

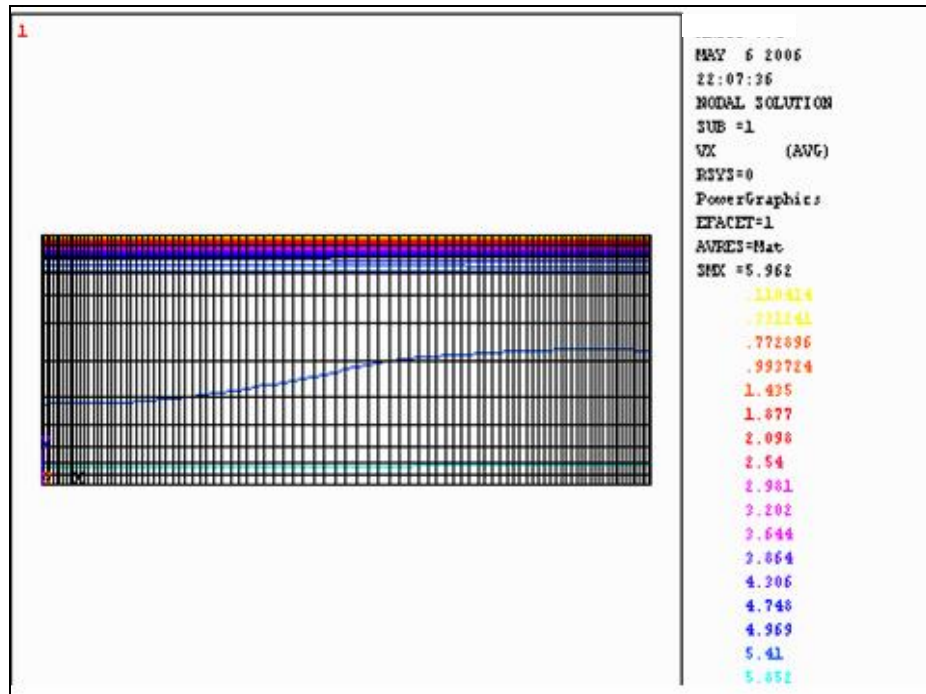


Figure (58): nodal solution for axial velocity under cold conditions.

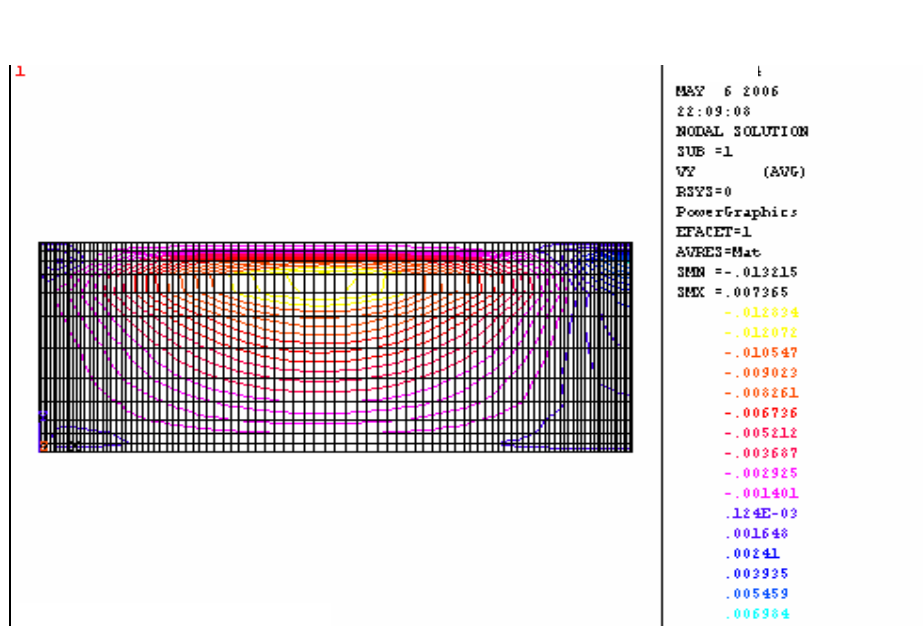


Figure (59): transverse velocity VY distribution at cold conditions.

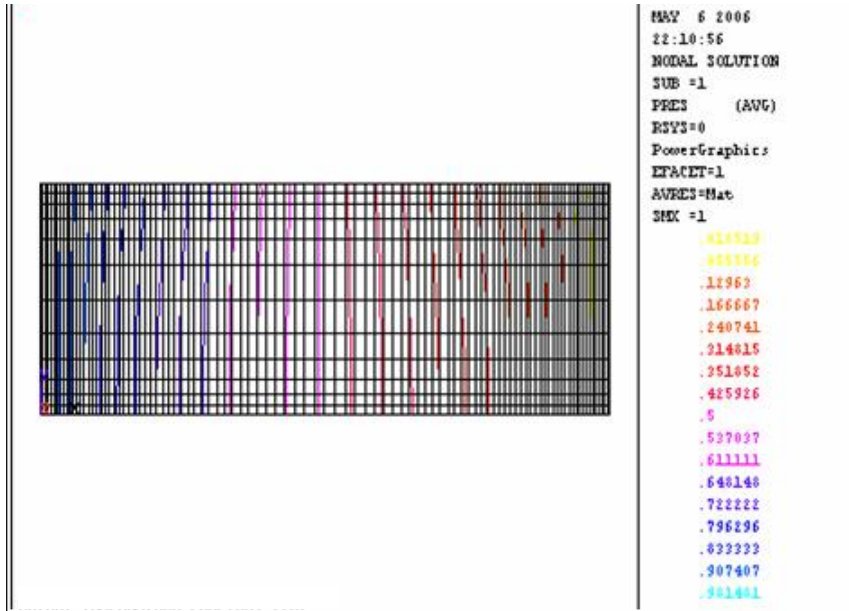


Figure (60): pressure distribution through the porous media under cold conditions.

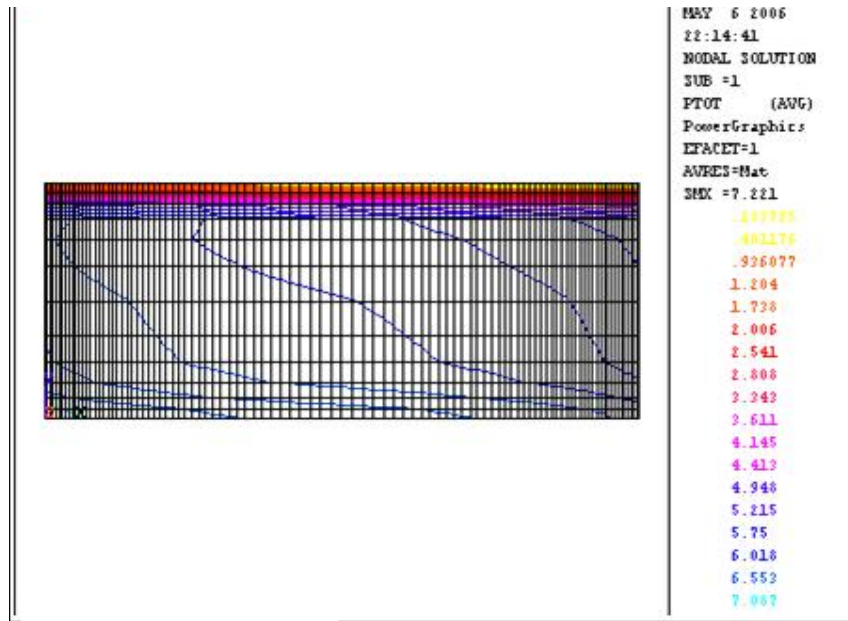


Figure (61): total pressure change across the porous media under cold conditions.

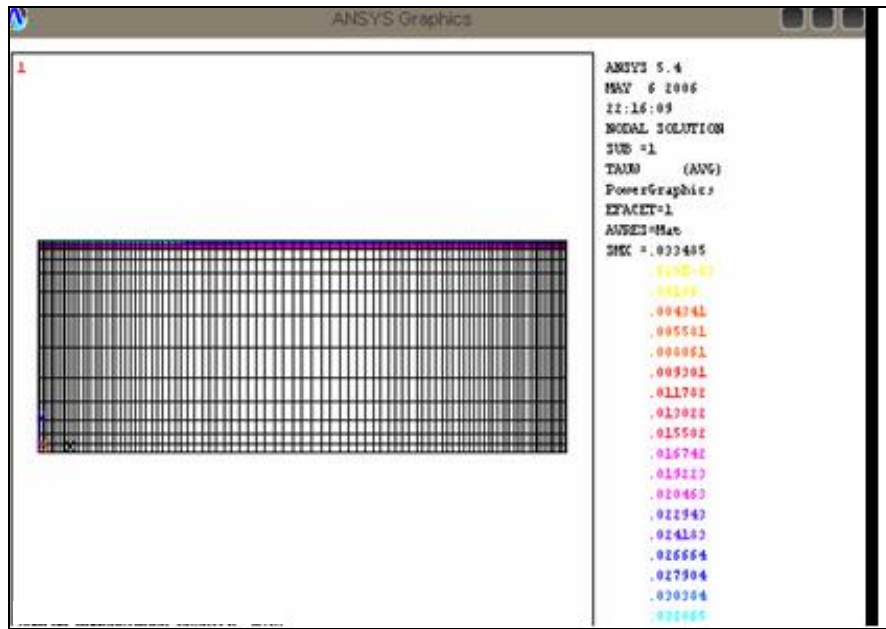


Figure (62): wall shear for the porous media under cold conditions.

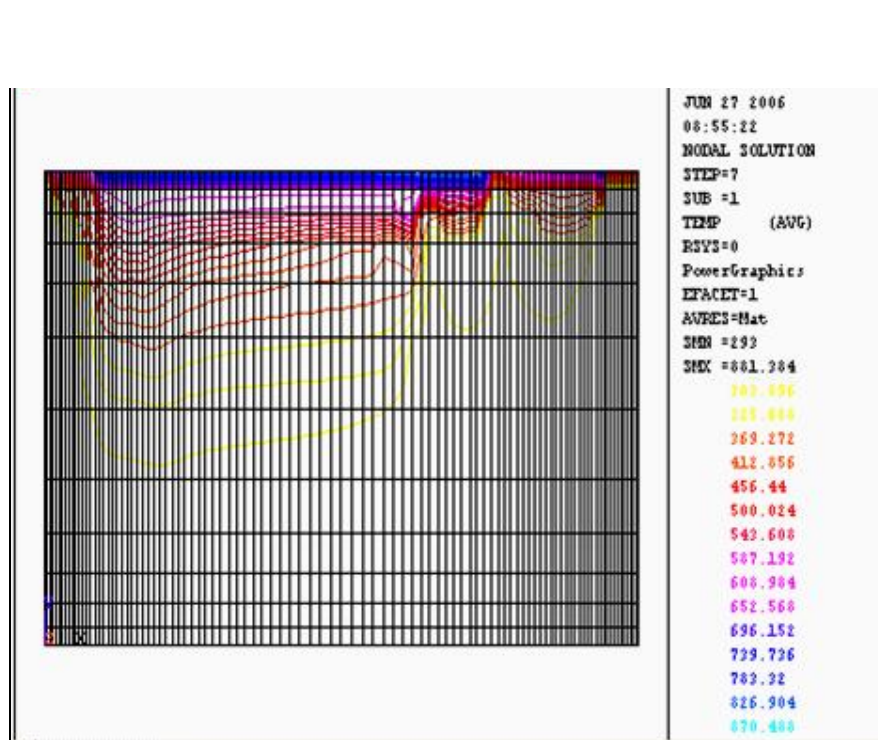


Figure (63): temperature distributions through porous media under cold conditions.

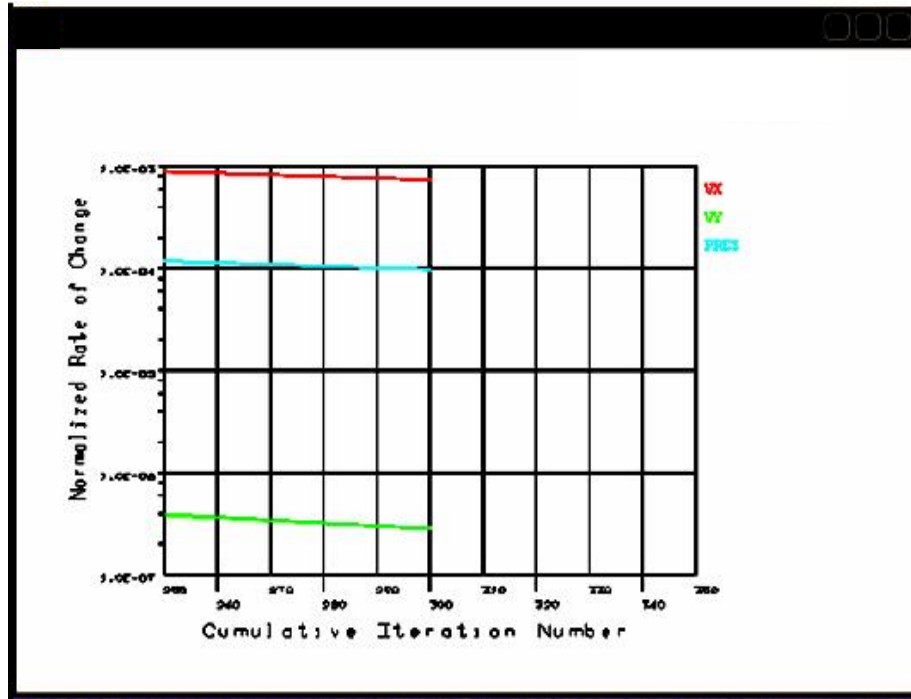


Figure (64): VX, VY, and Pressure rate of change for the gas flow through porous media under hot conditions.

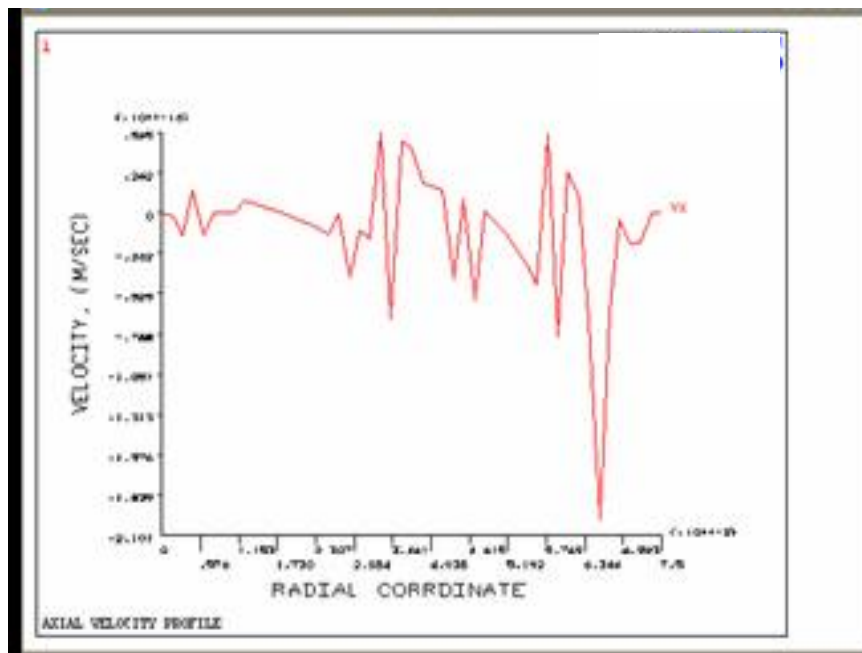


Figure (65): axial velocity profile for gases emission through the porous media under hot conditions.

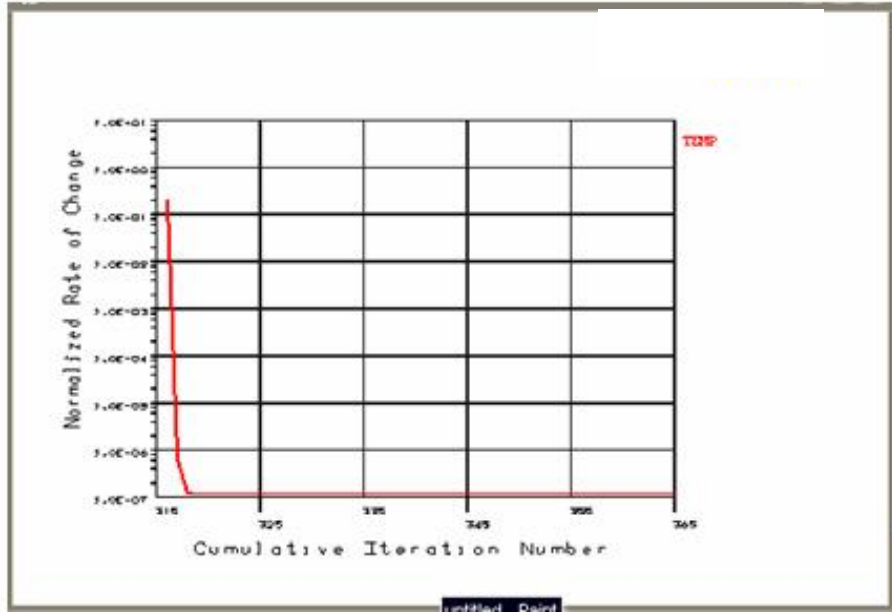


Figure (66): outlet temperature profile for gases emission through the porous media under hot conditions.

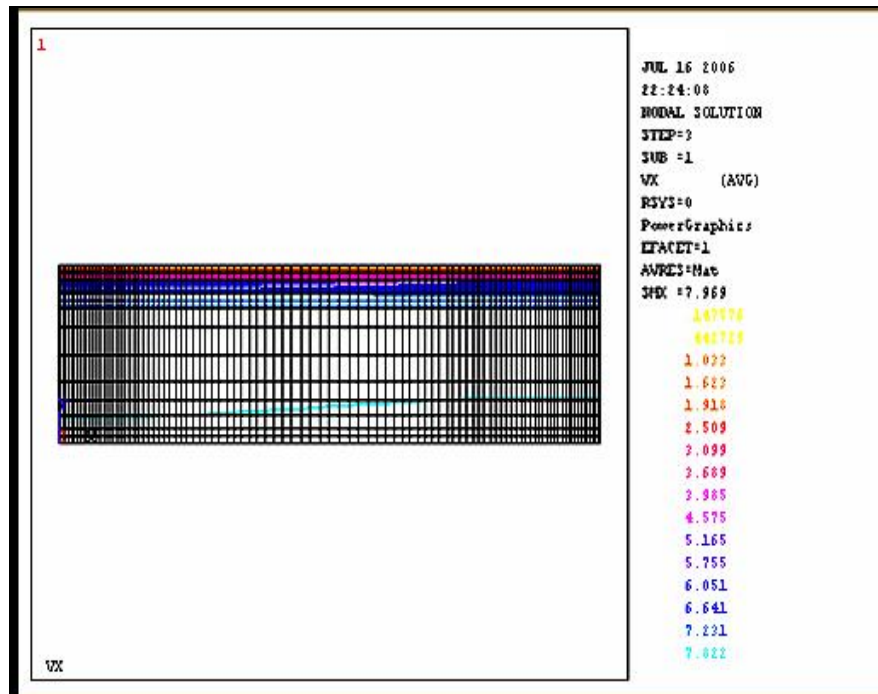


Figure (67): nodal solution for axial velocity under hot conditions.

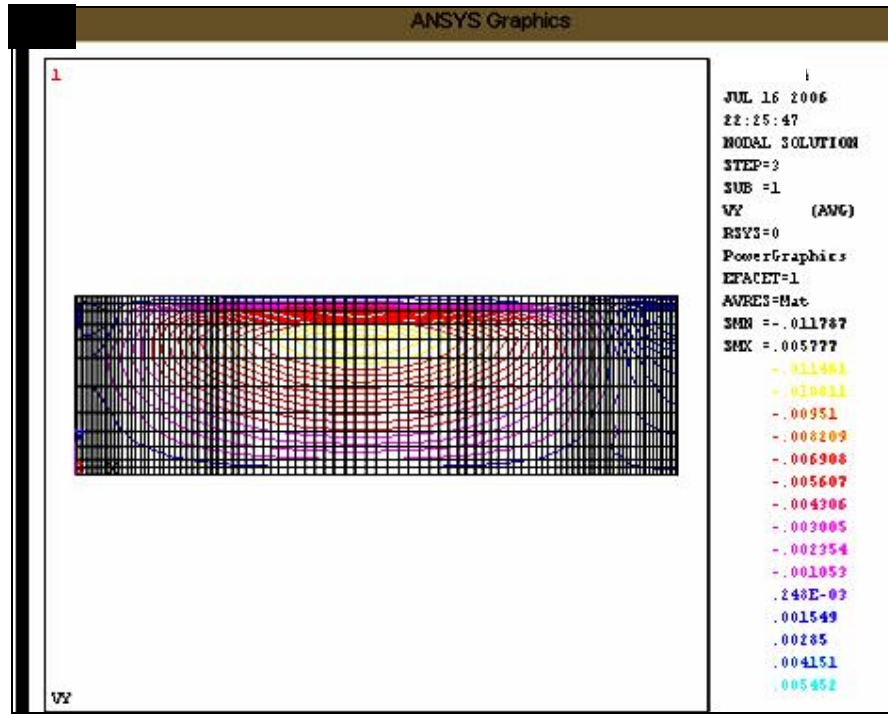


Figure (68): nodal solution for transverse velocity under hot conditions (T=773°K).

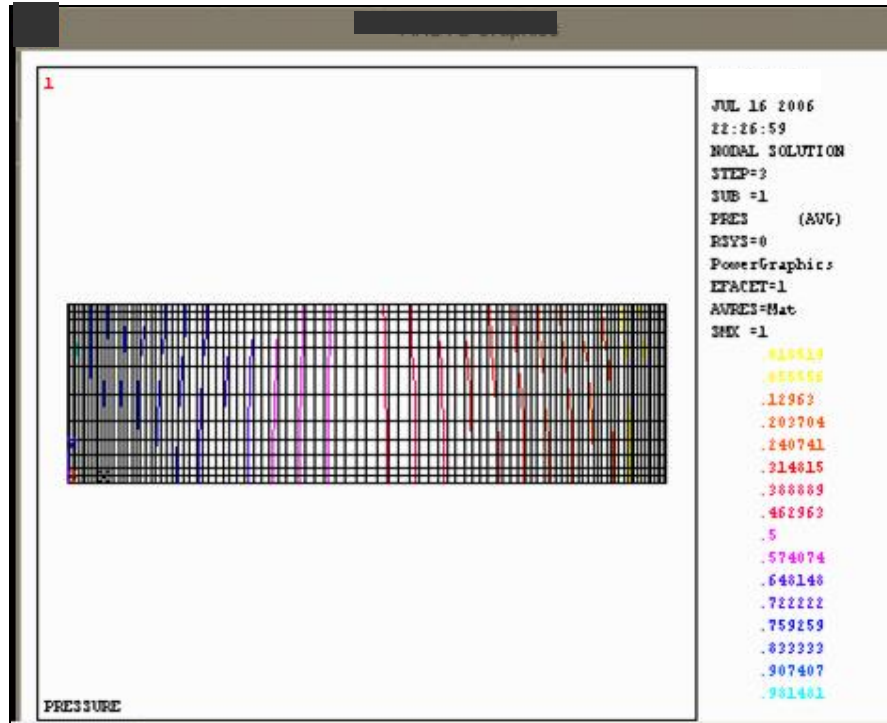


Figure (69): pressure distribution through the porous media under hot conditions.

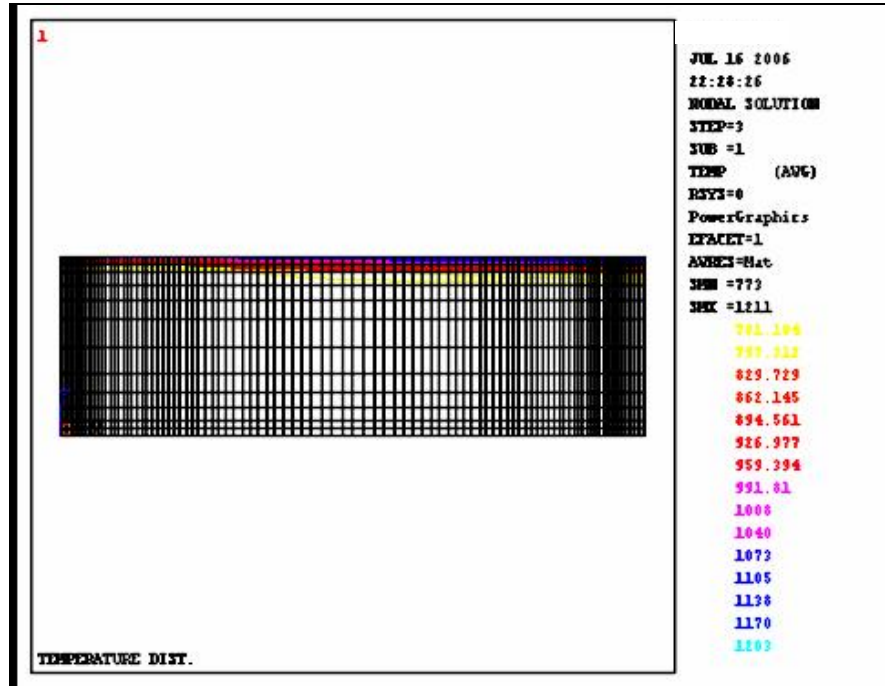


Figure (70): nodal solution for temperature distribution under hot conditions.

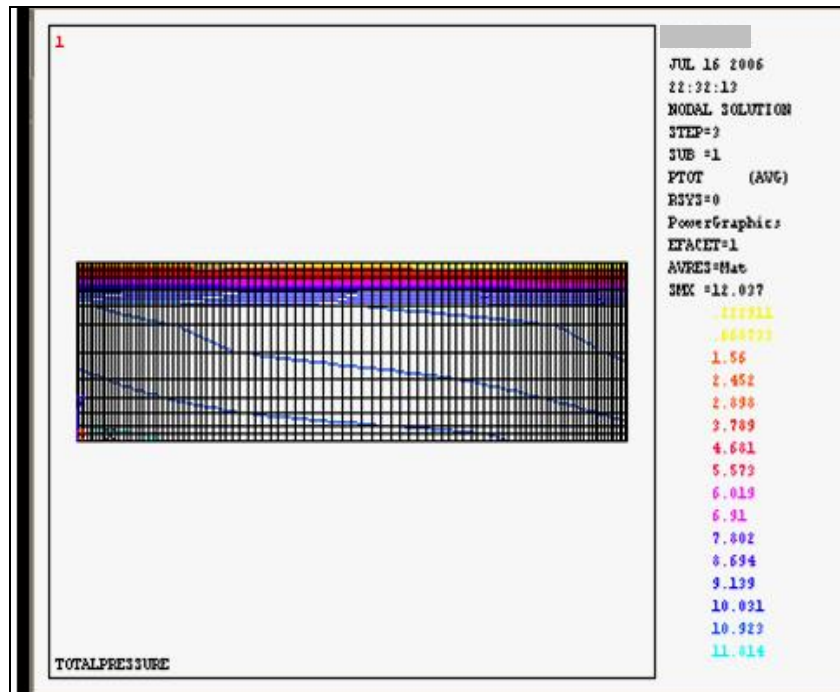


Figure (71): total pressure change across the porous media under hot conditions.

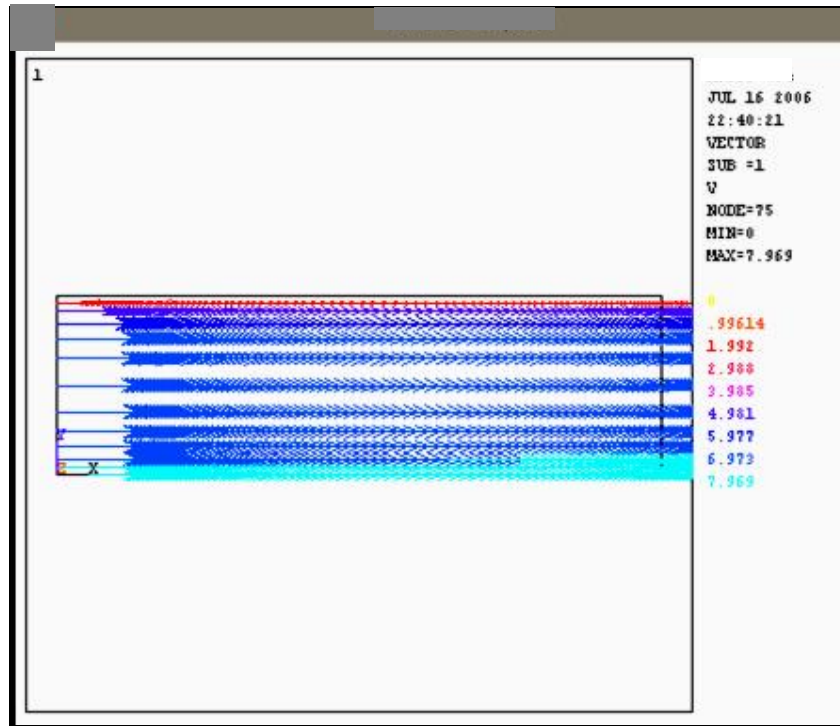
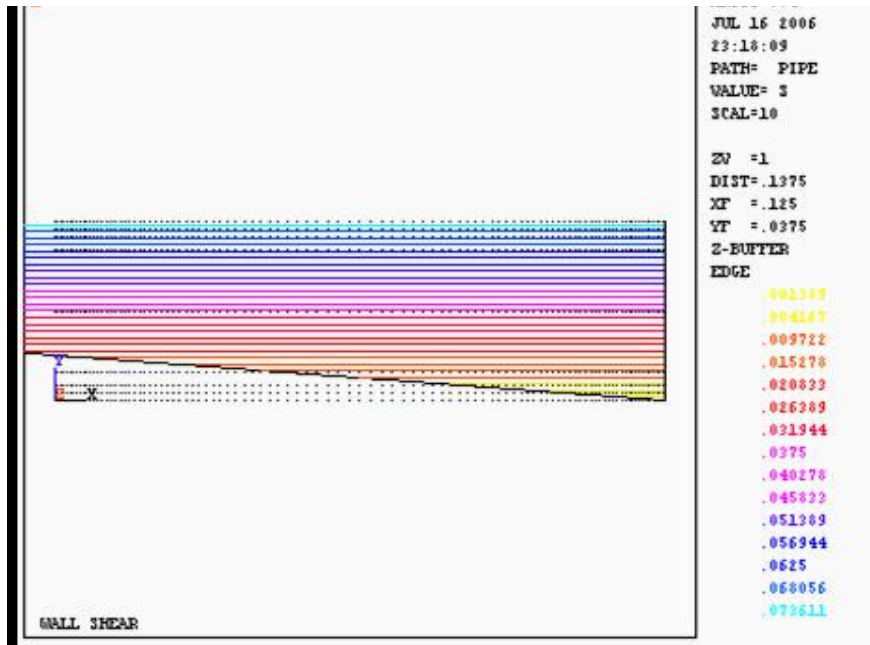


Figure (72): vector solution for velocity under hot conditions.



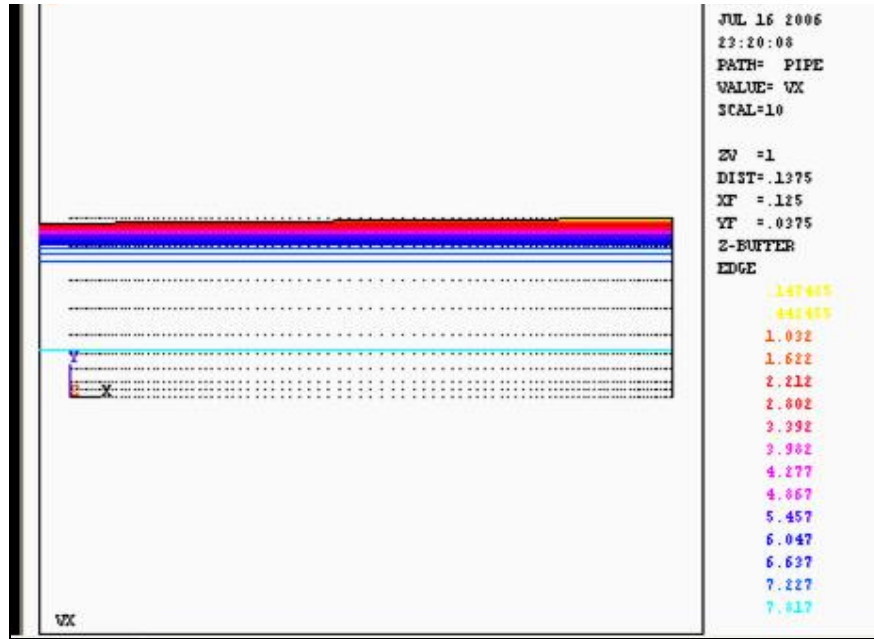


Figure (74): axial velocity under hot conditions distributions.

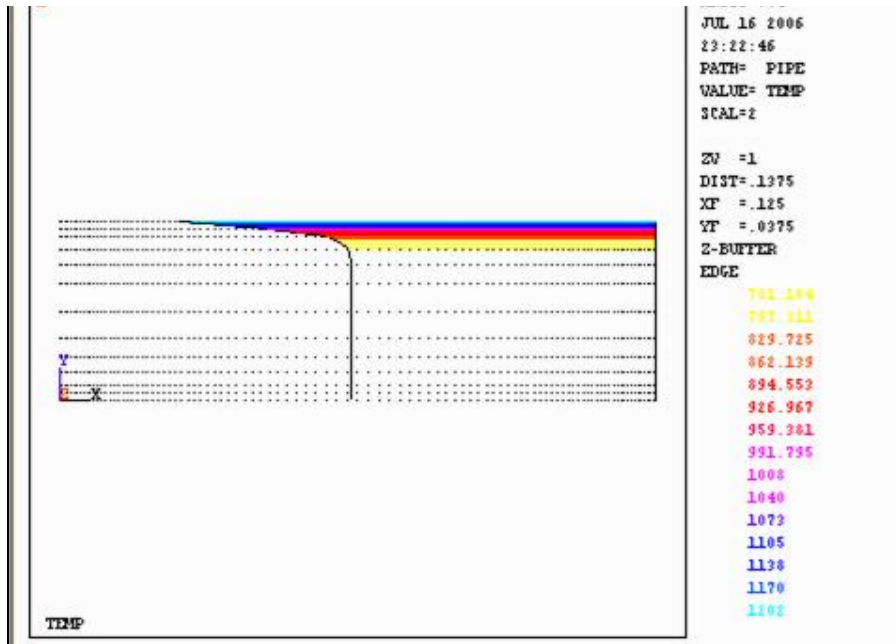


Figure (75): temperature distributions under hot conditions.


```

SF,ALL,HFLUX,QW
LSEL,S,,,1
NSLL,S,1
D,ALL,VY
LSEL,S,,,4
NSLL,S,1
D,ALL,VY
D,ALL,PRES,PIN
D,ALL,TEMP,TIN
LSEL,S,,,2
NSLL,S,1
D,ALL,VY
D,ALL,PRES
ALLSEL
VSEL,ALL
ASEL,ALL
LSEL,ALL
KSEL,ALL
ESEL,ALL
NSEL,ALL
FINISH
/SOLU
FLDATA,ITER,EXEC,300
FLDATA,ITER,CHEC,10
FLDATA,TEMP,NOMI,TIN
FLDATA,NOMI,DENS,RHO
FLDATA,NOMI,VISC,MU
FLDATA,NOMI,COND,K
FLDATA,NOMI,SPHT,CP
FLDATA,OUTP,TAUW,T
SAVE
SOLVE
/BATCH
***** UP19970828      21:28:19  07/16/2006
/input,menust,tmp      ,,1
/GRA,POWER
/GST,ON
/FILNAM,LAMINAR FLOW IN POROUS MEDIA
/TITLE,LAMINAR FLOW IN POROUS MEDIA
/PREP7
SMART,OFF
ET,1,FLUID141,,,2
MSHK,1
MSHA,0,2D
PI=ACOS(-1)
L=0.25
R=0.075
PIN=1
TIN=773
QW=5000

```

```

RHO=0.35
MU=4.15E-5
K=0.0674
CP=1141
RECTNG,,L,,R
LSEL,S,,2,4,2
LSEL,S,,,2,4,2
LESIZE,ALL,,,12,-4
LSEL,INVE
LESIZE,ALL,,,100,-4
ALLSEL
VSEL,ALL
ASEL,ALL
LSEL,ALL
KSEL,ALL
ESEL,ALL
NSEL,ALL
AMESH,1
LSEL,S,,,3
NSLL,S,1
D,ALL,VX
D,ALL,VY
SF,ALL,HFLUX,QW
LSEL,S,,,1
NSLL,S,1
D,ALL,VY
LSEL,S,,,4
NSLL,S,1
D,ALL,VY
D,ALL,PRES,PIN
D,ALL,TEMP,TIN
LSEL,S,,,2
NSLL,S,1
D,ALL,VY
D,ALL,PRES
ALLSEL
VSEL,ALL
ASEL,ALL
LSEL,ALL
KSEL,ALL
ESEL,ALL
NSEL,ALL
FINISH
/DOLU
!/DOLU
/SOLU
FLDATA,ITER,EXEC,300
FLDATA,ITER,CHEC,10
FLDATA,TEMP,NOMI,TIN
FLDATA,NOMI,DENS,RHO

```

```

FLDATA,NOMI,VISC,MU
FLDATA,NOMI,COND,K
FLDATA,NOMI,SPHT,CP
FLDATA,OUTP,TAUW,T
SAVE
SOLVE
SOLVE
FLDATA,ITER,EXEC,50
FLDATA,SOLU,TEMP,T
FLDATA,SOLU,FLOW,F
FLDATA,RELX,TEMP,1.0
SOLVE
FINISH
/POST1
/DEVICE,VECTOR,ON
SET,LAST
/RATIO,,,10
EPLOT
/EDGE
/EDGE,1,1
/CONTOUR,1,27
/TITLE,CONTOURS OF AXIAL VELOCITY
PLNSOL,VX
VXC=VX(2)
PATH,PIPE,2,,48
PPATH,1,,L,0,0
PPATH,2,,L,R,0
PDEF,VX,VY
PDEF,TEMP,TEMP
PCALC,MULT,PROD1,VX,S
PCALC,INTG,VXM,PROD1,S,2/R**2
*GET,VXM,PATH,,LAST,VXM
MDOT=RHO*VXM*PI*R**2
/TITLE,CONTOURS OF WALL SHEAR STRESS
PLNSOL,TAUW
*GET,TAU,PLNSOL,,MAX
PCALC,MULT,PROD2,VX,TEMP
PCALC,MULT,PROD3,PROD2,S
PCALC,INTG,TM,PROD3,S,2/VXM/R**2
*GET,TM_0,PATH,,LAST,TM
/TITLE,CONTOURS OF TEMPERATURE
PLNSOL,TEMP
*GET,TW_0,PLNSOL,,MAX
TC_0=TEMP(2)
*STATUS
/RATIO
/TITLE,AXIAL VELOCITY PROFILE
/AXIAL X,RADIAL CORRDIATE,
!/AXIAL X,RADIAL CORRDIATE,
/AXIAL,X,RADIAL CORRDIATE

```

```

!/AXIAL,X,RADIAL CORRDATE
/AXLAB,X,RADIAL CORRDATE
/AXLAB,Y,VELOCITY, (M/SEC)
/DEVICE,RASTOR,ON
PLPATH,VX
/TITLE,OUTLET TEMPERATURE PROFILE, T
/AXLAB,Y,TEMPERATURE, (K)
PLPATH,TEMP
PLPATH,TEMP
FINISH
/POST1
PLNSOL,V,X,0,
/TITLE, VX
PLNSOL,V,X,0,
PLNSOL,V,X,0,
/TITLE,VY
PLNSOL,V,Y,0,
PLNSOL,V,Y,0,
/TITLE,PRESSURE
PLNSOL,PRES, ,0,
PLNSOL,PRES, ,0,
/TITLE,TEMPERATURE DIST.
PLNSOL,TEMP, ,0,
PLNSOL,DENS, ,0,
PLESOL,CENT,X,0,
PLESOL,CENT,Y,0,
PLESOL,CENT,Z,0,
PLTRAC,FLUID,TEMP,, , , , ,0
PLTRAC,FLUID,V,X, , , , ,0
PLTRAC,FLUID,PRES,, , , , ,0
PLTRAC,FLUID,TEMP,, , , , ,0
PLNSOL,TAUW, ,0,
PLNSOL,PTOT, ,0,
/TITLE,TOTALPRESSURE
PLNSOL,PTOT, ,0,
PLNSOL,TTOT, ,0,
PLNSOL,MACH, ,0,
PLNSOL,HFLM, ,0,
PLNSOL,EVIS, ,0,
PLPAGM, ,1,'NODE'
PLNSOL,STRM, ,0,
PLNSOL,STRM, ,1,
PLNSOL,STRM, ,0,
PLNSOL,MACH, ,1,
PLESOL,CENT,Z,1,
PLNSOL,TTOT, ,1,
/POST26
FINISH
/POST26
/SOLU

```

```

FINISH
/SOLU
SOLVE
/POST1
FINISH
/POST1
PLTRAC,FLUID,TEMP,, , , , ,0
PLNSOL,TEMP, ,1,
PLNSOL,V,X,1,
PLNSOL,V,Y,1,
PLNSOL,V,SUM,1,
PLETAB, ,NOAV
PLPATH,
!*
/VSCALE,1,1,0
!
!*
PLVECT,V, , , ,VECT,ELEM,ON,0
/TITLE VELOCITY VECTORS
!*
/VSCALE,1,1,0
!
!*
PLVECT,V, , , ,VECT,ELEM,ON,0
PLVECT, , , , ,VECT,NODE
!*
/VSCALE,1,1,0
!
!*
PLVECT,V, , , ,RAST,ELEM,ON,0
!*
/VSCALE,1,1,0
!
!*
PLVECT,V, , , ,RAST,NODE,ON,0
!*
/VSCALE,1,1,1
!
!*
PLVECT,V, , , ,RAST,NODE,ON,0
PLPAGM, ,1,Blank
PLNSOL,ENKE, ,1,
PLNSOL,ENDS, ,1,
PLNSOL,TEMP, ,1,
PLNSOL,SPHT, ,1,
PLNSOL,EVIS, ,1,
PLNSOL,PCOE, ,1,
PLESOL,CENT,X,1,
PLESOL,CENT,Y,1,
PLTRAC,FLUID,V,X, , , , , ,0

```

```

PLNSOL,V,X,1,
PLNSOL,V,Y,1,
PLNSOL,V,Z,1,
PLNSOL,PRES, ,1,
PLNSOL,PRES, ,0,
PLNSOL,PRES, ,2,
PLNSOL,V,X,2,
PLESOL,CENT,Y,0,
PLNSOL,PRES, ,2,
PLNSOL,ENKE, ,2,
PLNSOL,ENDS, ,0,
/AUX12
FINISH
/AUX12
/POST1
PLNSOL,TEMP, ,1,
PLNSOL,TEMP, ,2,
PLETAB, ,AVG
PLNSOL,TTOT, ,2,
PLNSOL,TTOT, ,0,
TRTIME,0,0, ,0,0,
/SOLU
FINISH
/SOLU
/POST1
FINISH
/POST1
!*
RSYS,0
AVRES,2
AVPRIN,0
!*
SET,LIST,2
SET,LIST,2
PLNSOL,PRES, ,0,
PLNSOL,ENKE, ,0,
PLNSOL,ENDS, ,0,
PLNSOL,TEMP, ,0,
PLESOL,CENT,Z,0,
PLESOL,CENT,Y,0,
PLESOL,CENT,X,0,
PLESOL,CENT,X,0,
PLNSOL,TEMP, ,0,
PLESOL,CENT,Y,0,
PLNSOL,PRES, ,0,
!*
/VSCALE,1,1,1
!
!*
PLVECT,V, , , ,RAST,ELEM,ON,0

```

```

PLTRAC,FLUID,TEMP,, , , , ,0
PLPATH,
FLREAD, ,rsf, ,,,,
PLNSOL,TEMP, ,0,
/TITLE,TEMPERATURE PROFILE
/AXLAB,Y,TEMPERATURE, (K)
PLPATH,TEMP
PLNSOL,TEMP, ,0,
PLPATH,TEMP
PATH,PIPE,2,,48
PPATH,1,,L,0,0
PPATH,2,,L,R,0
PDEF,VX,VX
PDEF,TEMP,TEMP
PLPATH,TEMP
/TITLE, OUTLET TEMP PROFILE
/AXLAB,X,RADIAL COORDINATE
/AXLAB,Y,TEMPERATURE, (K)
PLPATH,TEMP

```

Appendix E

Cleaning and regeneration unit of DPFs



Figure (76): diesel particulate filter cleaning unit, (source: www.meca.com).

انتشار الصوت في المواد المسامية مع تطبيقات على فلتر الديزل الحبيبي

إعداد

صايل " محمد علي " مقبل فياض

المشرف الرئيسي

ا.د. محمد احمد حمدان

المشرف المساعد

ا.د. محمد نادر حمدان

الملخص

يقدم هذا العمل نموذجاً ثنائي الأبعاد (2-D) لانتشار الصوت في فلتر ديزل 'حبيبي (Diesel Particulate Filter). لقد تم بناء هذا النموذج باستخدام معادلة نافير ستوكس، معادلة الطاقة، معادلة الاستمرارية، و بمساعدة كل من معادلة دارسي للمواد المسامية و قانون الحالة في الغازات المثالية. لقد تم الإبقاء هنا على السرعة العمودية (transverse velocity) و لم يتم حذفها كما في الدراسات السابقة كذلك تم التعامل مع الفلتر كمادة مسامية بشكل جزئي. لقد تم في المرحلة الأولى اعتبار كل من درجة الحرارة، الضغط، الكثافة، السرعة الأفقية، و السرعة العمودية متغيرات مع الزمن فقط (Time Harmonic Variation)، ثم تم اشتقاق هذه الكميات بالنسبة للزمن. و من ثم تم تعويض المشتقات في المعادلات الأساسية السابقة الذكر، حيث تم الحصول على معادلات تفاضلية مشتقة بالنسبة للمستوى (plane)، ثم تم افتراض حلول مناسبة لها بدلالة المستويات و بمساعدة سلاسل فوريير الجيبية (Fourier sinus series) تم حل هذه المعادلات. و تم الحصول على معادلة نهائية من الدرجة الرابعة تم حلها و تم الحصول على أربعة جذور لثابت الانتشار الموجي (Γ) و لهذه الجذور الأربعة أربعة متجهات مرافقة لذلك تم تسمية هذا النموذج بنموذج الأبواب الأربعة (Four-port model). في المرحلة الثانية من هذه الدراسة تم اعتبار الكميات السابقة متغيرة مع كل من الزمن و الفراغ أو المستوى (Harmonic in time and in 2-D space) مع إهمال البعد الثالث (Z-direction) و بنفس الطريقة في المرحلة الأولى تم الحصول على معادلة تم حلها و نتج عنها ستة جذور، لهذه الجذور ستة متجهات لذلك تم هنا اكتشاف نموذج جديد لوصف السلوك الصوتي لفلتر الديزل الحبيبي تم تسميته بالنموذج ذواالبواب الستة (Six-Port Model). إن الأهداف الرئيسية لهذه الدراسة قد تضمنت إيجاد كل من ثابت الانتشار الموجي الذي يتضمن كل من التخامد الموجي (Attenuation) و الانحراف الموجي (Phase shift)، حساب مقدار الضياع في الانتشار الموجي خلال مسير الموجة داخل الفلتر (Transmission Losses)، معرفة مقدار تخفيض الفلتر للإزعاج (Noise Reduction Factor)، المقارنة بين الأنواع المختلفة لهذا الفلتر و قدرتها على القيام بعملية تقليل الإزعاج وتضييعه، و معرفة تأثير كل من النفاذية

(Porosity) و السماحية (permeability) و أبعاد الفلتر و مواصفاته على قدرته و كفاءته. لقد تم مقارنة النتائج الحالية بنتائج الدراسات السابقة خاصة ما حصل عليه علام (Allam (2006)) و كذلك مع الدراسات العملية (Experimental works) التي قام بها علام وتم ملاحظة أن النتائج الحالية أفضل من السابقة و أن التطابق كبير بين هذه النتائج و النتائج السابقة و العملية. لقد تضمنت هذه الدراسة توليد نموذج ثنائي الأبعاد لوصف انتشار الأمواج الصوتية في المواد المسامية (DPF unit) تم تسميته نموذج الأبواب الستة (Six-port model) . كما تم في هذه الدراسة القيام بحل عددي (Numerical Solution) لجريان الغازات في مادة مسامية باستخدام برنامج مناسب و قد تم إيجاد سلوك كل من السرعة الأفقية، العمودية، توزيع الضغط و درجات الحرارة للجريان داخل المادة المسامية التي تمثل في الواقع فلتر الديزل الحبيبي.